Author Manuscript

Author Manuscript

Author Manuscript

Author Manuscript

HHS Public Access

Author manuscript

J Med Chem. Author manuscript; available in PMC 2022 August 26.

Published in final edited form as:

J Med Chem. 2021 August 26; 64(16): 12109–12131. doi:10.1021/acs.jmedchem.1c00742.

Discovery of an Orally Bioavailable Small-Molecule Inhibitor for the β-Catenin/B-Cell Lymphoma 9 Protein–Protein Interaction

Zhen Wang,
Drug Discovery Department, H. Lee Moffitt Cancer Center and Research Institute, Tampa, Florida 33612-9497, United States

Min Zhang,
Drug Discovery Department, H. Lee Moffitt Cancer Center and Research Institute, Tampa, Florida 33612-9497, United States

Victor Quereda,
Drug Discovery Department, H. Lee Moffitt Cancer Center and Research Institute, Tampa, Florida 33612-9497, United States

Sylvia M. Frydman,
Drug Discovery Department, H. Lee Moffitt Cancer Center and Research Institute, Tampa, Florida 33612-9497, United States

Qianqian Ming,
Drug Discovery Department, H. Lee Moffitt Cancer Center and Research Institute, Tampa, Florida 33612-9497, United States

Vincent C. Luca,
Drug Discovery Department, H. Lee Moffitt Cancer Center and Research Institute, Tampa, Florida 33612-9497, United States

Derek R. Duckett,
Drug Discovery Department, H. Lee Moffitt Cancer Center and Research Institute, Tampa, Florida 33612-9497, United States

Haitao Ji

Corresponding Authors Phone: (813) 745-5410; Derek.Duckett@moffitt.org, Phone: (813) 745-8070; Haitao.Ji@moffitt.org.

Author Contributions

Z.W., M.Z., and V.Q. contributed equally to this work. The manuscript was written through contributions of all authors. All authors have given approval to the final version of the manuscript.

ASSOCIATED CONTENT

Supporting Information

The Supporting Information is available free of charge at https://pubs.acs.org/doi/10.1021/acs.jmedchem.1c00742.

Dose–response curves for AlphaScreen competitive inhibition assays, SPR competitive inhibition assays, AlphaScreen competitive binding assays of full-length β-catenin and **Biotin-ZW4864**, fluorescence anisotropy binding assays, AlphaScreen competitive binding assays, TOPFlash luciferase reporter, and MTS growth inhibition assays; uncropped Western blot gels for protein pull-down, co-IP, and Western blot experiments; original data plots of C57BL/6 mouse PK studies; original images for clonogenic assays, matrigel invasion, and 3D spheroid BME cell invasion; HPLC condition and traces; NMR spectra; and original FACS reports (PDF)

Molecular formula strings (CSV)

Complete contact information is available at: https://pubs.acs.org/10.1021/acs.jmedchem.1c00742

The authors declare the following competing financial interest(s): A provisional patent application has been filed based on these results.

Author Manuscript Author Manuscript Author Manuscript Author Manuscript

Drug Discovery Department, H. Lee Moffitt Cancer Center and Research Institute, Tampa, Florida 33612-9497, United States

Abstract

Aberrant activation of Wnt/β-catenin signaling is strongly associated with many diseases including cancer invasion and metastasis. Small-molecule targeting of the central signaling node of this pathway, β-catenin, is a biologically rational approach to abolish hyperactivation of β-catenin signaling but has been demonstrated to be a difficult task. Herein, we report a drug-like small molecule, **ZW4864**, that binds with β-catenin and selectively disrupts the protein–protein interaction (PPI) between B-cell lymphoma 9 (BCL9) and β-catenin while sparing the β-catenin/E-cadherin PPI. **ZW4864** dose-dependently suppresses β-catenin signaling activation, downregulates oncogenic β-catenin target genes, and abrogates invasiveness of β-catenin-dependent cancer cells. More importantly, **ZW4864** shows good pharmacokinetic properties and effectively suppresses β-catenin target gene expression in the patient-derived xenograft mouse model. This study offers a selective chemical probe to explore β-catenin-related biology and a drug-like small-molecule β-catenin/BCL9 disruptor for future drug development.

Graphical Abstract

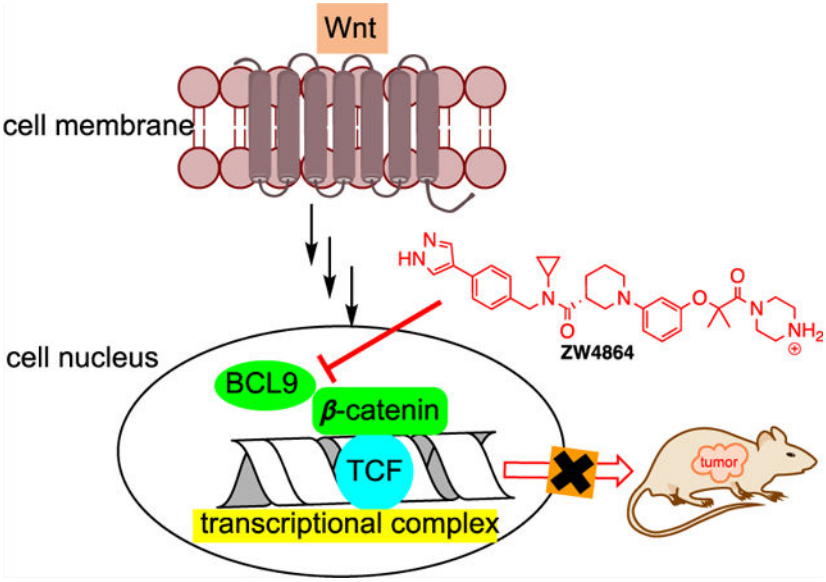

INTRODUCTION

The hyperactivation of the Wnt/β-catenin signaling pathway has a profound connection with initiation and progression of many cancers.[1] When the suppressor genes of this pathway, such as *APC* and *Axin*, suffer from loss-of-function mutations or the N-terminal phosphorylation sites of *CTNNB1* (β-catenin gene) are mutated inappropriately, β-catenin is stabilized into the dephosphorylated active form and translocated into the cell nucleus. Nuclear active β-catenin then binds with the DNA-binding lymphoid enhancer-binding factor (LEF)/T-cell factor (TCF) family of transcriptional factors and recruits CREB-binding

Author Manuscript Author Manuscript Author Manuscript Author Manuscript

protein (CBP)/p300, B-cell lymphoma 9 (BCL9)/BCL9-like (BCL9L), Pygo 1/Pygo2, etc., as coactivators to transcribe β-catenin target genes. These target genes induce the epithelial-to-mesenchymal transition (EMT), sustain stem-like cancer cells or cancer stem cells, and promote tumor immune evasion. β-Catenin signaling can also be activated by autocrine activation of frizzled (Fzd), Wnt ligands, and disheveled (Dvl), epigenetic silencing of Wnt suppressors, and/or crosstalk with other signaling pathways.

Substantial work has been conducted to search for inhibitors of the upstream effectors of the Wnt/β-catenin pathway,[2] with porcupine inhibitors LGK974,[3] ETC-159,[4] CGX1321,[5] and RXC004,[6] soluble Wnt receptor OMP-54F28,[7,8] and Fzd receptor blocker OMP-18R5[9] being tested in clinical trials. However, inhibition of these upstream Wnt targets (1) cannot produce efficacy against disease-causing loss-of-function mutations of *APC* and *Axin* and activation mutations of *CTNNB1*; (2) is ineffective against cancers owing to the crosstalk with the other signaling pathways to upregulate β-catenin; and (3) increases the risk of undesirable off-pathway effects by inhibiting noncanonical Wnt signaling pathways. The most appealing target for inhibitor development might be nuclear β-catenin-containing transcriptional complex because the penultimate step of the signaling cascade is the formation of this complex that confers activation of the β-catenin signaling circuit. However, direct targeting of β-catenin has proven to be a difficult task.[1,10–12] Most β-catenin-targeting efforts were focused on antagonizing β-catenin interaction with TCF/LEF,[12] but none of the compounds were advanced beyond the early stage of inhibitor development, probably due to two challenges: (1) β-catenin and TCF have a very large protein–protein interaction (PPI) area (3500 $Å^2$) and strong binding affinity (K_D = 7–10 nM)[13] and (2) β-catenin adopts the same PPI area to interact with APC, E-cadherin, and TCF.[13–20]

The β-catenin/BCL9 PPI is a promising alternative target for inhibitor development. BCL9 or BCL9L is the scaffolding protein of the Wnt enhanceosome that captures newly stabilized, nuclear-localized β-catenin, facilitating β-catenin access to LEF/TCF and activating the transcription complex.[21,22] The homology domain 2 (HD2) of BCL9 or BCL9L adopts a single α-helical structure to bind with β-catenin.[13] The β-catenin/BCL9 PPI interface is much smaller (1450 $Å^2$), and this PPI displays a moderate K_D of 0.47 μM. The surface area of β-catenin for interacting with BCL9 has little overlap with that for other β-catenin partners, and E-cadherin (region V) is the only other known protein that binds this PPI interface.[13] BCL9 and BCL9L are significantly overexpressed in many cancers, possibly through chromosomal 1q21 amplification and downregulation of BCL9-suppressing microRNAs.[23–25] The β-catenin/BCL9 complex can also be upregulated through downregulation of endogenous negative regulators of this PPI.[26] Dominant negative constructs of BCL9/BCL9L prohibit Wnt/β-catenin signaling.[27,28] Knock-down of BCL9/BCL9L using siRNA or shRNA suppresses β-catenin signaling, blocks transcription of β-catenin target genes, and impedes migration and invasion of Wnt-activated cancer cells.[23,24,27–30] Deletion of BCL9 and BCL9L suppresses Wnt-driven tumorigenesis, inhibits invasion and metastasis of Wnt-active tumors, and increases disease-free survival in mouse models that authentically mimic human cancer.[31–33]

In addition to peptide-based inhibitors that have been reported to disrupt the β-catenin/BCL9 PPI,[34–37] Bienz and co-workers discovered carnosic acid and its analogues as small-

Author Manuscript Author Manuscript Author Manuscript Author Manuscript

molecule β-catenin/BCL9 PPI inhibitors through compound screening.[38,39] We designed 3-(4-fluorophenyl)-*N*-phenylbenzamide (PNPB) derivatives as small-molecule β-catenin/BCL9 disruptors based on PPI hot-spot interactions.[40–43] Through modifying a screening hit **CP-868388** discovered in AlphaScreen assays,[44] we obtained 2-(3-(3-carbamoylpiperidin-1-yl)phenoxy)acetic acid (CPPAA) derivatives as β-catenin/BCL9 PPI inhibitors (Figure 1).[45] The best compound **CPPAA-30** exhibited a K_i of 3.6 μM for β-catenin/BCL9 disruption and showed on-target activities in cell-based experiments. In this study, we set out to perform alternative optimization on **CP-868388**, which yields a drug-like small-molecule β-catenin/BCL9 PPI inhibitor **ZW4864** that shows in vivo on-target effects (Figure 1).

RESULTS

Inhibitor Design and Biochemical Characterizations.

We first synthesized both *R*- and *S*-isomers of the reported inhibitor **CPPAA-2**, resulting in compounds **1** and **2** in Table 1, respectively. The AlphaScreen assays indicated that **1** displayed a K_i of 46 μM for β-catenin/BCL9 PPI disruption, while **2** was less active (K_i > 90 μM). Therefore, compound **1** was employed as a starting point for further optimization. Within the BCL9-binding surface area of β-catenin, there are a few acidic residues, including the acidic knobs (D162, E163, and D164), D144, D145, E147, and E155. Our previous structure-based design of PNPB derivatives demonstrated that introduction of positively charged groups increased the binding affinity.[40,41] Indeed, addition of a piperazine moiety led to 3, which disrupted the β-catenin/BCL9 PPI with a K_i of 5.8 μM and is 8 times more potent than 1 (Table 1). Another modification was the introduction of small substituents to the amide group (**4–7** in Table 1). The cyclopropyl group was identified as the optimal group to yield **7**, which disrupted the β-catenin/BCL9 interaction with a K_i of 2.7 μM and is 2-fold more potent than **3**.

Further optimization was focused on the isopropyl group on the benzyl ring in Table 1. Different groups (**8–18**) including heterocycles were investigated, and 1*H*-pyrazol was found to be most suitable for this position. Compound **15** (**ZW4864**) inhibited β-catenin/BCL9 PPI with a K_i of 0.76 μM and is 3.5-fold more potent than 7. The importance of the 1*H*-pyrazol group was also demonstrated by analogues **17** and **18**, which displayed the K_is of 8.0 and 68 μM and were 10- and 89-fold less potent than **ZW4864**, respectively. The enantiomer (**16**) of **ZW4864** was synthesized. Consistent with the **1/2** pair, compound **16** disrupted β-catenin/BCL9 PPI with a K_i of 32 μM and is much less potent than **ZW4864**. The importance of the piperazine moiety was investigated by designing analogues **19** and **20**, both of which displayed low inhibitory activities with the K_is of 32 and 43 μM, respectively.

We also developed an orthogonal surface plasmon resonance (SPR) assay to assess β-catenin/BCL9 competitive inhibition. As shown in Figure 2A, **ZW4864** disrupted the β-catenin/BCL9 PPI with an IC_{50} of 1.2 μM. Our structure–activity relationship (SAR) studies revealed that compounds with the linear *N*-alkyl substituents, such as **21** with an *N*-ethyl group and **22** with an *N*-ethoxyethyl group in Figure 2B, maintained low μM inhibitory affinities. Biotinylated **ZW4864** (**Biotin-ZW4864** in Figure 2C) was synthesized and its binding affinity with the purified full-length β-catenin was determined by AlphaScreen

Author Manuscript Author Manuscript Author Manuscript Author Manuscript

saturation binding assays. As shown in Figure S3, the AlphaScreen K_D between **Biotin-ZW4864** and β-catenin is 0.77 ± 0.063 μM and comparable with AlphaScreen competitive inhibition assay results of **ZW4864** in Table 1. **Biotin-ZW4864** was incubated with the purified full-length β-catenin or SW480 cell lysates. The proteins that bound with **Biotin-ZW4864** were "pulled down" by streptavidin-conjugated beads and examined by Western blot using the β-catenin-specific antibody. As shown in Figure 2D, **Biotin-ZW4864** bound with the purified full-length β-catenin in a concentration-dependent manner starting at 1 μM. **Biotin-ZW4864** can also effectively bind with β-catenin in SW480 cell lysates at 10 μM (Figure 2D, lower panel). These pull-down experiments demonstrated that **ZW4864** can directly bind with full-length β-catenin. On the other hand, **Biotin-ZW4864** did not pull down β-catenin R1C (residues 138–781) at 10 μM, indicating that the N-terminal disordered region of β-catenin participated in **ZW4864** binding (Figure 2E, upper panel). **Biotin-ZW4864** pulled down β-catenin R1C when its concentration was increased to 50 μM (Figure 2E, lower panel). This result was confirmed by AlphaScreen competitive inhibition assays (Figure 2F). **ZW4864** disrupted the β-catenin R1C/BCL9 PPI with a K_i of 8.9 μM, which is 10-fold higher than that of the full-length β-catenin/BCL9 PPI.

Because the PPI interface of β-catenin for interacting with BCL9 also binds with E-cadherin region V and the formation of β-catenin/E-cadherin complex is essential for cell–cell adhesion, **ZW4864** was assessed for its inhibitory selectivity for β-catenin/BCL9 over β-catenin/E-cadherin PPIs using AlphaScreen selectivity assays.[44] Noting the importance of β-catenin N-terminal disordered region (residues 1–137) in developing β-catenin/BCL9 inhibitors, we have modified our AlphaScreen selectivity assays[44] to include this β-catenin region. The K_D values between full-length wild-type β-catenin and wild-type BCL9 HD2 peptide (residues 350–375) in fluorescence anisotropy (FA) and AlphaScreen competitive binding experiments are 0.27 and 0.23 μM, respectively, which match the result of ITC studies[13] and are consistent with the K_D values we previously obtained using two β-catenin truncates (residues 138–686 or residues 138–781).[44] The K_D values between wild-type β-catenin (residues 1–686) and wild-type E-cadherin peptide (residues 824–877) in FA binding and AlphaScreen competitive binding assays are 80 and 67 nM, respectively, which are consistent with the K_D values obtained from ITC studies[46,47] or the previous FA and AlphaScreen studies using β-catenin truncates (residues 138–686 or residues 138–781).[44] This AlphaScreen selectivity assay system was employed to examine the selectivity of β-catenin/BCL9 inhibitors. The data in Figure 2G demonstrated that **ZW4864** exhibited a 229-fold selectivity for β-catenin/BCL9 over β-catenin/E-cadherin PPIs.

Cell-Based Activities of ZW4864 for Inhibition of β-catenin/BCL9 Interaction and β-Catenin-Dependent Transcription.

Both BCL9 and BCL9L use their HD2 domain to bind with the N-terminal domain of β-catenin armadillo repeats, as illustrated in Figure 3A. The homology domain 1 (HD1) of BCL9 or BCL9L binds with the PHD finger of Pygo, which regulates transcription of β-catenin target genes. Cell-based coimmunoprecipitation (co-IP) assays were performed to evaluate effects of **ZW4864 (15)** on disruption of the β-catenin/BCL9 interaction in HCT116 cells. As shown in Figure 3B, **ZW4864** disrupted the β-catenin/BCL9 interaction in a concentration-dependent manner, while input and immunoprecipitation controls were

Author Manuscript Author Manuscript Author Manuscript Author Manuscript

unchanged in the experiments. The parallel study revealed that the β-catenin/E-cadherin interaction was not affected by **ZW4864** at the highest concentrations used, demonstrating its cell-based selectivity for β-catenin/BCL9 over β-catenin/E-cadherin PPIs. Cell-based co-IP experiments in Figure 3C showed that **ZW4864** did not affect the interaction between BCL9 and Pygo but disrupted the association of β-catenin with Pygo, suggesting that **ZW4864** selectively disrupts the β-catenin/BCL9 interaction in the β-catenin–BCL9–Pygo complex.

Wnt-specific TOPFlash/FOPFlash luciferase reporter assays were performed to evaluate effects of **ZW4864** on β-catenin-dependent transcriptional activity using three cell lines, HEK293 cells transfected with pcDNA3.1–β-catenin to activate β-catenin signaling, colorectal cancer SW480 cells, and Wnt 3a-stimulated triple-negative breast cancer (TNBC) MDA-MB-468 cells. The firefly luciferase reporter gene was placed downstream of three wild-type TCF binding sites in the TOPFlash reporter construct and of three mutant TCF binding sites in the FOPFlash reporter construct. The firefly luciferase expression in TOPFlash assays is controlled by three tandem TCF binding sites. The Wnt/β-catenin signaling independent renilla luciferase reporter (pCMV-RL) was applied as the internal control to eliminate systematic errors, such as cell viability and transfection effects, and normalize luciferase reporter signals. As shown in Figure 3D, **ZW4864** suppressed TOPFlash luciferase activities in β-catenin-expressing HEK293 cells in a dose-dependent manner with an IC_{50} of 11 μM. The negative control, compound **19**, did not show any activity at 200 μM. **ZW4864** also dose-dependently suppressed the TOPFlash luciferase activities in SW480 and Wnt 3a-activated MDA-MB-468 cells with the IC_{50}s of 7.0 and 6.3 μM, respectively. The inhibitory activities of **ZW4864** in TOPFlash luciferase reporter assays were comparable with that of **ICG-001**, a compound that was reported to bind CBP and disrupt CBP/β-catenin PPI[48] (the IC_{50}s of **ICG-001** were 4.9 and 11 μM for SW480 and Wnt 3a-activated MDA-MB-468 cells, respectively). FOPFlash luciferase reporter assays revealed that **ZW4864** did not show obvious inhibitory activity up to 25 μM in all these three cell lines (Figure 3E), indicating that **ZW4864** selectively suppresses transactivation of β-catenin signaling.

Effects of **ZW4864** on the transcription of Wnt-specific target gene *Axin2* and other Wnt target genes *CCND1* (cyclin D1 gene), *LEF1*, and *BCL9L* were assessed. Quantitative realtime PCR (qPCR) experiments showed that **ZW4864** suppressed the transcription of these β-catenin target genes in a concentration-dependent manner without affecting the expression of *HPRT*, a house-keeper gene, in both SW480 and Wnt 3a-activated MDA-MB-231 cells (Figure 3F). Consistent with the results of qPCR studies, Western blot experiments showed that the expression levels of proteins Axin2 and cyclin D1 were also substantially decreased after **ZW4864** treatment without affecting the internal control β-tubulin in SW480 and Wnt 3a-activated MDA-MB-231 cells (Figure 3G).

Figure 3H shows the IC_{50} values of the 3-day MTS cell growth inhibition assay results of **ZW4864** and control compounds. **ZW4864** inhibited the growth of TNBC cells with hyperactive β-catenin signaling, while transfection of constitutively active β-catenin to these TNBC cells rescued the inhibitory effects of **ZW4864** (Figure 3I), demonstrating on-target effects of **ZW4864**.[49] **ZW4846** also inhibited colony formation in TNBC cells (Figure

Author Manuscript Author Manuscript Author Manuscript Author Manuscript

3J). Fluorescence-activated cell sorting (FACS) analyses revealed that **ZW4864** treatment selectively triggered rapid apoptosis of TNBC cells with hyperactive β-catenin signaling while sparing normal mammary epithelial MCF10A cells, as shown in Figure 3K,L.

Drug Metabolism and Pharmacokinetic (DMPK) Properties of ZW4864.

ZW4864 (15) displays great aqueous solubility >3 mM, and **ZW4864** at 2 mg/mL was completely soluble in saline (0.9% NaCl), EtOH/saline (5/95), or DMSO/Tween-80/H_2O (10/10/80). Hepatic microsomal stability of **ZW4864** and **21** was evaluated. As shown in Table 2A, these two compounds have moderate microsomal stability similar to the marketed drug, sunitinib. **ZW4864** was then advanced for PK studies using C57BL/6 mice. As shown in Table 2B, **ZW4864** exhibited good PK properties with an oral bioavailability (F) of 83%.

Inhibitory Effects of ZW4864 on Migration and Invasion of Cancer Cells Induced by β-Catenin Signaling.

β-Catenin signaling plays a key role in inducing and maintaining invasion and metastasis of cancer cells including TNBC cells. β-Catenin signaling activates the expression of the EMT-promoting genes, such as *Twist*[50] and *Snail*,[51,52] to induce and maintain breast cells in the mesenchymal and stem cell states[53] and cause breast cancer cell invasion and metastasis.[54,55] β-Catenin signaling also upregulates the expression of metastasis-associated genes such as *tenascin C*.[56,57] TNBC cells express tenascin C as a metastatic niche component to establish lung metastasis.[57] *LGR5* is a marker of adult stem cells and the target gene of β-catenin signaling.[58,59] It maintains stem-like properties of cancer cells including TNBC cells.[60–62] As shown in Figure 4A, disruption of β-catenin/BCL9 interaction with **ZW4864** dramatically suppressed the expression of β-catenin target genes that are associated with TNBC metastasis and EMT. **ZW4864** suppressed MDA-MB-231 cell migration in a dose-dependent manner in scratch wound healing assays (Figure 4B). As shown in Figure 4C, **ZW4864** at 20 μM reduced the Matrigel-coated transwell invasion of MDA-MB-231 cells to 13% of the DMSO-treated control. Figure 4D shows the 96-well three-dimensional (3D) spheroid cell invasion assay of **ZW4864**. The use of basement membrane extracts (BMEs) resulted in a larger invasion area of MDA-MB-231 cells on day 6. The use of **ZW4864** suppressed MDA-MB-231 cell invasion in a dose-dependent manner.

Pharmacodynamic (PD) Properties of ZW4864 in the Patient-Derived TNBC Xenograft Mouse Model.

To test the in vivo antitumor effects of **ZW4864**, we used a patient-derived xenograft (PDX) model, PDX 4013, derived from a TNBC patient that had limited response to treatment with dasatinib and docetaxel.[63] The 4013 cells were implanted into the mammary fat pad of immunocompromised SCID/Beige mice. The hyperactive β-catenin signaling circuit drives the metastatic cascade of this clinically relevant TNBC model.[64] We tested 90 mg/kg dose given orally in saline daily to mice with PDX 4013 tumors (~200 mm^3, $n = 4$) grown orthotopically for 5 days. The tumor tissue was collected 3 h after the last dose to assess the PD properties of the compound. The results showed a variation in tumor growth in mice that were treated with **ZW4864** compared to those treated only with vehicle, while no significant decrease in weight or major toxicity issues were observed over the treatment (Figure 5A,B).

Author Manuscript Author Manuscript Author Manuscript Author Manuscript

Moreover, we observed significant decreases in the expression of key β-catenin target genes in tumors treated with **ZW4864** vs vehicle-treated tumors (Figure 5C). Collectively, these data support on-target effects and the promising antitumor effect of **ZW4864** and grant development of specific antitumor efficacy studies with our β-catenin inhibitors.

Chemistry.

Scheme 1 shows the synthetic route for 1–2. The key intermediate 23 was obtained by the nucleophilic substitution reaction between 3-bromophenol and *tert*-butyl 2-bromo-2-methylpropanoate. The amide bond coupling reaction between *(R)*- or *(S)*-1-(*tert*-butoxycarbonyl)piperidine-3-carboxylic acid and (4-isopropylphenyl)methanamine generated intermediates **24a** and **24b**, which underwent Boc deprotection and Buchwald–Hartwig amination reactions with **23** to yield **25a** and **25b**. Removal of the *tert*-butyl group of 25a and 25b by TFA in CH_2Cl_2 solution offered final products **1** and **2**.

Scheme 2 shows the synthetic route for 3–7. The amide bond coupling between *(R)*-1-(*tert*-butoxycarbonyl)piperidine-3-carboxylic acid and (4-isopropylphenyl)methanamine derivatives offered intermediates **24a** and **26**. Compounds **24a** and **26** went through Boc deprotection and Buchwald–Hartwig amination reactions with **23** to yield **25a** and **27**. Removal of the *tert*-butyl groups in **25a** and **27** by TFA in CH_2Cl_2 solution and then condensation with *tert*-butyl piperazine-1-carboxylate provided **28**, Boc deprotection of which under the acidic condition offered final products 3–7.

The synthetic route for **8–15**, **17**, and **18** is illustrated in Scheme 3. The Buchwald–Hartwig amination reaction between compound **23** and ethyl *(R)*-piperidine-3-carboxylate produced intermediate 29. Removal of the *tert*-butyl group of **29** and then coupling with *tert*-butyl piperazine-1-carboxylate produced **30**. Hydrolysis of **30** and condensation with *N*-benzylcyclopropanamine derivatives yielded **31**, which went through the Boc deprotection reaction to afford final compounds **8–10** and **12–14**.

Hydrolysis of **30** and then condensation with *N*-(4-bromobenzyl)cyclopropanamine yielded **32**, which went through the Suzuki coupling reaction with various boronic acids to afford **33**. Deprotection of the Boc protecting group of **33** produced final products **11, 15, 17**, and **18**.

The route for synthesis of **19** and **20** is described in Scheme 4. Removal of the *tert*-butyl in **29** and then condensation with 1-methylpiperazine or piperidine produced intermediate **34**. Hydrolysis of **34** and then condensation with *N*-(4-bromobenzyl)cyclopropanamine yielded **35**, which underwent the Suzuki coupling reaction with (1*H*-pyrazol-4-yl)boronic acid to afford final products **19** and **20**.

The route for synthesis of **21** and **22** is shown in Scheme 5. Hydrolysis of **30** and then condensation with (4-bromophenyl)methanamine derivatives yielded **36**, which was coupled with (1*H*-pyrazol-4-yl)boronic acid by the Suzuki reaction to produce intermediate **37**. Removal of the Boc protecting group of **37** under the acidic condition afforded final compounds **21** and **22**.

Author Manuscript Author Manuscript Author Manuscript Author Manuscript

The route for the synthesis of **16** is described in Scheme 6. The Buchwald–Hartwig amination reaction between **23** and ethyl (*S*)-piperidine-3-carboxylate produced **38**. Removal of *tert*-butyl of **38** and then condensation with *tert*-butyl piperazine-1-carboxylate produced **39**. Hydrolysis of **39** and condensation with *N*-benzylcyclopropanamine derivatives yielded **40**, which went through Suzuki coupling with (1-pyrazol-4-yl)boronic acid and the Boc deprotection reaction to afford the final compound **16**.

Scheme 7 shows the synthetic route for **Biotin-ZW4864**. The reductive-amination reaction between 4-bromobenzaldehyde and benzyl (2-(2-(2-aminoethoxy)ethoxy)ethyl)carbamate produced intermediate **42**, which was condensed with (*R*)-1-(3-((1-(4-(*tert*-butoxycarbonyl)piperazin-1-yl)-2-methyl-1-oxopropan-2-yl)oxy)phenyl)piperidine-3-carboxylic acid to yield **43**. Compound **43** was coupled with (1-trityl-1*H*-pyrazol-4-yl)boronic acid using the Suzuki reaction to give **44**, which went through the Cbz deprotection and then the coupling reaction with Biotin-*N*-hydroxysuccinimide (Biotin-NHS) to yield **45**. Deprotection of Boc and trityl protecting groups of **45** under the acidic condition and then putting back the Boc protecting group resulted in **46**, which afforded the final product after applying 10% TFA in CH_2Cl_2.

DISCUSSION AND CONCLUSIONS

There is compelling evidence that dysregulation of the β-catenin signaling circuit plays a key role in initiation and progression of many cancers. However, development of small-molecule PPI disruptors that directly bind with β-catenin has been highly challenging. Herein, we described **ZW4864**, a small molecule that selectively disrupts the β-catenin/BCL9 PPI without interfering the β-catenin/E-cadherin PPI. Using pull-down assays, co-IP experiments, and β-catenin rescue experiments, we provide evidence that **ZW4864** binds directly with β-catenin and selectively disrupts the β-catenin/BCL9 PPI in both the protein level and the cellular context. **ZW4864** also suppresses transactivation of β-catenin signaling and downregulates the transcription and expression of oncogenic β-catenin target genes in vitro and in vivo in a dose-dependent manner. This compound selectively suppresses growth and promotes apoptosis of cancer cells with hyperactive Wnt/β-catenin signaling. It is worth noting that the only other β-catenin/BCL9 inhibitor that has been characterized in vivo is the natural product carnosic acid, although its catechol group is known as a substructure of pan-assay interference compounds (PAINS). **ZW4864** is orally bioavailable with high tolerability in mice. In a therapy-resistant TNBC PDX model, **ZW4864** showed promising therapeutic effects. Importantly, **ZW4864** displayed on-target activity in vivo in our 5 day assay and in the long efficacy experiment, as observed in the reduced expression of β-catenin target genes. Therefore, **ZW4864** represents a better chemical probe to explore β-catenin-related biology and a drug-like small-molecule β-catenin/BCL9 inhibitor for further drug development.

It is worth noting that the N-terminal disordered region of β-catenin (residues 1–137) was found to be important for **ZW4864** binding. **Biotin-ZW4864** pulled down the full-length β-catenin at 1 μM, and **ZW4864** displayed a K_i of 0.76 μM in the full-length β-catenin/BCL9 AlphaScreen assay. However, **Biotin-ZW4864** was not able to pull down β-catenin R1C (residues 138–781) even at 10 μM, and **ZW4864** showed an increased K_i of 8.9 μM to

Author Manuscript Author Manuscript Author Manuscript Author Manuscript

disrupt β-catenin R1C/BCL9 PPI in AlphaScreen assays. These data indicate that full-length β-catenin should be taken into consideration when developing β-catenin/BCL9 inhibitors or biochemical assays to evaluate β-catenin/BCL9 inhibitors.

EXPERIMENTAL SECTION

Chemical Synthesis.

All reagents were purchased from commercial sources and used as received. ^{1}H NMR and ^{13}C NMR spectra were recorded on Bruker AVANCE III HD 500 (500 MHz) spectrometers (125.7 MHz for ^{13}C NMR spectra) in $CDCl_3$, DMSO-d_6, acetone-d_6, and CD_3OD. Chemical shifts were reported as values in parts per million (ppm), and the reference resonance peaks were set at 7.26 ppm ($CHCl_3$), 3.31 ppm (CD_2HOD), 2.50 ppm [$(CD_2H)_2SO$], and 2.05 ppm [$(CD_2H)_2CO$] for ^{1}H NMR spectra and 77.23 ppm ($CDCl_3$), 49.00 ppm (CD_3OD), 39.52 ppm (DMSO-d_6), and 29.84 ppm (acetone-d_6) for ^{13}C NMR spectra. Low-resolution mass spectra were determined on an Agilent 6120 single quadrupole MS with a 1220 infinity LC system (high-performance liquid chromatography-mass spectrometry (HPLC-MS)) and an electrospray ionization (ESI) source. High-resolution mass spectra were determined on an Agilent G6230BA TOF LC-MS Mass Spectrometer with a TOF mass detector. Thin-layer chromatography was carried out on E. Merck precoated silica gel 60 F254 plates with a UV–visible lamp. Column chromatography was performed with SilicaFlash@F60 (230–400 mesh). The purity of the final compounds was determined by HPLC analyses. The instrument was an Agilent 1260 Infinity II HPLC system with a quaternary pump, a vial sampler, and a DAD detector. A Kromasil 300–5-C18 column (4.6 × 250 mm^2) was used. The DAD detector was set to 254 nm. The purity of all tested compounds was >95%.

General Procedure for Amide Bond Coupling Reaction.—At 0 °C, to a suspension of carboxylic acid (1 mmol), amine (1.1 mmol), and 1-[bis(dimethylamino)methylene]-1*H*-1,2,3-triazolo[4,5-*b*]pyridinium 3-oxide hexafluorophosphate (HATU) (1.5 mmol) in dichloromethane (CH_2Cl_2) (10 mL) was added *N*,*N*-diisopropylethylamine (DIPEA) (2 mmol) dropwise. The reaction mixture was warmed to room temperature and stirred overnight. After completion of the reaction, more CH_2Cl_2 was added. The organic phase was washed with 1 M HCl, saturated $NaHCO_3$, and brine, dried over anhydrous Na_2SO_4, and concentrated under reduced pressure. Column chromatography was used to purify the target compound.

General Procedure for Suzuki Coupling Reaction.—To a solution of bromobenzene derivatives (1 mmol) in dioxane/water (12/4 mL) were added boronic acid (1.2 mmol), $Pd(PPh_3)_4$ (0.1 mmol), and K_2CO_3 (2 mmol). The reaction mixture was heated to 90 °C under argon and stirred overnight. The reaction mixture was cooled to room temperature, concentrated under reduced pressure, then redissolved with ethyl acetate, washed with water and brine, and dried over Na_2SO_4. The solution obtained was concentrated under vacuum. The residue was purified by column chromatography to yield the target compound.

General Procedure for Buchwald–Hartwig Amination Reaction.—A solution of bromobenzene derivatives (1 mmol), amine (1.1 mmol), $Pd_2(dba)_3$ (0.1 mmol), Ruphos (0.2

Author Manuscript Author Manuscript Author Manuscript Author Manuscript

mmol), and Cs_2CO_3 (2 mmol) in dioxane (10 mL) was heated to 80 °C under argon and stirred overnight. The reaction mixture was cooled to room temperature. The solid was removed, and the filtrate was concentrated under reduced pressure and purified by column chromatography to yield the target compound.

General Procedure for Deprotection of Boc Using 4 M HCl in Dioxane.—At 0 °C, 4 M HCl (8 mL) in dioxane was added to Boc-protected amine (1 mmol) in a 20 mL vial. The reaction was kept at 0 °C for 2 h. Upon completion, the solvent was removed under reduced pressure. Dioxane residue was removed by evaporation with additional methanol twice. Then, water (HPLC grade) was added and dried over a Labconco lyophilizer.

General Procedure for Deprotection of Boc Using 10% Trifluoroacetic Acid (TFA) in CH_2Cl_2.—To Boc-protected amine (1 mmol) in 10 mL of CH_2Cl_2 at room temperature was added TFA (1 mL). The reaction was stirred at room temperature for 6 h. TFA was removed by adding CH_2Cl_2 three times to afford the desired product. Then, water (HPLC grade) was added and dried over a Labconco lyophilizer.

General Procedure for Deprotection of tert-Butyl and Boc Using 50% TFA in CH_2Cl_2.—At 0 °C, to a solution of the *tert*-butyl ester or Boc-protected amine (1 mmol) in CH_2Cl_2 (5 mL) was added TFA (5 mL) dropwise. The reaction was stirred at 0 °C for 6 h. Upon completion, the solvent was removed under reduced pressure. TFA was removed by adding CH_2Cl_2 three times to afford the desired product, which was used directly in the next step.

General Procedure for Hydrolysis of Ethyl Ester.—To a solution of ethyl ester (1 mmol) in THF (4 mL) and methanol (2 mL) was added a solution of LiOH (2 mmol) in H_2O (1 mL). The mixture was stirred at room temperature for 3 h. After completion of the reaction, the solvent was removed under reduced pressure. The residue was redissolved in H_2O and acidified using 1 M HCl. Ethyl acetate was added, and the organic phase was washed with brine, dried over anhydrous Na_2SO_4, and concentrated under reduced pressure to yield the target compound, which was used directly in the next step.

General Procedure for Reductive-Amination Reaction.—A solution of aldehyde (1 mmol) and amine (2 mmol) in anhydrous methanol (5 mL) was stirred under Ar at room temperature overnight. Then, $NaBH_4$ (1.5 mmol) was added portionwise to the mixture at 0 °C. The mixture was stirred at 0 °C for 1 h. Saturated NH_4Cl was added, followed by addition of ethyl acetate. The organic phase was collected and washed with brine, dried over anhydrous Na_2SO_4, concentrated under reduced pressure, and purified by column chromatography to yield the target compound.

General Procedure for Boc-Protection Reaction.—To a solution of amine (1 mmol) in CH_2Cl_2 (10 mL) were added $(Boc)_2O$ (1.5 mmol) and triethylamine (Et_3N) (2 mmol). The mixture was stirred at room temperature for 2 h. After completion of the reaction, the mixture was concentrated under reduced pressure and purified by column chromatography to yield the target compound.

Author Manuscript Author Manuscript Author Manuscript Author Manuscript

General Procedure for Deprotection of the Cbz Group.—To the solution of the Cbz-protected amine (1 mmol) in methanol (10 mL) was added 10% Pd/C under Ar. The mixture was stirred overnight at room temperature under H_2. The resulting product was collected by removal of the Pd/C catalyst and used directly in the next step.

General Procedure for Reaction between Amine and (+)-Biotin-N-Hydroxysuccinimide Ester (NHS-Biotin).—To a solution of amine (1 mmol) in dimethylformamide (DMF) (10 mL) were added NHS-Biotin (1 mmol) and DIPEA (2 mmol) under Ar. The mixture was stirred overnight. After completion of the reaction, DMF was evaporated and water and ethyl acetate were added. The organic phase was collected and washed with brine, dried over anhydrous Na_2SO_4, and purified by column chromatography to yield the target compound.

Synthesis of tert-Butyl 2-(3-Bromophenoxy)-2-methylpropanoate.—A solution of 3-bromophenol (1 mmol), *tert*-butyl 2-bromo-2-methylpropanoate (5 mmol), K_2CO_3 (4 mmol), and $MgSO_4$ (1 mmol) in DMF was stirred at 100 °C overnight. The DMF was removed under reduced pressure. Water and ethyl acetate were added. The obtained organic phase was washed with brine, dried over Na_2SO_4, and concentrated under vacuum. The residue was purified by column chromatography to yield the target compound.

(*R*)-2-(3-(3-((4-Isopropylbenzyl)carbamoyl)piperidin-1-yl)phenoxy)-2-methylpropanoic Acid (1).—^{1}H NMR (500 MHz, chloroform-d) δ 7.17 (d, J = 1.5 Hz, 4H), 7.08 (t, J = 8.3 Hz, 1H), 6.91 (t, J = 5.8 Hz, 1H), 6.63 (d, J = 5.8 Hz, 2H), 6.50 (d, J = 8.1 Hz, 1H), 4.56−4.28 (m, 2H), 3.50−3.33 (m, 1H), 3.28 (dt, J = 10.3, 4.4 Hz, 1H), 3.19 (dd, J = 12.4, 8.6 Hz, 1H), 3.08−2.92 (m, 1H), 2.94−2.78 (m, 1H), 2.65 (dq, J = 9.5, 4.8, 4.3 Hz, 1H), 1.90−1.65 (m, 4H), 1.57 (d, J = 2.7 Hz, 6H), 1.22 (dd, J = 6.9, 1.5 Hz, 6H). ^{13}C NMR (126 MHz, chloroform-*d*) δ 176.6, 173.9, 156.0, 148.2, 135.4, 129.7, 127.7, 126.8, 113.1, 112.1, 109.6, 79.7, 53.4, 51.4, 43.2, 41.9, 33.8, 26.9, 25.20, 25.16, 24.0, 23.1. HRMS (ESI) calcd for $C_{26}H_{34}N_2O_4$ $(M - H)^-$ 437.2446, found 437.2443. HPLC purity 98.6%, t_R = 12.48 min.

(*S*)-2-(3-(3-((4-Isopropylbenzyl)carbamoyl)piperidin-1-yl)phenoxy)-2-methylpropanoic Acid (2).—^{1}H NMR (500 MHz, methanol-d_4) δ 7.19 (d, J = 1.0 Hz, 4H), 7.09 (t, J = 8.2 Hz, 1H), 6.68−6.62 (m, 1H), 6.53 (t, J = 2.3 Hz, 1H), 6.38 (dd, J = 8.1, 2.2 Hz, 1H), 4.48−4.23 (m, 2H), 3.62 (ddt, J = 12.2, 3.5, 1.6 Hz, 1H), 3.53 (ddt, J = 12.5, 3.7, 2.1 Hz, 1H), 3.02−2.82 (m, 2H), 2.81−2.71 (m, 1H), 2.59 (ddd, J = 10.5, 6.7, 3.7 Hz, 1H), 2.00−1.90 (m, 1H), 1.80 (qd, J = 7.2, 3.4 Hz, 1H), 1.73−1.62 (m, 2H), 1.54 (s, 6H), 1.22 (d, J = 7.0 Hz, 6H). ^{13}C NMR (126 MHz, methanol-d_4) δ 175.1, 156.4, 152.5, 147.7, 136.0, 129.0, 127.2, 126.1, 111.0, 110.6, 108.4, 78.8, 52.6, 50.0, 42.6, 42.3, 33.7, 27.4, 24.42, 24.37, 23.8, 23.1. HRMS (ESI) calcd for $C_{26}H_{34}N_2O_4$ $(M - H)^-$ 437.2446, found 437.2443. HPLC purity 98.9%, t_R = 12.51 min.

(*R*)-*N*-(4-Isopropylbenzyl)-1-(3-((2-methyl-1-oxo-1-(piperazin-1-yl)propan-2-yl)oxy)phenyl)piperidine-3-carboxamide (3 as HCl Salt).—^{1}H NMR (500 MHz, methanol-d_4) δ 7.52 (t, J = 8.3 Hz, 1H), 7.43−7.33 (m, 1H), 7.32−7.12 (m, 5H), 6.99 (dd, J = 8.4, 2.2 Hz, 1H), 4.37 (q, J = 14.8 Hz, 2H), 4.02 (d, J = 117.9 Hz, 4H), 3.71(td,

Author Manuscript Author Manuscript Author Manuscript Author Manuscript

J = 11.0, 10.0, 5.5 Hz, 3H), 3.55 (d, J = 8.1 Hz, 1H), 3.25−2.82 (m, 6H), 2.13 (q, J = 12.4, 11.3 Hz, 3H), 1.92 (s, 1H), 1.68 (d, J = 1.0 Hz, 6H), 1.22 (d, J = 6.9 Hz, 6H). ^{13}C NMR (126 MHz, methanol-d_4) δ 171.5, 156.3, 147.9, 143.9, 135.7, 131.4, 127.3, 126.2, 117.8, 114.2, 111.1, 81.7, 57.5, 43.1, 42.5, 39.6, 33.7, 25.3, 24.9, 24.7, 23.0, 21.9. HRMS (ESI) calcd for $C_{30}H_{42}N_4O_3$ $(M + Na)^+$ 529.3149, found 529.3140. HPLC purity 97.6%, t_R = 10.96 min.

(*R*)-*N*-(4-Isopropylbenzyl)-*N*-methyl-1-(3-((2-methyl-1-oxo-1-(piperazin-1-yl)propan-2-yl)oxy)phenyl)piperidine-3-carboxamide (4 as HCl Salt).—^{1}H NMR (500 MHz, methanol-d_4) δ 7.47 (dt, J = 25.8, 8.2 Hz, 1H), 7.38−7.01 (m, 6H), 6.90 (d, J = 30.1 Hz, 1H), 4.75−4.50 (m, 2H), 4.02 (d, J = 122.4 Hz, 4H), 3.78−3.41 (m, 5H), 3.25−2.87 (m, 8H), 2.20−1.79 (m, 4H), 1.70−1.65 (m, 6H), 1.24 (dd, J = 6.9, 3.5 Hz, 6H). ^{13}C NMR (126 MHz, methanol-d_4) δ 171.7, 171.6, 156.3, 148.5, 148.2, 134.1, 131.3, 127.6, 126.7, 126.5, 126.4, 81.6, 52.7, 50.3, 43.1, 34.1, 33.7 (d, J = 2.2 Hz), 33.2, 24.9, 24.8, 24.7, 23.01, 23.00. HRMS (ESI) calcd for $C_{31}H_{44}N_4O_3$ $(M + H)^+$ 521.3486, found 521.3478. HPLC purity 100%, t_R = 11.37 min.

(*R*)-*N*-Ethyl-*N*-(4-isopropylbenzyl)-1-(3-((2-methyl-1-oxo-1-(piperazin-1-yl)propan-2-yl)oxy)phenyl)piperidine-3-carboxamide (5 as HCl Salt).—^{1}H NMR (500 MHz, methanol-d_4) δ 7.48 (dt, J = 17.8, 8.1 Hz, 1H), 7.40−7.08 (m, 6H), 6.91 (s, 1H), 4.79−4.36 (m, 2H), 4.03 (d, J = 121.8 Hz, 4H), 3.78−3.34 (m, 7H), 3.27−2.79 (m, 5H), 2.30−1.74 (m, 4H), 1.68 (d, J = 3.3 Hz, 6H), 1.30−1.11 (m, 9H). ^{13}C NMR (126 MHz, methanol-d_4) δ 171.62, 171.61, 156.3, 148.5, 148.0, 134.6, 134.1, 131.3, 131.2, 127.4, 126.6, 126.6, 126.3, 113.9, 81.6, 81.5, 54.8, 50.3, 43.1, 42.7, 41.9, 41.2, 39.6, 33.7, 24.9, 24.80, 24.79, 23.04, 23.03, 21.9, 13.1, 11.4. HRMS (ESI) calcd for $C_{32}H_{46}N_4O_3$ $(M + H)^+$ 535.3643, found 535.3640. HPLC purity 98.0%, t_R = 11.55 min.

(*R*)-*N*-Isopropyl-*N*-(4-isopropylbenzyl)-1-(3-((2-methyl-1-oxo-1-(piperazin-1-yl)propan-2-yl)oxy)phenyl)piperidine-3-carboxamide (6 as HCl Salt).—^{1}H NMR (500 MHz, methanol-d_4) δ 7.46 (dt, J = 35.6, 8.2 Hz, 1H), 7.21 (d, J = 133.2 Hz, 6H), 7.00−6.79 (m, 1H), 4.73−4.57 (m, 2H), 4.50−4.35 (m, 1H), 4.03 (d, J = 124.8 Hz, 4H), 3.81−3.32 (m, 5H), 3.22−2.86 (m, 5H), 2.25−1.77 (m, 4H), 1.67 (t, J = 1.6 Hz, 6H), 1.27−1.13 (m, 12H). ^{13}C NMR (126 MHz, methanol-d_4) δ 171.7, 171.6, 156.3, 156.2, 148.1, 147.2, 136.2, 135.5, 131.3, 131.1, 126.6, 126.3, 126.0, 114.0, 113.4, 110.8, 81.6, 81.4, 54.8, 49.3, 46.2, 43.3, 43.1, 42.7, 39.5, 33.64, 33.62, 24.9, 24.83, 24.77, 23.10, 23.06, 20.6, 20.2, 19.1, 18.9. HRMS (ESI) calcd for $C_{33}H_{48}N_4O_3$ $(M + H)^+$ 549.3799, found 549.3790. HPLC purity 100%, t_R = 12.33 min.

(*R*)-*N*-Cyclopropyl-*N*-(4-isopropylbenzyl)-1-(3-((2-methyl-1-oxo-1-(piperazin-1-yl)propan-2-yl)oxy)phenyl)piperidine-3-carboxamide (7 as HCl Salt).—^{1}H NMR (500 MHz, methanol-d_4) δ 7.45 (d, J = 8.4 Hz, 1H), 7.34−7.02 (m, 6H), 6.87 (s, 1H), 4.47−4.38 (m, 1H), 4.21−3.84 (m, 5H), 3.76−3.38 (m, 5H), 3.26−2.67 (m, 6H), 2.22−1.73 (m, 4H), 1.67 (d, J = 2.4 Hz, 6H), 1.23 (d, J = 6.9 Hz, 6H), 1.09−0.64 (m, 4H). ^{13}C NMR (126 MHz, methanol-d_4) δ 171.71, 156.26, 147.81, 135.17, 131.09, 127.16, 126.63, 126.24, 81.45, 49.34, 43.13, 33.67, 29.81, 24.90, 24.78, 23.04, 9.17, 7.36. HRMS (ESI) calcd for $C_{33}H_{46}N_4O_3$ $(M + H)^+$ 547.3643, found 547.3646. HPLC purity 100%, t_R = 12.15 min.

Author Manuscript Author Manuscript Author Manuscript Author Manuscript

(*R*)-*N*-(4-(*tert*-Butyl)benzyl)-*N*-cyclopropyl-1-(3-((2-methyl-1-oxo-1-(piperazin-1-yl)propan-2-yl)oxy)phenyl)piperidine-3-carboxamide (8 as HCl Salt).— ^{1}H NMR (500 MHz, methanol-d_4) δ 7.54 (t, J = 8.3 Hz, 1H), 7.47−7.33 (m, 3H), 7.29 (s, 1H), 7.19 (d, J = 7.9 Hz, 2H), 7.00 (dd, J = 8.4, 2.3 Hz, 1H), 4.89 (s, 1H), 4.40 (d, J = 14.8 Hz, 1H), 4.02 (d, J = 116.9 Hz, 5H), 3.80−3.57 (m, 4H), 3.07 (d, J = 107.6 Hz, 4H), 2.84−2.74 (m, 1H), 2.38−1.79 (m, 4H), 1.68 (d, J = 2.7 Hz, 6H), 1.30 (s, 9H), 1.12−0.78 (m, 4H). ^{13}C NMR (126 MHz, methanol-d_4) δ 171.5, 156.3, 150.0, 143.9, 134.7, 131.4, 126.9, 125.1, 118.0, 114.2, 111.3, 81.7, 55.5, 49.3, 43.1, 42.6, 39.6, 33.9, 30.4, 29.8, 24.9, 24.7, 9.3, 7.2. HRMS (ESI) calcd for $C_{34}H_{48}N_4O_3$ $(M + H)^+$ 561.3799, found 561.3791. HPLC purity 100%, t_R = 12.49 min.

(*R*)-*N*-(4-Cyclohexylbenzyl)-*N*-cyclopropyl-1-(3-((2-methyl-1-oxo-1-(piperazin-1-yl)propan-2-yl)oxy)phenyl)piperidine-3-carboxamide (9 as HCl Salt).— ^{1}H NMR (500 MHz, methanol-d_4) δ 7.46 (t, J = 8.2 Hz, 1H), 7.24 (d, J = 9.8 Hz, 1H), 7.17 (s, 5H), 6.87 (s, 1H), 4.80 (s, 1H), 4.42 (d, J = 14.8 Hz, 1H), 4.25−3.83 (m, 5H), 3.73 (dd, J = 12.2, 3.6 Hz, 2H), 3.68−3.40 (m, 2H), 3.24−2.88 (m, 4H), 2.82−2.73 (m, 1H), 2.49 (ddt, J = 11.8, 8.5, 3.2 Hz, 1H), 2.21−2.01 (m, 3H), 1.89−1.72 (m, 6H), 1.67 (d, J = 2.5 Hz, 6H), 1.47−1.39 (m, 4H), 1.34−1.25 (m, 1H), 1.09−0.84 (m, 4H). ^{13}C NMR (126 MHz, methanol-d_4) δ 171.7, 156.3, 147.0, 135.2, 131.1, 127.1, 126.7, 113.6, 81.5, 49.4, 44.3, 43.1, 42.7, 34.3, 29.8, 26.6, 25.8, 24.9, 24.8, 9.2, 7.4. HRMS (ESI) calcd for $C_{36}H_{50}N_4O_3$ $(M + H)^+$ 587.3956, found 587.3948. HPLC purity 99.4%, t_R = 13.42 min.

(*R*)-*N*-([1,1′-Biphenyl]-4-ylmethyl)-*N*-cyclopropyl-1-(3-((2-methyl-1-oxo-1-(piperazin-1-yl)propan-2-yl)oxy)phenyl)piperidine-3-carboxamide (10 as HCl Salt).— ^{1}H NMR (500 MHz, methanol-d_4) δ 7.64−7.55 (m, 4H), 7.43 (dd, J = 8.3, 7.1 Hz, 3H), 7.39−6.62 (m, 6H), 4.88 (d, J = 11.1 Hz, 1H), 4.55 (d, J = 14.9 Hz, 1H), 4.28−3.79 (m, 5H), 3.74 (dt, J = 11.1, 5.4 Hz, 2H), 3.68−3.35 (m, 2H), 3.23−2.82 (m, 5H), 2.23−1.79 (m, 4H), 1.67 (d, J = 2.6 Hz, 6H), 1.12−0.79 (m, 4H). ^{13}C NMR (126 MHz, methanol-d_4) δ 171.8, 156.3, 140.6, 140.1, 137.0, 131.0, 128.5, 127.7, 127.0, 126.8, 126.5, 81.4, 49.4, 43.1, 42.7, 39.6, 29.9, 24.9, 24.8, 9.2, 7.5. HRMS (ESI) calcd for $C_{36}H_{44}N_4O_3$ $(M + Na)^+$ 603.3306, found 603.3293. HPLC purity 100%, t_R = 12.29 min.

(*R*)-*N*-Cyclopropyl-1-(3-((2-methyl-1-oxo-1-(piperazin-1-yl)propan-2-yl)oxy)phenyl)-*N*-(4-(thiophen-3-yl)benzyl)piperidine-3-carboxamide (11 as HCl Salt).— ^{1}H NMR (500 MHz, methanol-d_4) δ 7.68−7.55 (m, 3H), 7.51−7.41 (m, 3H), 7.30 (d, J = 7.9 Hz, 3H), 7.00 (d, J = 127.8 Hz, 2H), 4.87 (d, J = 12.4 Hz, 1H), 4.50 (d, J = 14.9 Hz, 1H), 4.20−3.82 (m, 5H), 3.74 (ddd, J = 12.4, 8.4, 4.0 Hz, 2H), 3.68−3.40 (m, 2H), 3.20−2.81 (m, 5H), 2.20−1.86 (m, 4H), 1.67 (d, J = 2.6 Hz, 6H), 1.10−0.88 (m, 4H). ^{13}C NMR (126 MHz, methanol-d_4) δ 171.7, 156.3, 141.7, 136.6, 134.9, 131.1, 127.7, 126.1, 126.0, 125.6, 119.9, 81.5, 49.4, 43.1, 42.7, 39.5, 29.9, 24.9, 24.8, 9.2, 7.4. HRMS (ESI) calcd for $C_{34}H_{42}N_4O_3S$ $(M + Na)^+$ 609.2870, found 609.2861. HPLC purity 99.4%, t_R = 11.90 min.

(*R*)-*N*-Cyclopropyl-1-(3-((2-methyl-1-oxo-1-(piperazin-1-yl)propan-2-yl)oxy)phenyl)-*N*-(4-(pyridin-2-yl)benzyl)piperidine-3-carboxamide (12

Author Manuscript Author Manuscript Author Manuscript Author Manuscript

as HCl Salt).—^{1}H NMR (500 MHz, methanol-d_4) δ 8.84 (dd, J = 6.0, 1.5 Hz, 1H), 8.68 (td, J = 8.0, 1.6 Hz, 1H), 8.41 (d, J = 8.2 Hz, 1H), 8.07−8.03 (m, 1H), 7.97 (d, J = 8.2 Hz, 2H), 7.61−7.50 (m, 3H), 7.50−7.27 (m, 2H), 7.02 (dd, J = 8.4, 2.3 Hz, 1H), 4.93 (s, 1H), 4.68 (d, J = 15.6 Hz, 1H), 4.36−3.85 (m, 5H), 3.84−3.66 (m, 4H), 3.27−2.88 (m, 5H), 2.36−1.83 (m, 4H), 1.68 (d, J = 2.0 Hz, 6H), 1.13−0.88 (m, 4H). ^{13}C NMR (126 MHz, methanol-d_4) δ 171.5, 156.3, 152.4, 146.9, 143.6, 143.2, 141.6, 131.5, 129.7, 128.4, 128.2, 125.9, 125.2, 118.3, 114.4, 111.5, 81.8, 57.8, 55.8, 49.7, 43.1, 42.6, 39.6, 30.3, 24.9, 24.7, 9.2, 7.3. HRMS (ESI) calcd for $C_{35}H_{43}N_5O_3$ $(M + H)^+$ 582.3439, found 582.3432. HPLC purity 97.1%, t_R = 8.05 min.

(*R*)-*N*-Cyclopropyl-1-(3-((2-methyl-1-oxo-1-(piperazin-1-yl)propan-2-yl)oxy)phenyl)-*N*-(4-(pyridin-3-yl)benzyl)piperidine-3-carboxamide (13 as HCl Salt).—^{1}H NMR (500 MHz, methanol-d_4) δ 9.20 (d, J = 2.1 Hz, 1H), 8.94 (dt, J = 8.3, 1.8 Hz, 1H), 8.84 (dt, J = 5.6, 1.0 Hz, 1H), 8.19 (dd, J = 8.3, 5.7 Hz, 1H), 7.91−7.75 (m, 2H), 7.65−7.23 (m, 5H), 7.03 (dd, J = 8.4, 2.3 Hz, 1H), 4.92 (d, J =15.8 Hz, 1H), 4.60 (d, J = 15.4 Hz, 1H), 4.35−3.83 (m, 5H), 3.82−3.63 (m, 4H), 3.27−2.73 (m, 5H), 2.43−1.76 (m, 4H), 1.68 (d, J = 2.1 Hz, 6H), 1.15−0.86 (m, 4H). ^{13}C NMR (126 MHz, methanol-d_4) δ 171.5, 156.3, 144.2, 143.5, 140.6, 140.3, 139.5, 139.4, 132.4, 131.5, 128.4, 127.4, 118.4, 114.4, 111.5, 81.8, 49.5, 43.1, 30.2, 24.9, 24.7, 9.2, 7.3. HRMS (ESI) calcd for $C_{35}H_{43}N_5O_3$ $(M + Na)^+$ 604.3258, found 604.3249. HPLC purity 99.2%, t_R = 8.21 min.

(*R*)-*N*-Cyclopropyl-1-(3-((2-methyl-1-oxo-1-(piperazin-1-yl)propan-2-yl)oxy)phenyl)-*N*-(4-(pyridin-4-yl)benzyl)piperidine-3-carboxamide (14 as HCl Salt).—^{1}H NMR (500 MHz, methanol-d_4) δ 8.90−8.83 (m, 2H), 8.45−8.38 (m, 2H), 8.00 (d, J = 8.3 Hz, 2H), 7.64−7.25 (m, 5H), 7.04 (dd, J = 8.4, 2.2 Hz, 1H), 4.93 (d, J = 15.7 Hz, 1H), 4.64 (d, J = 15.5 Hz, 1H), 4.35−3.85 (m, 5H), 3.83−3.65 (m, 4H), 3.27−2.87 (m, 5H), 2.43−1.85 (m, 4H), 1.68 (d, J = 2.0 Hz, 6H), 1.14−0.90 (m, 4H). ^{13}C NMR (126 MHz, methanol-d_4) δ 171.5, 157.7, 156.3, 143.5, 142.8, 141.4, 133.2, 131.5, 128.4, 128.1, 124.0, 118.5, 114.4, 111.6, 81.8, 49.6, 43.1, 30.2, 24.9, 24.7, 9.2, 7.3. HRMS (ESI) calcd for $C_{35}H_{43}N_5O_3$ $(M + Na)^+$ 604.3258, found 604.3251. HPLC purity 98.8%, t_R = 13.07 min.

(*R*)-*N*-(4-(1H-Pyrazol-4-yl)benzyl)-*N*-cyclopropyl-1-(3-((2-methyl-1-oxo-1-(piperazin-1-yl)propan-2-yl)oxy)phenyl)piperidine-3-carboxamide (15 as HCl Salt).—^{1}H NMR (500 MHz, methanol-d_4) δ 8.55 (d, J = 8.3 Hz, 2H), 7.76−7.62 (m, 2H), 7.56 (t, J = 8.3 Hz, 1H), 7.46 (d, J = 8.0 Hz, 1H), 7.35 (d, J = 7.9 Hz, 3H), 7.04 (dd, J = 8.4, 2.3 Hz, 1H), 4.90 (s, 1H), 4.50 (d, J = 15.0 Hz, 1H), 4.04 (d, J = 128.1 Hz, 5H), 3.82−3.66 (m, 4H), 3.26−2.73 (m, 5H), 2.35−1.84 (m, 4H), 1.68 (d, J = 2.2 Hz, 6H), 1.13−0.85 (m, 4H). ^{13}C NMR (126 MHz, methanol-d_4) δ 171.5, 156.3, 143.4, 137.8, 131.5, 130.7, 128.6, 128.0, 125.9, 123.8, 118.6, 114.5, 111.6, 81.8, 58.2, 55.9, 49.5, 43.1, 42.7, 39.5, 30.0, 24.9, 24.7, 9.3, 7.2. HRMS (ESI) calcd for $C_{33}H_{42}N_6O_3$ $(M + Na)^+$ 593.3211, found 593.3204. HPLC purity 96.8%, t_R = 9.35 min.

(*S*)-*N*-(4-(1*H*-Pyrazol-4-yl)benzyl)-*N*-cyclopropyl-1-(3-((2-methyl-1-oxo-1-(piperazin-1-yl)propan-2-yl)oxy)phenyl)piperidine-3-carboxamide (16 as HCl Salt).—^{1}H NMR (500 MHz, methanol-d_4) δ 8.52 (s, 2H), 7.66 (d, J = 8.0 Hz, 2H), 7.55

Author Manuscript Author Manuscript Author Manuscript Author Manuscript

(t, J = 8.2 Hz, 1H), 7.50 (dd, J = 8.1, 2.1 Hz, 1H), 7.40 (s, 1H), 7.33 (d, J = 7.9 Hz, 2H), 7.03 (dd, J = 8.4, 2.3 Hz, 1H), 4.85 (d, J = 15.1 Hz, 1H), 4.50 (d, J = 15.1 Hz, 1H), 4.36−3.85 (m, 5H), 3.82−3.67 (m, 4H), 3.28−2.75 (m, 5H), 2.40−2.08 (m, 3H), 1.95 (d, J = 12.2 Hz, 1H), 1.68 (d, J = 2.1 Hz, 6H), 1.15−0.84 (m, 4H). ^{13}C NMR (126 MHz, methanol-d_4) δ 171.4, 156.3, 143.4, 137.7, 131.5, 130.7, 128.9, 127.9, 125.9, 123.6, 118.5, 114.5, 111.6, 81.8, 58.0, 56.0, 49.5, 43.1, 42.7, 39.6, 37.1, 30.0, 25.0, 24.8, 23.9, 21.9, 9.3, 7.3. calcd for $C_{33}H_{42}N_6O_3$ $(M + H)^+$ 571.3391, found 571.3389. HPLC purity 98.8%, t_R = 9.34 min.

(*R*)-*N*-(4-(1*H*-Pyrazol-5-yl)benzyl)-*N*-cyclopropyl-1-(3-((2-methyl-1-oxo-1-(piperazin-1-yl)propan-2-yl)oxy)phenyl)piperidine-3-carboxamide (17 as HCl Salt).—^{1}H NMR (500 MHz, methanol-d_4) δ 8.23 (d, J = 2.7 Hz, 1H), 7.83 (d, J = 8.2 Hz, 2H), 7.64 (ddt, J = 9.9, 6.7, 1.8 Hz, 1H), 7.56 (td, J = 7.8, 7.4, 2.4 Hz, 2H), 7.46 (d, J = 7.9 Hz, 3H), 7.37 (s, 1H), 7.09 (d, J = 2.7 Hz, 1H), 7.04 (dd, J = 8.4, 2.3 Hz, 1H), 4.91 (s, 1H), 4.59 (d, J = 15.4 Hz, 1H), 4.37−3.84 (m, 5H), 3.82−3.63 (m, 4H), 3.26−2.81 (m, 5H), 2.39−1.84 (m, 4H), 1.68 (d, J = 2.1 Hz, 6H), 1.14−0.85 (m, 4H). ^{13}C NMR (126 MHz, methanol-d_4) δ 171.5, 156.3, 147.6, 143.4, 141.0, 134.8, 132.4, 131.7, 131.6, 131.5, 128.6, 128.5, 128.1, 126.7, 125.8, 118.6, 114.5, 111.6, 104.4, 81.8, 55.9, 49.6, 43.1, 42.7, 39.6, 30.2, 24.9, 24.7, 9.3, 7.3. HRMS (ESI) calcd for $C_{33}H_{42}N_6O_3$ $(M + Na)^+$ 593.3211, found 593.3203. HPLC purity 99.1%, t_R = 9.41 min.

(*R*)-*N*-Cyclopropyl-1-(3-((2-methyl-1-oxo-1-(piperazin-1-yl)propan-2-yl)oxy)phenyl)-*N*-(4-(1-methyl-1*H*-pyrazol-4-yl)benzyl)piperidine-3-carboxamide (18 as HCl Salt).—^{1}H NMR (500 MHz, methanol-d_4) δ 8.11 (s, 1H), 8.00 (d, J = 0.9 Hz, 1H), 7.60−7.50 (m, 3H), 7.48−7.37 (m, 1H), 7.37−7.24 (m, 3H), 7.04 (dd, J = 8.3, 2.3 Hz, 1H), 4.89 (s, 1H), 4.45 (d, J = 14.9 Hz, 1H), 4.23−3.61 (m, 12H), 3.27−2.77 (m, 5H), 2.34−1.79 (m, 4H), 1.68 (d, J = 2.6 Hz, 6H), 1.12−0.86 (m, 4H). ^{13}C NMR (126 MHz, methanol-d_4) δ 171.5, 156.3, 143.4, 136.4, 134.8, 131.5, 130.7, 129.0, 127.8, 125.4, 123.1, 118.6, 114.4, 111.6, 81.8, 49.5, 43.1, 37.5, 29.9, 24.9, 24.7, 9.3, 7.2. HRMS (ESI) calcd for $C_{34}H_{44}N_6O_3$ $(M + Na)^+$ 607.3367, found 607.3356. HPLC purity 98.0%, t_R = 9.86 min.

(*R*)-*N*-(4-(1*H*-Pyrazol-4-yl)benzyl)-*N*-cyclopropyl-1-(3-((2-methyl-1-(4-methylpiperazin-1-yl)-1-oxopropan-2-yl)oxy)phenyl)piperidine-3-carboxamide (19).—^{1}H NMR (500 MHz, chloroform-d) δ 7.83 (s, 2H), 7.45 (d, J = 7.8 Hz, 2H), 7.24 (d, J = 7.8 Hz, 2H), 7.06 (t, J = 8.2 Hz, 1H), 6.54 (dd, J = 8.3, 2.3 Hz, 1H), 6.42 (t, J = 2.4 Hz, 1H), 6.28 (dd, J = 8.2, 2.3 Hz, 1H), 4.69 (d, J = 14.6 Hz, 1H), 4.54 (d, J = 14.7 Hz, 1H), 3.87 (s, 2H), 3.73−3.59 (m, 4H), 3.45 (tt, J = 11.0, 3.5 Hz, 1H), 2.99 (dd, J = 12.4, 11.0 Hz, 1H), 2.75 (td, J = 12.1, 3.0 Hz, 1H), 2.64 (ddd, J = 10.7, 6.9, 4.1 Hz, 1H), 2.31 (d, J = 6.1 Hz, 2H), 2.17 (s, 3H), 2.08 (s, 2H), 1.95 (d, J = 10.7 Hz, 1H), 1.85−1.70 (m, 3H), 1.63−1.60 (m, 6H), 0.93−0.80 (m, 4H). ^{13}C NMR (126 MHz, chloroform-d) δ 176.9, 171.9, 156.3, 152.7, 136.7, 131.4, 129.6, 128.3, 125.9, 109.8, 107.7, 106.0, 80.7, 54.9, 54.7, 52.3, 49.9, 49.6, 45.9, 45.6, 42.8, 39.9, 29.8, 27.8, 26.23, 26.21, 24.5, 9.5, 9.1. HRMS (ESI) calcd for $C_{34}H_{44}N_6O_3$ $(M + H)^+$ 585.3548, found 585.3546. HPLC purity 98.5%, t_R = 9.23 min.

(*R*)-*N*-(4-(1*H*-Pyrazol-4-yl)benzyl)-*N*-cyclopropyl-1-(3-((2-methyl-1-oxo-1-(piperidin-1-yl)propan-2-yl)oxy)phenyl)piperidine-3-carboxamide (20).—^{1}H

Author Manuscript Author Manuscript Author Manuscript Author Manuscript

NMR (500 MHz, methanol-d_4) δ 7.92 (s, 2H), 7.57−7.51 (m, 2H), 7.24 (d, J = 8.1 Hz, 2H), 7.09 (t, J = 8.2 Hz, 1H), 6.59 (dd, J = 8.3, 2.3 Hz, 1H), 6.44 (t, J = 2.3 Hz, 1H), 6.30 (dd, J = 8.1, 2.3 Hz, 1H), 4.66−4.56 (m, 2H), 3.81 (p, J = 7.2, 6.5 Hz, 2H), 3.72−3.63 (m, 2H), 3.59−3.49 (m, 3H), 2.88 (dd, J = 12.3, 10.9 Hz, 1H), 2.78−2.71 (m, 2H), 1.98 (d, J = 9.8 Hz, 1H), 1.83 (dq, J = 8.6, 2.8 Hz, 1H), 1.72 (qd, J = 12.1, 11.7, 3.4 Hz, 2H), 1.59−1.44 (m, 10H), 1.25 (dd, J = 7.2, 3.9 Hz, 2H), 0.89 (pd, J = 8.5, 7.7, 4.8 Hz, 4H). ^{13}C NMR (126 MHz, methanol-d_4) δ 177.6, 172.0, 156.4, 152.5, 136.2, 131.6, 129.3, 127.7, 125.3, 122.0, 109.7, 108.2, 105.5, 80.2, 52.5, 49.7, 49.2, 46.6, 44.0, 39.7, 29.8, 27.4, 25.8, 25.4, 25.3, 25.2, 24.1, 23.9, 8.5, 8.2. HRMS (ESI) calcd for $C_{34}H_{43}N_5O_3$ $(M + H)^+$ 570.3439, found 570.3446. HPLC purity 99.7%, t_R = 11.52 min.

(*R*)-*N*-(4-(1*H*-Pyrazol-4-yl)benzyl)-*N*-ethyl-1-(3-((2-methyl-1-oxo-1-(piperazin-1-yl)propan-2-yl)oxy)phenyl)piperidine-3-carboxamide (21 as HCl Salt).—^{1}H NMR (500 MHz, methanol-d_4) δ 8.45 (d, J = 4.4 Hz, 2H), 7.69 (dd, J = 29.3, 8.0 Hz, 2H), 7.55 (q, J = 8.1 Hz, 1H), 7.49−7.25 (m, 4H), 7.03 (ddd, J = 8.8, 6.7, 2.3 Hz, 1H), 4.84−4.47 (m, 2H), 4.31−3.83 (m, 4H), 3.84−3.62 (m, 5H), 3.60−3.41 (m, 2H), 3.28−2.77 (m, 4H), 2.37−1.80 (m, 4H), 1.68 (d, J = 3.4 Hz, 6H), 1.20 (dt, J = 63.2, 7.1 Hz, 3H). ^{13}C NMR (126 MHz, methanol-d_4) δ 171.5, 156.3, 143.3, 136.9, 136.1, 131.5, 130.7, 130.0, 129.4, 128.1, 127.5, 126.1, 125.9, 123.4, 118.5, 118.3, 114.5, 111.60, 111.56, 81.8, 58.3, 55.7, 50.3, 43.1, 42.2, 41.3, 39.6, 24.9, 24.7, 21.4, 13.2, 11.4. HRMS (ESI) calcd for $C_{32}H_{42}N_6O_3$ $(M + Na)^+$ 581.3211, found 581.3204. HPLC purity 99.9%, t_R = 8.99 min.

(*R*)-*N*-(4-(1*H*-Pyrazol-4-yl)benzyl)-*N*-(2-ethoxyethyl)-1-(3-((2-methyl-1-oxo-1-(piperazin-1-yl)propan-2-yl)oxy)phenyl)piperidine-3-carboxamide (22 as HCl Salt).—^{1}H NMR (500 MHz, methanol-d_4) δ 8.43 (d, J = 4.1 Hz, 2H), 7.68 (dd, J = 31.4, 8.0 Hz, 2H), 7.57−7.52 (m, 1H), 7.46−7.28 (m, 4H), 7.02 (ddd, J = 7.3, 4.9, 2.2 Hz, 1H), 4.80 (d, J = 16.9 Hz, 1H), 4.57 (d, J = 15.3 Hz, 1H), 4.22−3.57 (m, 13H), 3.50−3.42 (m, 2H), 3.26−2.81 (m, 4H), 2.30−1.85 (m, 4H), 1.68 (d, J = 3.5 Hz, 6H), 1.15 (dt, J = 16.7, 7.0 Hz, 3H). ^{13}C NMR (126 MHz, methanol-d_4) δ 171.5, 156.3, 143.3, 136.9, 131.53, 131.49, 130.7, 129.4, 128.0, 127.4, 126.1, 125.8, 118.4, 118.3, 114.5, 114.4, 111.65, 111.56, 81.80, 81.77, 67.7, 67.3, 66.3, 66.1, 55.7, 43.1, 42.5, 39.5, 24.9, 24.7, 21.4, 14.2, 14.1. HRMS (ESI) calcd for $C_{34}H_{46}N_6O_4$ $(M + H)^+$ 603.3653, found 603.3650. HPLC purity 99.7%, t_R = 9.34 min.

***tert*-Butyl 2-(3-Bromophenoxy)-2-methylpropanoate (23).—**^{1}H NMR (500 MHz, chloroform-d) δ 7.16−7.04 (m, 2H), 7.01 (dd, J = 2.7, 1.3 Hz, 1H), 6.82−6.71 (m, 1H), 1.56 (s, 6H), 1.44 (s, 9H). MS (ESI) m/z = 315.1 $[M + H]^+$.

***tert*-Butyl (*R*)-3-((4-Isopropylbenzyl)carbamoyl)piperidine-1-carboxylate (24a).—**^{1}H NMR (500 MHz, chloroform-d) δ 7.14 (s, 4H), 4.37 (d, J = 19.2 Hz, 2H), 4.05−3.61 (m, 2H), 3.15 (dd, J = 13.5, 9.3 Hz, 1H), 2.86−2.77 (m, 2H), 2.26 (dq, J = 9.8, 5.3, 4.9 Hz, 1H), 1.92−1.77 (m, 2H), 1.70−1.53 (m, 1H), 1.38 (s, 10H), 1.22 (d, J = 7.0 Hz, 6H). MS (ESI) m/z = 383.3 $[M + Na]^+$.

***tert*-Butyl (*S*)-3-((4-Isopropylbenzyl)carbamoyl)piperidine-1-carboxylate (24b).—**^{1}H NMR (500 MHz, chloroform-d) δ 7.15 (s, 4H), 4.37 (d, J = 19.2 Hz, 2H), 4.03−3.60

Author Manuscript Author Manuscript Author Manuscript Author Manuscript

(m, 2H), 3.14 (dd, J = 13.5, 9.3 Hz, 1H), 2.86 (hept, J = 6.8 Hz, 2H), 2.28 (dq, J = 9.8, 5.3, 4.9 Hz, 1H), 1.91−1.77 (m, 2H), 1.69−1.54 (m, 1H), 1.38 (s, 10H), 1.21 (d, J = 7.0 Hz, 6H). MS (ESI) m/z = 361.3 $[M + H]^+$, 383.3 $[M + Na]^+$.

***tert*-Butyl (*R*)-2-(3-(3-((4-Isopropylbenzyl)carbamoyl)piperidin-1-yl)phenoxy)-2-methylpropanoate (25a).—**^{1}H NMR (500 MHz, chloroform-*d*) δ 7.18 (d, J = 1.6 Hz, 4H), 7.06 (t, J = 8.2 Hz, 1H), 6.91 (t, J = 5.7 Hz, 1H), 6.54 (dd, J = 8.3, 2.3 Hz, 1H), 6.48 (t, J = 2.3 Hz, 1H), 6.34 (dd, J = 8.2, 2.3 Hz, 1H), 4.43 (d, J = 5.6 Hz, 2H), 3.39 (dd, J = 12.5, 3.6 Hz, 1H), 3.30−3.15 (m, 2H), 3.02 (ddd, J = 11.8, 8.4, 3.1 Hz, 1H), 2.88 (p, J = 6.9 Hz, 1H), 2.55 (tt, J = 8.0, 4.1 Hz, 1H), 2.00−1.73 (m, 3H), 1.66 (tq, J = 8.7, 4.4 Hz, 1H), 1.56 (s, 6H), 1.42 (d, J = 0.9 Hz, 9H), 1.24 (d, J = 6.9 Hz, 6H). MS (ESI) m/z = 495.4 $[M + H]^+$.

***tert*-Butyl (*S*)-2-(3-(3-((4-Isopropylbenzyl)carbamoyl)piperidin-1-yl)phenoxy)-2-methylpropanoate (25b).—**^{1}H NMR (500 MHz, chloroform-*d*) δ 7.18 (d, J = 1.6 Hz, 4H), 7.06 (t, J = 8.2 Hz, 1H), 6.90 (t, J = 5.7 Hz, 1H), 6.54 (dd, J = 8.3, 2.3 Hz, 1H), 6.49 (t, J = 2.3 Hz, 1H), 6.34 (dd, J = 8.2, 2.3 Hz, 1H), 4.42 (d, J = 5.6 Hz, 2H), 3.39 (dd, J = 12.5, 3.6 Hz, 1H), 3.31−3.15 (m, 2H), 3.02 (ddd, J = 11.8, 8.4, 3.1 Hz, 1H), 2.88 (p, J = 6.9 Hz, 1H), 2.55 (tt, J = 8.0, 4.1 Hz, 1H), 2.02−1.72 (m, 3H), 1.66 (tq, J = 8.7, 4.4 Hz, 1H), 1.55 (s, 6H), 1.42 (d, J = 0.9 Hz, 9H), 1.23 (d, J = 6.9 Hz, 6H). MS (ESI) m/z = 495.4 $[M + H]^+$.

***tert*-Butyl (*R*)-3-((4-Isopropylbenzyl)(methyl)carbamoyl)piperidine-1-carboxylate (26a).—**^{1}H NMR (500 MHz, chloroform-*d*) δ 7.24−7.12 (m, 2H), 7.11−6.89 (m, 2H), 4.51 (s, 2H), 4.16 (s, 1H), 4.06 (s, 1H), 2.95 (s, 2H), 2.90−2.79 (m, 3H), 2.70−2.45 (m, 2H), 2.02−1.54 (m, 3H), 1.53−1.30 (m, 10H), 1.21 (t, J = 6.9 Hz, 6H). MS (ESI) m/z = 375.3 $[M + H]^+$.

***tert*-Butyl (*R*)-3-(Ethyl(4-isopropylbenzyl)carbamoyl)piperidine-1-carboxylate (26b).—**^{1}H NMR (500 MHz, chloroform-*d*) δ 7.20−7.14 (m, 1H), 7.14−6.90 (m, 3H), 4.85−3.96 (m, 4H), 3.26 (s, 2H), 2.84 (dp, J = 13.7, 6.9 Hz, 2H), 2.60 (tt, J = 31.9, 17.1 Hz, 2H), 1.97−1.55 (m, 3H), 1.38 (d, J = 30.3 Hz, 10H), 1.19 (dd, J = 8.0, 6.9 Hz, 6H), 1.08 (dt, J = 48.7, 7.1 Hz, 3H). MS (ESI) m/z = 389.3 $[M + H]^+$.

***tert*-Butyl (*R*)-3-(Isopropyl(4-isopropylbenzyl)carbamoyl)piperidine-1-carboxylate (26c).—**^{1}H NMR (500 MHz, chloroform-*d*) δ 7.19−7.12 (m, 1H), 7.12−6.97 (m, 3H), 4.94−3.85 (m, 5H), 3.19−2.20 (m, 4H), 2.04−1.62 (m, 2H), 1.64−1.52 (m, 1H), 1.44 (s, 4H), 1.36 (s, 6H), 1.29−1.10 (m, 9H), 1.04 (d, J = 6.8 Hz, 3H). MS (ESI) m/z = 403.3 $[M + H]^+$, 425.3 $[M + Na]^+$.

***tert*-Butyl (*R*)-3-(Cyclopropyl(4-isopropylbenzyl)carbamoyl)piperidine-1-carboxylate (26d).—**^{1}H NMR (500 MHz, chloroform-*d*) δ 7.12 (t, J = 6.7 Hz, 4H), 4.91−3.94 (m, 4H), 3.19 (tt, J = 11.5, 3.8 Hz, 1H), 2.87 (dq, J = 13.8, 6.8 Hz, 2H), 2.65 (d, J = 69.8 Hz, 2H), 1.90 (d, J = 13.3 Hz, 1H), 1.85−1.63 (m, 2H), 1.45 (s, 10H), 1.22 (d, J = 6.9 Hz, 6H), 0.97−0.70 (m, 4H). MS (ESI) m/z = 401.4 $[M + H]^+$, 423.3 $[M + Na]^+$.

***tert*-Butyl (*R*)-2-(3-(3-((4-Isopropylbenzyl)(methyl)carbamoyl)piperidin-1-yl)phenoxy)-2- methylpropanoate (27a).—**^{1}H NMR (500 MHz, chloroform-*d*) δ

Author Manuscript Author Manuscript Author Manuscript Author Manuscript

7.17−7.06 (m, 3H), 7.04−6.83 (m, 2H), 6.57−6.30 (m, 2H), 6.21 (ddd, J = 16.6, 8.1, 2.2 Hz, 1H), 4.62−4.28 (m, 2H), 3.87−3.51 (m, 2H), 3.00−2.76 (m, 6H), 2.67 (dtd, J = 18.5, 12.0, 2.7 Hz, 1H), 2.05−1.61 (m, 4H), 1.54−1.43 (m, 6H), 1.36 (d, J = 3.4 Hz, 9H), 1.17 (dd, J = 6.9, 3.2 Hz, 6H). MS (ESI) m/z = 509.4 $[M + H]^+$.

***tert*-Butyl (*R*)-2-(3-(3-(Ethyl(4-isopropylbenzyl)carbamoyl)piperidin-1-yl)phenoxy)-2-methylpropanoate (27b).—**^{1}H NMR (500 MHz, chloroform-d) δ 7.16−7.04 (m, 3H), 7.04−6.87 (m, 2H), 6.54−6.27 (m, 2H), 6.21 (ddd, J = 19.7, 7.9, 2.2 Hz, 1H), 4.62−4.31 (m, 2H), 3.75−3.49 (m, 2H), 3.42−3.16 (m, 2H), 3.03−2.52 (m, 4H), 1.96−1.57 (m, 4H), 1.50−1.41 (m, 6H), 1.35 (d, J = 3.3 Hz, 9H), 1.16 (dd, J = 6.9, 3.5 Hz, 6H), 1.05 (dt, J = 25.1, 7.1 Hz, 3H). MS (ESI) m/z = 523.4 $[M + H]^+$.

***tert*-Butyl (*R*)-2-(3-(3-(Isopropyl(4-isopropylbenzyl)carbamoyl)piperidin-1-yl)phenoxy)-2-methylpropanoate (27c).—**^{1}H NMR (500 MHz, chloroform-d) δ 7.19 (d, J = 8.2 Hz, 1H), 7.15−7.04 (m, 3H), 6.98 (t, J = 8.2 Hz, 1H), 6.63−6.21 (m, 3H), 5.07−4.21 (m, 3H), 3.71 (ddt, J = 16.2, 12.0, 2.0 Hz, 1H), 3.57 (td, J = 9.8, 7.6, 3.0 Hz, 1H), 3.18−2.56 (m, 4H), 2.05−1.63 (m, 4H), 1.59−1.52 (m, 6H), 1.43 (d, J = 7.8 Hz, 9H), 1.33−1.00 (m, 12H). MS (ESI) m/z = 537.4 $[M + H]^+$.

***tert*-Butyl (*R*)-2-(3-(3-(Cyclopropyl(4-isopropylbenzyl)carbamoyl)piperidin-1-yl)phenoxy)-2-methylpropanoate (27d).—**^{1}H NMR (500 MHz, chloroform-d) δ 7.20−7.12 (m, 4H), 7.07 (t, J = 8.2 Hz, 1H), 6.55 (dd, J = 8.2, 2.3 Hz, 1H), 6.49 (t, J = 2.4 Hz, 1H), 6.30 (dd, J = 8.1, 2.3 Hz, 1H), 4.71−4.37 (m, 2H), 3.85−3.61 (m, 2H), 3.43 (ddt, J = 11.0, 7.1, 3.4 Hz, 1H), 2.99 (dd, J = 12.4, 10.9 Hz, 1H), 2.88 (p, J = 6.9 Hz, 1H), 2.77 (td, J = 12.1, 2.6 Hz, 1H), 2.59 (tt, J = 6.9, 4.1 Hz, 1H), 2.00−1.89 (m, 1H), 1.88−1.65 (m, 3H), 1.55 (s, 6H), 1.44 (s, 9H), 1.24 (d, J = 6.9 Hz, 6H), 0.97−0.75 (m, 4H). MS (ESI) m/z = 535.4 $[M + H]^+$.

***tert*-Butyl (*R*)-4-(2-(3-(3-((4-Isopropylbenzyl)carbamoyl)piperidin-1-yl)phenoxy)-2-methylpropanoyl)piperazine-1-carboxylate (28a).—**^{1}H NMR (500 MHz, chloroform-d) δ 7.14 (d, J = 8.2 Hz, 2H), 7.10 (d, J = 8.1 Hz, 2H), 6.99 (t, J = 8.2 Hz, 1H), 6.88 (s, 1H), 6.45 (dd, J = 8.3, 2.2 Hz, 1H), 6.33 (t, J = 2.3 Hz, 1H), 6.23 (dd, J = 8.1, 2.2 Hz, 1H), 4.37 (qd, J = 14.7, 5.6 Hz, 2H), 3.72 (d, J = 5.6 Hz, 2H), 3.50−3.36 (m, 3H), 3.33 (dt, J = 12.5, 4.4 Hz, 1H), 3.21 (s, 2H), 3.12 (dd, J = 12.8, 8.8 Hz, 1H), 2.94 (ddd, J = 22.2, 12.9, 4.5 Hz, 3H), 2.82 (p, J = 6.9 Hz, 1H), 2.54−2.32 (m, 1H), 1.82 (qd, J = 9.1, 3.9 Hz, 2H), 1.67 (dt, J = 13.3, 4.8 Hz, 1H), 1.55 (d, J = 5.0 Hz, 7H), 1.34 (s, 9H), 1.16 (d, J = 7.0 Hz, 6H). MS (ESI) m/z = 607.4 $[M + H]^+$.

***tert*-Butyl (*R*)-4-(2-(3-(3-((4-Isopropylbenzyl)(methyl)carbamoyl)piperidin-1-yl)phenoxy)-2-methylpropanoyl)piperazine-1-carboxylate (28b).—**^{1}H NMR (500 MHz, chloroform-d) δ 7.24−7.10 (m, 3H), 7.09−6.88 (m, 2H), 6.55−6.32 (m, 2H), 6.24 (ddd, J = 19.9, 8.1, 2.3 Hz, 1H), 4.84−4.37 (m, 2H), 3.80 (dd, J = 10.7, 5.5 Hz, 2H), 3.72−3.53 (m, 4H), 3.32 (d, J = 6.0 Hz, 2H), 3.07 (d, J = 6.4 Hz, 2H), 3.02−2.92 (m, 4H), 2.92−2.84 (m, 2H), 2.72 (qd, J = 12.4, 2.6 Hz, 1H), 1.98−1.66 (m, 4H), 1.68−1.44 (m, 6H), 1.41 (s, 9H), 1.23 (dd, J = 6.9, 4.1 Hz, 6H). MS (ESI) m/z = 621.4 $[M + H]^+$.

Author Manuscript Author Manuscript Author Manuscript Author Manuscript

***tert*-Butyl (*R*)-4-(2-(3-(3-(Ethyl(4-isopropylbenzyl)carbamoyl)piperidin-1-yl)phenoxy)-2-methylpropanoyl)piperazine-1-carboxylate (28c).—**^{1}H NMR (500 MHz, chloroform-*d*) δ 7.24−7.11 (m, 3H), 7.11−6.89 (m, 2H), 6.65−6.32 (m, 2H), 6.30−6.12 (m, 1H), 4.86−4.43 (m, 2H), 3.80 (dt, *J* = 11.2, 5.2 Hz, 2H), 3.71−3.55 (m, 4H), 3.48−3.24 (m, 4H), 3.17−2.66 (m, 6H), 1.99−1.67 (m, 4H), 1.66−1.52 (m, 7H), 1.42 (s, 9H), 1.24 (dd, *J* = 7.0, 4.2 Hz, 6H), 1.14 (dt, *J* = 27.5, 7.1 Hz, 3H). MS (ESI) *m/z* = 635.4 $[M + H]^+$.

***tert*-Butyl (*R*)-4-(2-(3-(3-(Isopropyl(4-isopropylbenzyl)carbamoyl)piperidin-1-yl)phenoxy)-2-methylpropanoyl)piperazine-1-carboxylate (28d).—**^{1}H NMR (500 MHz, chloroform-*d*) δ 7.22−6.90 (m, 5H), 6.62−6.14 (m, 3H), 4.95−4.19 (m, 3H), 3.90−3.45 (m, 6H), 3.32 (d, *J* = 6.9 Hz, 2H), 3.23−2.54 (m, 6H), 2.00−1.65 (m, 4H), 1.62 (dd, *J* = 7.7, 1.9 Hz, 6H), 1.52−1.39 (m, 10H), 1.34−1.05 (m, 12H). MS (ESI) *m/z* =649.5 $[M + H]^+$, 671.5 $[M + Na]^+$.

***tert*-Butyl (*R*)-4-(2-(3-(3-(Cyclopropyl(4-isopropylbenzyl)carbamoyl)piperidin-1-yl)phenoxy)-2-methylpropanoyl)piperazine-1-carboxylate (28e).—**^{1}H NMR (500 MHz, chloroform-*d*) δ 7.21−7.13 (m, 4H), 7.07 (t, *J* = 8.2 Hz, 1H), 6.54 (dd, *J* = 8.3, 2.2 Hz, 1H), 6.43 (t, *J* = 2.4 Hz, 1H), 6.28 (dd, *J* = 8.1, 2.3 Hz, 1H), 4.68 (d, *J* = 14.5 Hz, 1H), 4.51 (d, *J* = 14.6 Hz, 1H), 3.83 (q, *J* = 5.5 Hz, 2H), 3.73−3.53 (m, 4H), 3.49−3.28 (m, 3H), 3.17−2.83 (m, 4H), 2.77 (td, *J* = 12.2, 3.0 Hz, 1H), 2.66−2.54 (m, 1H), 2.01−1.92 (m, 1H), 1.89−1.69 (m, 3H), 1.71−1.54 (m, 7H), 1.43 (s, 9H), 1.25 (d, *J* = 6.9 Hz, 6H), 1.02−0.74 (m, 4H). MS (ESI) *m/z* =647.4 $[M + H]^+$.

Ethyl (*R*)-1-(3-((1-(*tert*-Butoxy)-2-methyl-1-oxopropan-2-yl)oxy)phenyl)piperidine-3-carboxylate (29).—^{1}H NMR (500 MHz, chloroform-*d*) δ 7.04 (t, *J* = 8.2 Hz, 1H), 6.54 (dd, *J* = 8.1, 2.3 Hz, 1H), 6.45 (t, *J* = 2.4 Hz, 1H), 6.31−6.21 (m, 1H), 4.12 (q, *J* = 7.1 Hz, 2H), 3.67 (ddt, *J* = 12.4, 3.5, 1.5 Hz, 1H), 3.42 (ddd, *J* = 12.3, 4.9, 3.1 Hz, 1H), 2.95 (dd, *J* = 12.4, 9.9 Hz, 1H), 2.80−2.68 (m, 1H), 2.60 (tt, *J* = 10.0, 3.9 Hz, 1H), 2.05−1.93 (m, 1H), 1.74 (th, *J* = 9.2, 3.1 Hz, 1H), 1.69−1.59 (m, 2H), 1.53 (s, 6H), 1.41 (s, 9H), 1.24 (t, *J* = 7.2 Hz, 3H). MS (ESI) *m/z* =392.3 $[M + H]^+$, 414.3 $[M + Na]^+$.

***tert*-Butyl (*R*)-4-(2-(3-(3-(Ethoxycarbonyl)piperidin-1-yl)phenoxy)-2-methylpropanoyl)piperazine-1-carboxylate (30).—**^{1}H NMR (500 MHz, chloroform-*d*) δ 7.05 (t, *J* = 8.2 Hz, 1H), 6.55 (dd, *J* = 8.0, 2.3 Hz, 1H), 6.41 (t, *J* = 2.3 Hz, 1H), 6.27 (ddd, *J* = 8.2, 2.5, 0.7 Hz, 1H), 4.15 (q, *J* = 7.1 Hz, 2H), 3.81 (t, *J* = 5.2 Hz, 2H), 3.67 (ddt, *J* = 12.4, 3.5, 1.5 Hz, 1H), 3.59 (t, *J* = 5.2 Hz, 2H), 3.50−3.39 (m, 1H), 3.33 (q, *J* = 5.5 Hz, 2H), 3.07 (t, *J* = 5.2 Hz, 2H), 2.97 (dd, *J* = 12.4, 9.9 Hz, 1H), 2.81−2.70 (m, 1H), 2.62 (tt, *J* = 10.0, 3.9 Hz, 1H), 2.07−1.92 (m, 1H), 1.78 (qq, *J* = 4.9, 3.2, 2.2 Hz, 1H), 1.62 (s, 8H), 1.41 (s, 9H), 1.26 (t, *J* = 7.1 Hz, 3H). MS (ESI) *m/z* =504.3 $[M + H]^+$, 526.3 $[M + Na]^+$.

***tert*-Butyl (*R*)-4-(2-(3-(3-((4-(*tert*-Butyl)benzyl)(cyclopropyl)carbamoyl)piperidin-1-yl)phenoxy)-2-methylpropanoyl)piperazine-1-carboxylate (31a).—**^{1}H NMR (500 MHz, chloroform-*d*) δ 7.35−7.29 (m, 2H), 7.18−7.12 (m, 2H), 7.06 (t, *J* = 8.2 Hz, 1H), 6.53 (dd, *J* = 8.3, 2.3 Hz, 1H), 6.42 (t, *J* = 2.3 Hz, 1H), 6.27 (dd, *J* = 8.1, 2.3 Hz,

Author Manuscript Author Manuscript Author Manuscript Author Manuscript

1H), 4.67 (d, J = 14.6 Hz, 1H), 4.49 (d, J = 14.6 Hz, 1H), 3.88−3.74 (m, 2H), 3.74−3.49 (m, 4H), 3.43 (tt, J = 10.9, 3.5 Hz, 1H), 3.33 (s, 2H), 3.15−2.91 (m, 3H), 2.75 (td, J = 12.2, 2.9 Hz, 1H), 2.62 (tt, J = 6.6, 4.4 Hz, 1H), 2.00−1.89 (m, 1H), 1.87−1.67 (m, 3H), 1.63 (d, J = 1.4 Hz, 6H), 1.42 (s, 9H), 1.30 (s, 9H), 0.89−0.75 (m, 4H). MS (ESI) m/z = 661.5 $[M + H]^+$.

***tert*-Butyl (*R*)-4-(2-(3-(3-((4-Cyclohexylbenzyl)(cyclopropyl)carbamoyl)piperidin-1-yl)phenoxy)-2-methylpropanoyl)piperazine-1-carboxylate (31b).—** ^{1}H NMR (500 MHz, chloroform-d) δ 7.13 (s, 4H), 7.05 (t, J = 8.2 Hz, 1H), 6.52 (dd, J = 8.3, 2.3 Hz, 1H), 6.41 (t, J = 2.3 Hz, 1H), 6.26 (dd, J = 8.2, 2.3 Hz, 1H), 4.65 (d, J = 14.6 Hz, 1H), 4.48 (d, J = 14.6 Hz, 1H), 3.86−3.72 (m, 2H), 3.71−3.50 (m, 4H), 3.47−3.20 (m, 3H), 3.15−2.92 (m, 3H), 2.75 (td, J = 12.2, 2.9 Hz, 1H), 2.66−2.54 (m, 1H), 2.53−2.33 (m, 1H), 1.95 (d, J = 11.2 Hz, 1H), 1.90−1.66 (m, 8H), 1.62 (d, J = 1.3 Hz, 6H), 1.41 (s, 12H), 1.29−1.18 (m, 2H), 0.91−0.75 (m, 4H). MS (ESI) m/z = 687.5 $[M + H]^+$, 709.4 $[M + Na]^+$.

***tert*-Butyl (*R*)-4-(2-(3-(3-(([1,1′-Biphenyl]-4-ylmethyl)(cyclopropyl)carbamoyl)piperidin-1-yl)phenoxy)-2-methylpropanoyl)piperazine-1-carboxylate (31c).—** ^{1}H NMR (500 MHz, chloroform-d) δ 7.63−7.52 (m, 4H), 7.46−7.39 (m, 2H), 7.37−7.28 (m, 3H), 7.06 (t, J = 8.2 Hz, 1H), 6.54 (dd, J = 8.3, 2.2 Hz, 1H), 6.43 (t, J = 2.4 Hz, 1H), 6.27 (dd, J = 8.2, 2.3 Hz, 1H), 4.74 (d, J = 14.7 Hz, 1H), 4.57 (d, J = 14.7 Hz, 1H), 3.81 (s, 2H), 3.72−3.50 (m, 4H), 3.45 (tt, J = 11.0, 3.6 Hz, 1H), 3.32 (s, 2H), 3.13−2.94 (m, 3H), 2.82−2.60 (m, 2H), 2.01−1.94 (m, 1H), 1.88−1.67 (m, 3H), 1.62 (s, 6H), 1.41 (s, 9H), 0.95−0.78 (m, 4H). MS (ESI) m/z = 681.4 $[M + H]^+$.

***tert*-Butyl (*R*)-4-(2-(3-(3-(Cyclopropyl(4-(pyridin-2-yl)benzyl) carbamoyl) piperidin-1-yl) phenoxy)-2-methylpropanoyl)piperazine-1-carboxylate (31d).—** ^{1}H NMR (500 MHz, chloroform-d) δ 8.67 (dt, J = 4.9, 1.3 Hz, 1H), 7.97−7.89 (m, 2H), 7.79−7.65 (m, 2H), 7.34 (d, J = 8.1 Hz, 2H), 7.21 (ddd, J = 6.6, 4.8, 1.5 Hz, 1H), 7.05 (t, J = 8.2 Hz, 1H), 6.52 (dd, J = 8.4, 2.3 Hz, 1H), 6.41 (t, J = 2.4 Hz, 1H), 6.26 (dd, J = 8.1, 2.3 Hz, 1H), 4.75 (d, J = 14.6 Hz, 1H), 4.58 (d, J = 14.6 Hz, 1H), 3.88−3.73 (m, 2H), 3.73−3.63 (m, 2H), 3.63−3.49 (m, 2H), 3.43 (tt, J = 11.0, 3.6 Hz, 1H), 3.32 (s, 2H), 3.14−2.93 (m, 3H), 2.76 (td, J = 12.2, 2.8 Hz, 1H), 2.61 (tt, J = 6.9, 3.2 Hz, 1H), 2.01−1.89 (m, 1H), 1.89−1.65 (m, 3H), 1.62 (d, J = 1.6 Hz, 6H), 1.41 (s, 9H), 0.91−0.77 (m, 4H). MS (ESI) m/z = 682.4 $[M + H]^+$.

***tert*-Butyl (*R*)-4-(2-(3-(3-(Cyclopropyl(4-(pyridin-3-yl)benzyl) carbamoyl) piperidin-1-yl) phenoxy)–2-methylpropanoyl)piperazine-1-carboxylate (31e).—** ^{1}H NMR (500 MHz, chloroform-d) δ 8.73−8.56 (m, 2H), 7.59 (dd, J = 8.1, 1.8 Hz, 2H), 7.51−7.45 (m, 2H), 7.37−7.29 (m, 2H), 7.05 (t, J = 8.2 Hz, 1H), 6.52 (dd, J = 8.3, 2.3 Hz, 1H), 6.41 (t, J = 2.3 Hz, 1H), 6.27 (dd, J = 8.2, 2.3 Hz, 1H), 4.74 (d, J = 15.1 Hz, 1H), 4.58 (d, J = 14.9 Hz, 1H), 3.80 (d, J = 6.3 Hz, 2H), 3.72−3.63 (m, 2H), 3.57 (p, J = 9.7, 7.7 Hz, 2H), 3.44 (tt, J = 11.1, 3.4 Hz, 1H), 3.31 (s, 2H), 3.13−2.95 (m, 3H), 2.81−2.64 (m, 2H), 1.96 (d, J = 10.7 Hz, 1H), 1.88−1.69 (m, 3H), 1.41 (d, J = 2.4 Hz, 9H), 0.94−0.76 (m, 4H). MS (ESI) m/z = 682.4 $[M + H]^+$.

Author Manuscript Author Manuscript Author Manuscript Author Manuscript

***tert*-Butyl (*R*)-4-(2-(3-(3-(Cyclopropyl(4-(pyridin-4-yl)benzyl) carbamoyl) piperidin-1-yl) phenoxy)-2-methylpropanoyl)piperazine-1-carboxylate (31f).—** ^{1}H NMR (500 MHz, chloroform-*d*) δ 8.71−8.55 (m, 2H), 7.59 (dd, J = 8.1, 1.8 Hz, 2H), 7.52−7.45 (m, 2H), 7.38−7.29 (m, 2H), 7.05 (t, J = 8.2 Hz, 1H), 6.52 (dd, J = 8.3, 2.3 Hz, 1H), 6.41 (t, J = 2.3 Hz, 1H), 6.27 (dd, J = 8.2, 2.3 Hz, 1H), 4.74 (d, J = 15.1 Hz, 1H), 4.58 (d, J = 14.9 Hz, 1H), 3.80 (d, J = 6.3 Hz, 2H), 3.73−3.63 (m, 2H), 3.57 (p, J = 9.7, 7.7 Hz, 2H), 3.44 (tt, J = 11.1, 3.4 Hz, 1H), 3.31 (s, 2H), 3.14−2.94 (m, 3H), 2.75 (td, J = 12.1, 3.0 Hz, 1H), 2.67 (tt, J = 6.6, 4.0 Hz, 1H), 1.96 (d, J = 10.7 Hz, 1H), 1.87−1.68 (m, 3H), 1.62 (s, 6H), 1.41 (d, J = 2.4 Hz, 9H), 0.97−0.74 (m, 4H). MS (ESI) *m/z* = 682.4 $[M + H]^+$.

***tert*-Butyl (*R*)-4-(2-(3-(3-((4-Bromobenzyl)(cyclopropyl)carbamoyl)piperidin-1-yl)phenoxy)-2-methylpropanoyl)piperazine-1-carboxylate (32).—** ^{1}H NMR (500 MHz, chloroform-*d*) δ 7.47−7.40 (m, 2H), 7.16−7.11 (m, 2H), 7.07 (t, J = 8.2 Hz, 1H), 6.53 (dd, J = 8.3, 2.2 Hz, 1H), 6.42 (t, J = 2.4 Hz, 1H), 6.29 (dd, J = 8.1, 2.3 Hz, 1H), 4.63 (d, J = 14.7 Hz, 1H), 4.49 (d, J = 14.7 Hz, 1H), 3.82 (q, J = 4.7 Hz, 2H), 3.72−3.49 (m, 4H), 3.42 (ddt, J = 10.9, 7.0, 3.5 Hz, 1H), 3.33 (s, 2H), 3.08 (d, J = 5.3 Hz, 2H), 3.02−2.92 (m, 1H), 2.80−2.72 (m, 1H), 2.62 (tt, J = 7.0, 3.9 Hz, 1H), 1.99−1.86 (m, 1H), 1.86−1.78 (m, 1H), 1.73 (td, J = 11.0, 5.6 Hz, 2H), 1.64 (d, J = 1.5 Hz, 6H), 1.43 (s, 9H), 0.96−0.76 (m, 4H). MS (ESI) *m/z* = 683.3 $[M + H]^+$.

***tert*-Butyl (*R*)-4-(2-(3-(3-(Cyclopropyl(4-(thiophen-3-yl)benzyl) carbamoyl)piperidin-1-yl)phenoxy)–2-methylpropanoyl)piperazine-1-carboxylate (33a).—** ^{1}H NMR (500 MHz, chloroform-*d*) δ 7.63−7.51 (m, 2H), 7.46 (t, J = 2.2 Hz, 1H), 7.40 (d, J = 2.1 Hz, 2H), 7.31−7.27 (m, 2H), 7.09 (t, J = 8.2 Hz, 1H), 6.56 (dd, J = 8.3, 2.3 Hz, 1H), 6.45 (t, J = 2.3 Hz, 1H), 6.30 (dd, J = 8.2, 2.3 Hz, 1H), 4.73 (d, J = 14.6 Hz, 1H), 4.57 (d, J = 14.6 Hz, 1H), 3.83 (s, 2H), 3.70 (t, J = 9.3 Hz, 2H), 3.66−3.53 (m, 2H), 3.46 (ddt, J = 10.9, 6.9, 3.5 Hz, 1H), 3.35 (s, 2H), 3.18−2.92 (m, 3H), 2.85−2.72 (m, 1H), 2.65 (tt, J = 6.5, 3.5 Hz, 1H), 2.03−1.92 (m, 1H), 1.88−1.67 (m, 3H), 1.65 (s, 6H), 1.44 (s, 9H), 0.98−0.79 (m, 4H). MS (ESI) *m/z* = 687.5 $[M + H]^+$.

***tert*-Butyl (*R*)-4-(2-(3-(3-((4-(1H-Pyrazol-4-yl)benzyl)(cyclopropyl)carbamoyl)piperidin-1-yl)phenoxy)-2-methylpropanoyl)piperazine-1-carboxylate (33b).—** ^{1}H NMR (500 MHz, chloroform-*d*) δ 7.80 (s, 2H), 7.43 (d, J = 7.9 Hz, 2H), 7.22 (d, J = 7.9 Hz, 2H), 7.05 (t, J = 8.2 Hz, 1H), 6.53 (dd, J = 8.4, 2.2 Hz, 1H), 6.42 (t, J = 2.3 Hz, 1H), 6.27 (dd, J = 8.2, 2.3 Hz, 1H), 4.69 (d, J = 14.7 Hz, 1H), 4.52 (d, J = 14.7 Hz, 1H), 3.88−3.72 (m, 2H), 3.72−3.63 (m, 2H), 3.63−3.52 (m, 2H), 3.44 (tt, J = 11.0, 3.5 Hz, 1H), 3.38−3.25 (m, 2H), 3.14−2.91 (m, 3H), 2.76 (td, J = 12.1, 2.8 Hz, 1H), 2.63 (td, J = 6.7, 3.2 Hz, 1H), 1.98−1.92 (m, 1H), 1.85−1.67 (m, 3H), 1.62 (s, 6H), 1.41 (s, 9H), 0.94−0.70 (m, 4H). MS (ESI) *m/z* = 671.5 $[M + H]^+$, 669.3 $[M - H]^-$.

***tert*-Butyl (*R*)-4-(2-(3-(3-((4-(1H-Pyrazol-5-yl)benzyl)(cyclopropyl)carbamoyl)piperidin-1-yl)phenoxy)-2-methylpropanoyl)piperazine-1-carboxylate (33c).—** ^{1}H NMR (500 MHz, chloroform-*d*) δ 7.76−7.66 (m, 2H), 7.61−7.53 (m, 1H), 7.47 (ddd, J = 8.4,

Author Manuscript Author Manuscript Author Manuscript Author Manuscript

6.9, 2.9 Hz, 1H), 7.33−7.24 (m, 2H), 7.07 (t, *J* = 8.2 Hz, 1H), 6.63−6.50 (m, 2H), 6.43 (t, *J* = 2.3 Hz, 1H), 6.29 (dd, *J* = 8.1, 2.3 Hz, 1H), 4.71 (d, *J* = 14.7 Hz, 1H), 4.59 (d, *J* = 14.6 Hz, 1H), 3.89−3.51 (m, 6H), 3.51−3.24 (m, 3H), 3.18−2.89 (m, 3H), 2.77 (td, *J* = 12.1, 2.8 Hz, 1H), 2.63 (td, *J* = 6.8, 3.3 Hz, 1H), 2.05−1.91 (m, 1H), 1.89−1.67 (m, 3H), 1.64 (d, *J* = 1.8 Hz, 6H), 1.43 (s, 9H), 0.94−0.77 (m, 4H). MS (ESI) *m/z* = 671.5 $[M + H]^+$, 669.4 $[M - H]^-$.

***tert*-Butyl (*R*)-4-(2-(3-(3-(Cyclopropyl(4-(1-methyl-1*H*-pyrazol-4-yl)benzyl)carbamoyl)piperidin-1-yl)phenoxy)-2-methylpropanoyl)piperazine-1-carboxylate (33d).—** ^{1}H NMR (500 MHz, chloroform-*d*) *δ* 7.76 (d, *J* = 0.9 Hz, 1H), 7.61 (s, 1H), 7.47−7.37 (m, 2H), 7.25 (d, *J* = 8.0 Hz, 2H), 7.08 (t, *J* = 8.2 Hz, 1H), 6.55 (dd, *J* = 8.3, 2.2 Hz, 1H), 6.44 (t, *J* = 2.3 Hz, 1H), 6.29 (dd, *J* = 8.2, 2.3 Hz, 1H), 4.70 (d, *J* = 14.6 Hz, 1H), 4.55 (d, *J* = 14.6 Hz, 1H), 3.96 (s, 3H), 3.83 (s, 2H), 3.75−3.52 (m, 4H), 3.51−3.24 (m, 3H), 3.15−2.94 (m, 3H), 2.78 (td, *J* = 12.1, 2.9 Hz, 1H), 2.69−2.56 (m, 1H), 1.97 (d, *J* = 11.1 Hz, 1H), 1.90−1.69 (m, 3H), 1.64 (s, 6H), 1.44 (s, 9H), 0.92−0.83 (m, 4H). MS (ESI) *m/z* = 685.4 $[M + H]^+$.

Ethyl (*R*)-1-(3-((2-Methyl-1-(4-methylpiperazin-1-yl)-1-oxopropan-2-yl)oxy)phenyl)piperidine-3-carboxylate (34a).— ^{1}H NMR (500 MHz, acetone-d_6) *δ* 6.95 (t, *J* = 8.2 Hz, 1H), 6.46 (ddd, *J* = 8.3, 2.3, 0.8 Hz, 1H), 6.31 (t, *J* = 2.3 Hz, 1H), 6.15 (ddd, *J* = 8.1, 2.4, 0.8 Hz, 1H), 4.00 (q, *J* = 7.1 Hz, 2H), 3.70 (s, 2H), 3.55−3.35 (m, 3H), 3.35−3.24 (m, 1H), 2.89 (dd, *J* = 12.4, 9.5 Hz, 1H), 2.69 (ddd, *J* = 12.3, 10.0, 3.2 Hz, 1H), 2.48 (tt, *J* = 9.6, 4.0 Hz, 1H), 2.13 (s, 2H), 1.98 (s, 3H), 1.93 (ddt, *J* = 8.8, 4.4, 2.4 Hz, 2H), 1.87−1.76 (m, 1H), 1.64 (dddd, *J* = 11.5, 6.8, 3.8, 2.0 Hz, 1H), 1.59−1.46 (m, 2H), 1.43 (s, 6H), 1.11 (t, *J* = 7.1 Hz, 3H). MS (ESI) *m/z* = 418.3 $[M + H]^+$.

Ethyl (*R*)-1-(3-((2-Methyl-1-oxo-1-(piperidin-1-yl)propan-2-yl)oxy)phenyl)piperidine-3-carboxylate (34b).— ^{1}H NMR (500 MHz, chloroform-*d*) *δ* 7.02 (t, *J* = 8.2 Hz, 1H), 6.51 (ddd, *J* = 8.2, 2.4, 0.8 Hz, 1H), 6.40 (t, *J* = 2.4 Hz, 1H), 6.28 (ddd, *J* = 8.2, 2.4, 0.7 Hz, 1H), 4.12 (q, *J* = 7.2 Hz, 2H), 3.73 (t, *J* = 5.4 Hz, 2H), 3.65 (ddt, *J* = 12.4, 3.6, 1.5 Hz, 1H), 3.53 (t, *J* = 4.9 Hz, 2H), 3.46−3.34 (m, 1H), 2.94 (dd, *J* = 12.4, 9.9 Hz, 1H), 2.80−2.65 (m, 1H), 2.60 (tt, *J* = 10.1, 4.0 Hz, 1H), 2.04−1.93 (m, 1H), 1.82−1.67 (m, 1H), 1.59 (s, 8H), 1.47 (t, *J* = 4.0 Hz, 4H), 1.24 (t, *J* = 7.1 Hz, 5H). MS (ESI) *m/z* = 403.3 $[M + H]^+$.

(*R*)-*N*-(4-Bromobenzyl)-*N*-cyclopropyl-1-(3-((2-methyl-1-(4-methylpiperazin-1-yl)-1-oxopropan-2-yl)oxy)phenyl)piperidine-3-carboxamide (35a).— ^{1}H NMR (500 MHz, chloroform-*d*) *δ* 7.45−7.36 (m, 2H), 7.15−7.08 (m, 2H), 7.05 (t, *J* = 8.2 Hz, 1H), 6.51 (dd, *J* = 8.3, 2.3 Hz, 1H), 6.40 (t, *J* = 2.4 Hz, 1H), 6.28 (dd, *J* = 8.1, 2.3 Hz, 1H), 4.61 (d, *J* = 14.7 Hz, 1H), 4.47 (d, *J* = 14.7 Hz, 1H), 3.85 (s, 2H), 3.67−3.53 (m, 4H), 3.41 (tt, *J* = 11.0, 3.7 Hz, 1H), 2.94 (dd, *J* = 12.4, 10.9 Hz, 1H), 2.79−2.65 (m, 1H), 2.65−2.55 (m, 1H), 2.31 (t, *J* = 5.6 Hz, 2H), 2.17 (s, 3H), 2.08 (d, *J* = 6.5 Hz, 2H), 1.91 (d, *J* = 8.8 Hz, 1H), 1.80 (tt, *J* = 10.8, 4.1 Hz, 1H), 1.76−1.65 (m, 2H), 1.61 (d, *J* = 1.1 Hz, 6H), 0.93−0.74 (m, 4H). MS (ESI) *m/z* = 597.3, 599.3 $[M + H]^+$.

(*R*)-*N*-(4-Bromobenzyl)-*N*-cyclopropyl-1-(3-((2-methyl-1-oxo-1-(piperidin-1-yl)propan-2-yl)oxy)phenyl)piperidine-3-carboxamide (35b).— ^{1}H NMR (500

Author Manuscript Author Manuscript Author Manuscript Author Manuscript

MHz, chloroform-*d*) δ 7.42−7.33 (m, 2H), 7.08 (d, J = 8.1 Hz, 2H), 7.02 (t, J = 8.2 Hz, 1H), 6.48 (dd, J = 8.2, 2.3 Hz, 1H), 6.44 (s, 1H), 6.28 (dd, J = 8.2, 2.3 Hz, 1H), 4.57 (d, J = 14.7 Hz, 1H), 4.46 (d, J = 14.8 Hz, 1H), 3.72 (q, J = 5.7 Hz, 2H), 3.67−3.59 (m, 2H), 3.51 (qd, J = 13.4, 12.4, 5.7 Hz, 2H), 3.39 (tt, J = 10.8, 3.4 Hz, 1H), 2.92 (dd, J = 12.5, 10.9 Hz, 1H), 2.76−2.66 (m, 1H), 2.60 (tt, J = 7.0, 3.9 Hz, 1H), 1.89 (d, J = 9.6 Hz, 1H), 1.83−1.74 (m, 1H), 1.73−1.64 (m, 2H), 1.59 (d, J = 1.4 Hz, 6H), 1.51−1.40 (m, 4H), 1.26−1.19 (m, 2H), 0.92−0.72 (m, 4H). MS (ESI) *m/z* = 582.3, 584.2 $[M + H]^+$.

***tert*-Butyl (*R*)-4-(2-(3-(3-((4-Bromobenzyl)(ethyl)carbamoyl)piperidin-1-yl)phenoxy)-2-methylpropanoyl)piperazine-1-carboxylate (36a).—** ^{1}H NMR (500 MHz, chloroform-*d*) δ 7.52−7.37 (m, 2H), 7.13−6.93 (m, 3H), 6.55−6.16 (m, 3H), 4.64−4.37 (m, 2H), 3.87−3.69 (m, 2H), 3.69−3.48 (m, 4H), 3.48−3.20 (m, 4H), 3.14−2.88 (m, 3H), 2.78 (s, 2H), 1.94−1.49 (m, 10H), 1.40 (s, 9H), 1.12 (dt, J = 27.6, 7.1 Hz, 3H). MS (ESI) *m/z* = 671.3 $[M + H]^+$.

***tert*-Butyl (*R*)-4-(2-(3-(3-((4-Bromobenzyl)(2-ethoxyethyl)carbamoyl)piperidin-1-yl)phenoxy)-2-methylpropanoyl)piperazine-1-carboxylate (36b).—** ^{1}H NMR (500 MHz, chloroform-*d*) δ 7.42−7.36 (m, 2H), 7.21−7.15 (m, 1H), 7.12−7.05 (m, 1H), 7.02 (dt, J = 8.2, 4.1 Hz, 1H), 6.54−6.34 (m, 1H), 6.34−6.06 (m, 2H), 4.72−4.41 (m, 2H), 3.82−3.22 (m, 14H), 3.11−2.61 (m, 5H), 1.95−1.64 (m, 4H), 1.62−1.57 (m, 6H), 1.39 (s, 9H), 1.12 (t, J = 7.0 Hz, 3H). MS (ESI) *m/z* = 715.4, 717.4 $[M + H]^+$.

***tert*-Butyl (*R*)-4-(2-(3-(3-((4-(1*H*-Pyrazol-4-yl)benzyl)(ethyl)carbamoyl)piperidin-1-yl)phenoxy)-2-methylpropanoyl)piperazine-1-carboxylate (37a).—** ^{1}H NMR (500 MHz, chloroform-*d*) δ 7.83 (d, J = 7.6 Hz, 2H), 7.54−7.41 (m, 2H), 7.23 (d, J = 7.9 Hz, 1H), 7.17 (d, J = 8.0 Hz, 1H), 7.00 (dt, J = 58.6, 8.4 Hz, 1H), 6.57−6.19 (m, 3H), 4.74−4.42 (m, 2H), 3.88−3.54 (m, 6H), 3.54−3.16 (m, 4H), 3.16−2.60 (m, 5H), 1.99−1.66 (m, 4H), 1.65−1.56 (m, 6H), 1.41 (s, 9H), 1.16 (dt, J = 26.5, 7.1 Hz, 3H). MS (ESI) *m/z* = 659.5 $[M + H]^+$, 657.5 $[M - H]^-$.

***tert*-Butyl (*R*)-4-(2-(3-(3-((4-(1H-Pyrazol-4-yl)benzyl)(2-ethoxyethyl)carbamoyl)piperidin-1-yl)phenoxy)-2-methylpropanoyl)piperazine-1-carboxylate (37b).—** ^{1}H NMR (500 MHz, chloroform-*d*) δ 7.83 (s, 2H), 7.46 (dd, J = 21.2, 7.9 Hz, 2H), 7.22 (d, J = 7.9 Hz, 1H), 7.16 (d, J = 8.0 Hz, 1H), 6.99 (dt, J = 56.4, 8.1 Hz, 1H), 6.61−6.40 (m, 1H), 6.37−6.30 (m, 1H), 6.23 (ddd, J = 26.8, 8.2, 2.3 Hz, 1H), 4.83−4.45 (m, 2H), 3.89−3.38 (m, 12H), 3.38−3.23 (m, 2H), 3.15−2.64 (m, 5H), 2.00−1.66 (m, 4H), 1.66−1.52 (m, 6H), 1.41 (s, 9H), 1.16 (td, J = 7.0, 4.2 Hz, 3H). MS (ESI) *m/z* = 703.5 $[M + H]^+$, 701.5 $[M - H]^-$.

Ethyl (*S*)-1-(3-((1-(*tert*-Butoxy)-2-methyl-1-oxopropan-2-yl)oxy)phenyl)piperidine-3-carboxylate (38).— ^{1}H NMR (500 MHz, chloroform-*d*) δ 7.07 (t, J = 8.2 Hz, 1H), 6.57 (ddd, J = 8.3, 2.4, 0.8 Hz, 1H), 6.48 (t, J = 2.4 Hz, 1H), 6.30 (ddd, J = 8.1, 2.3, 0.8 Hz, 1H), 4.20−4.11 (m, 2H), 3.70 (ddt, J = 12.3, 3.5, 1.5 Hz, 1H), 3.51−3.42 (m, 1H), 2.97 (dd, J = 12.4, 10.0 Hz, 1H), 2.77 (tdd, J = 10.2, 4.5, 3.1 Hz, 1H), 2.66−2.56 (m, 1H), 2.06−1.95 (m, 1H), 1.82−1.72 (m, 1H), 1.72−1.62 (m, 2H), 1.55 (s, 6H), 1.44 (s, 9H), 1.27 (t, J = 7.1 Hz, 3H). MS (ESI) *m/z* = 392.2 $[M + H]^+$.

Author Manuscript Author Manuscript Author Manuscript Author Manuscript

***tert*-Butyl (*S*)-4-(2-(3-(3-(Ethoxycarbonyl)piperidin-1-yl)phenoxy)-2-methylpropanoyl)piperazine-1-carboxylate (39).—**^{1}H NMR (500 MHz, chloroform-*d*) δ 7.04 (t, *J* = 8.2 Hz, 1H), 6.54 (dd, *J* = 8.2, 2.3 Hz, 1H), 6.40 (t, *J* = 2.3 Hz, 1H), 6.29−6.21 (m, 1H), 4.14 (q, *J* = 7.1 Hz, 2H), 3.80 (t, *J* = 5.1 Hz, 2H), 3.66 (ddt, *J* = 12.4, 3.5, 1.5 Hz, 1H), 3.58 (d, *J* = 5.3 Hz, 2H), 3.46−3.37 (m, 1H), 3.32 (d, *J* = 5.4 Hz, 2H), 3.06 (t, *J* = 5.2 Hz, 2H), 2.97 (dd, *J* = 12.4, 9.9 Hz, 1H), 2.82−2.68 (m, 1H), 2.61 (tq, *J* = 12.2, 4.3 Hz, 1H), 2.05−1.94 (m, 1H), 1.77 (dddd, *J* = 10.5, 9.1, 5.3, 3.5 Hz, 1H), 1.61 (s, 8H), 1.40 (s, 9H), 1.25 (t, *J* = 7.1 Hz, 3H). MS (ESI) *m/z* =504.3 $[M + H]^+$.

***tert*-Butyl (*S*)-4-(2-(3-(3-((4-Bromobenzyl)(cyclopropyl)carbamoyl)piperidin-1-yl)phenoxy)-2-methylpropanoyl)piperazine-1-carboxylate (40).—**^{1}H NMR (500 MHz, chloroform-*d*) δ 7.42−7.34 (m, 2H), 7.08 (d, *J* = 8.4 Hz, 2H), 7.02 (t, *J* = 8.2 Hz, 1H), 6.48 (dd, *J* = 8.5, 2.3 Hz, 1H), 6.37 (t, *J* = 2.4 Hz, 1H), 6.23 (dd, *J* = 8.2, 2.3 Hz, 1H), 4.58 (d, *J* = 14.7 Hz, 1H), 4.44 (d, *J* = 14.7 Hz, 1H), 3.77 (d, *J* = 7.2 Hz, 2H), 3.61 (d, *J* = 12.5 Hz, 2H), 3.57−3.46 (m, 2H), 3.37 (tt, *J* = 10.9, 3.5 Hz, 1H), 3.31 (s, 2H), 3.07−2.96 (m, 2H), 2.96−2.84 (m, 1H), 2.69 (dd, *J* = 12.0, 3.0 Hz, 1H), 2.56 (td, *J* = 6.6, 3.2 Hz, 1H), 1.89 (d, *J* = 10.9 Hz, 1H), 1.77 (ddd, *J* = 11.6, 7.3, 4.2 Hz, 1H), 1.74−1.65 (m, 2H), 1.58 (d, *J* = 1.4 Hz, 6H), 1.37 (s, 9H), 0.90−0.72 (m, 4H). MS (ESI) *m/z* = 683.4, 685.3 $[M + H]^+$.

***tert*-Butyl (*S*)-4-(2-(3-(3-((4-(1H-Pyrazol-4-yl)benzyl) (cyclopropyl)carbamoyl)piperidin-1-yl) phenoxy)-2-methylpropanoyl)piperazine-1-carboxylate (41).—**^{1}H NMR (500 MHz, chloroform-*d*) δ 7.80 (s, 2H), 7.49−7.38 (m, 2H), 7.22 (d, *J* = 8.0 Hz, 2H), 7.05 (t, *J* = 8.2 Hz, 1H), 6.53 (dd, *J* = 8.3, 2.2 Hz, 1H), 6.42 (t, *J* = 2.4 Hz, 1H), 6.27 (dd, *J* = 8.2, 2.3 Hz, 1H), 4.69 (d, *J* = 14.7 Hz, 1H), 4.53 (d, *J* = 14.7 Hz, 1H), 3.88−3.73 (m, 2H), 3.73−3.64 (m, 2H), 3.64−3.50 (m, 2H), 3.44 (ddt, *J* = 11.0, 7.0, 3.5 Hz, 1H), 3.32 (s, 2H), 3.14−2.95 (m, 3H), 2.76 (td, *J* = 12.1, 2.8 Hz, 1H), 2.63 (tt, *J* = 6.8, 3.2 Hz, 1H), 1.95 (d, *J* = 10.9 Hz, 1H), 1.85−1.71 (m, 3H), 1.62 (s, 6H), 1.41 (s, 9H), 0.92−0.78 (m, 4H). MS (ESI) *m/z* = 671.4 $[M + H]^+$, 669.4 $[M - H]^-$.

Benzyl (2-(2-(2-((4-Bromobenzyl)amino)ethoxy)ethoxy)ethyl)carbamate (42).—^{1}H NMR (500 MHz, chloroform-*d*) δ 7.46−7.39 (m, 2H), 7.39−7.27 (m, 5H), 7.18 (d, *J* = 8.0 Hz, 2H), 5.60 (t, *J* = 5.7 Hz, 1H), 5.09 (s, 2H), 3.72 (s, 2H), 3.64−3.47 (m, 8H), 3.37 (p, *J* = 8.2, 6.8 Hz, 2H), 2.76 (t, *J* = 5.2 Hz, 2H), 2.16 (s, 1H). MS (ESI) *m/z* = 451.2, 453.1 $[M + H]^+$.

***tert*-Butyl (*R*)-4-(2-(3-(3-((4-Bromobenzyl)(3-oxo-1-phenyl-2,7,10-trioxa-4-azadodecan-12-yl)carbamoyl)piperidin-1-yl)phenoxy)-2-methylpropanoyl)piperazine-1-carboxylate (43).—**^{1}H NMR (500 MHz, chloroform-*d*) δ 7.53−7.47 (m, 1H), 7.47− 7.40 (m, 1H), 7.39−7.29 (m, 5H), 7.16−6.97 (m, 3H), 6.60−6.41 (m, 1H), 6.37−6.22 (m, 2H), 5.31 (s, 1H), 5.09 (d, *J* = 2.6 Hz, 2H), 4.77−4.36 (m, 2H), 3.81 (dt, *J* = 10.2, 4.7 Hz, 2H), 3.73−3.28 (m, 18H), 3.17−2.65 (m, 5H), 1.96−1.70 (m, 4H), 1.64 (d, *J* = 2.8 Hz, 6H), 1.44 (s, 9H). MS (ESI) *m/z* = 908.4, 910.4 $[M + H]^+$.

***tert*-Butyl (*R*)-4-(2-Methyl-2-(3-(3-((3-oxo-1-phenyl-2,7,10-trioxa-4-azadodecan-12-yl)(4-(1-trityl-1H-**

Author Manuscript Author Manuscript Author Manuscript Author Manuscript

pyrazol-4-yl)benzyl)carbamoyl)piperidin-1-yl)phenoxy)propanoyl)piperazine-1-carboxylate (44).—^{1}H NMR (500 MHz, chloroform-*d*) δ 7.97−7.87 (m, 1H), 7.61 (dd, *J* = 9.5, 0.8 Hz, 1H), 7.43−7.26 (m, 16H), 7.23−7.14 (m, 7H), 7.14−6.90 (m, 2H), 6.57−6.17 (m, 3H), 5.29 (s, 1H), 5.07 (d, *J* = 3.8 Hz, 2H), 4.83−4.44 (m, 2H), 3.86−3.73 (m, 2H), 3.67−3.26 (m, 18H), 3.17−2.65 (m, 5H), 1.93−1.69 (m, 4H), 1.61 (dd, *J* = 13.3, 2.6 Hz, 6H), 1.42 (d, *J* = 1.3 Hz, 9H).

***tert*-Butyl 4-(2-Methyl-2-(3-((*R*)-3-((2-(2-(2-(5-((3a*S*,4*S*,6a*R*)-2-oxohexahydro-1*H*-thieno[3,4-*d*] imidazol-4-yl)pentanamido)ethoxy)ethoxy)ethyl)(4-(1-trityl-1*H*-pyrazol-4yl)benzyl)carbamoyl)piperidin-1-yl)phenoxy)propanoyl)piperazine-1-carboxylate (45).—**^{1}H NMR (500 MHz, chloroform-*d*) δ 7.93 (dd, *J* = 8.7, 0.8 Hz, 1H), 7.61 (dd, *J* = 11.7, 0.8 Hz, 1H), 7.46−7.40 (m, 1H), 7.40−7.35 (m, 1H), 7.32 (ddd, *J* = 4.5, 3.6, 1.9 Hz, 9H), 7.20−7.16 (m, 7H), 7.12 (d, *J* = 8.2 Hz, 1H), 6.99 (dt, *J* = 58.5, 8.2 Hz, 1H), 6.67−6.37 (m, 2H), 6.36−6.18 (m, 3H), 5.58 (d, *J* = 20.7 Hz, 1H), 4.80−4.40 (m, 3H), 4.32−4.19 (m, 1H), 3.80−3.30 (m, 17H), 3.16−2.89 (m, 5H), 2.86−2.81 (m, 1H), 2.75−2.60 (m, 4H), 2.25−2.12 (m, 2H), 1.97−1.53 (m, 15H), 1.41 (d, *J* = 1.8 Hz, 11H). ^{13}C NMR (126 MHz, chloroform-d) δ 175.0, 174.7, 173.4, 172.1, 156.3, 156.2, 154.4, 154.3, 152.7, 152.4, 143.05, 143.01, 137.2, 135.8, 135.0, 132.1, 131.7, 130.1, 129.6, 129.0, 128.4, 127.85, 127.81, 127.79, 126.7, 126.0, 125.8, 121.2, 121.0, 109.9, 109.8, 105.7, 105.4, 80.6, 80.5, 80.14, 80.12, 78.93, 78.88, 70.6, 70.3, 70.10, 70.06, 69.9, 69.0, 68.7, 61.9, 60.3, 60.2, 55.5, 52.3, 52.1, 52.0, 49.9, 49.6, 48.3, 46.5, 46.0, 45.7, 42.9, 40.5, 39.20, 39.18, 39.10, 38.8, 35.9, 35.8, 28.4, 28.2, 28.1, 28.0, 26.24, 26.18, 25.5, 25.4, 24.4, 24.2.

***tert*-Butyl 4-(2-(3-((*R*)-3-((4-(1*H*-Pyrazol-4-yl)benzyl)(2-(2-(2(5-((3a*S*,4*S*,6a*R*)-2-oxohexahydro-1*H*-thieno[3,4-*d*]imidazol-4-yl)pentanamido)ethoxy)ethoxy)ethyl)carbamoyl)piperidin-1-yl)phenoxy)-2-methylpropanoyl)piperazine-1-carboxylate (46).—**^{1}H NMR (500 MHz, chloroform-*d*) δ 8.31 (dd, *J* = 11.9, 0.9 Hz, 1H), 7.99 (dd, *J* = 8.5, 0.9 Hz, 1H), 7.59−7.52 (m, 1H), 7.52−7.44 (m, 1H), 7.26 (s, 1H), 7.23−7.13 (m, 2H), 7.01 (dt, *J* = 56.2, 8.2 Hz, 1H), 6.62−6.18 (m, 4H), 5.64 (d, *J* = 23.7 Hz, 1H), 4.92−4.50 (m, 3H), 4.47 (dt, *J* = 12.8, 6.4 Hz, 1H), 4.28 (dt, *J* = 13.4, 6.4 Hz, 1H), 3.84−3.25 (m, 18H), 3.19−2.63 (m, 8H), 2.24−2.15 (m, 2H), 1.99−1.54 (m, 15H), 1.42 (d, *J* = 1.7 Hz, 11H).

(*R*)-*N*-(4-(1*H*-Pyrazol-4-yl)benzyl)-1-(3-((2-methyl-1-oxo-1-(piperazin-1-yl)propan-2-yl)oxy)phenyl)-*N*-(2-(2-(2-(5-((3a*S*,4*S*,6a*R*)-2-oxohexahydro-1*H*-thieno[3,4-*d*]imidazol-4-yl)pentanamido)ethoxy)ethoxy)ethyl)piperidine-3-carboxamide (Biotin-ZW4864 as TFA Salt).—1H NMR (500 MHz, methanol-d_4) δ 7.98 (d, *J* = 16.4 Hz, 2H), 7.60 (dd, *J* = 38.8, 8.0 Hz, 2H), 7.26 (t, *J* = 7.7 Hz, 2H), 7.12 (dt, *J* = 88.7, 8.2 Hz, 1H), 6.82−6.58 (m, 1H), 6.54−6.18 (m, 2H), 4.85−4.53 (m, 4H), 4.45 (dd, *J* = 7.8, 4.9 Hz, 1H), 4.25 (dt, *J* = 7.8, 3.8 Hz, 1H), 4.11 (d, *J* = 36.6 Hz, 2H), 3.84 (s, 2H), 3.70 (ddd, *J* = 23.9, 12.2, 7.4 Hz, 3H), 3.62−3.51 (m, 8H), 3.46 (d, *J* = 5.5 Hz, 1H), 3.36 (d, *J* = 5.5 Hz, 1H), 3.29 (s, 1H), 3.19−2.64 (m, 10H), 2.19 (t, *J* = 7.4 Hz, 2H), 2.07−1.51 (m, 15H), 1.39 (p, *J* = 7.8 Hz, 2H). ^{13}C NMR (126 MHz, methanol-d_4) δ 175.5, 175.4, 174.7, 172.32, 172.28, 164.7, 156.15, 156.06, 151.4, 135.6, 135.4, 132.1, 131.8, 130.7, 130.0, 129.8, 127.9, 126.7, 125.7, 125.4, 121.8, 110.9,

Author Manuscript Author Manuscript Author Manuscript Author Manuscript

110.4, 107.9, 106.2, 105.7, 80.6, 80.4, 70.3, 70.0, 69.9, 69.23, 69.21, 68.7, 68.2, 61.9, 60.2, 55.6, 53.0, 51.9, 50.7, 49.8, 46.3, 43.1, 42.7, 39.7, 39.5, 39.1, 39.0, 38.7, 38.2, 35.35, 35.33, 28.37, 28.36, 28.1, 27.4, 27.1, 25.5, 25.05, 25.01, 24.9, 23.6, 23.4. HRMS (ESI) calcd for $C_{46}H_{65}N_9O_7S$ $(M + Na)^+$ 910.4620, found 910.4616. HPLC purity 96.0%, t_R = 8.83 min.

Protein Expression and Purification.

Full-length β-catenin (residues 1−781), β-catenin R1C (residues 138−781), and β-catenin (residues 1−686) were cloned into the pEHISTEV vector carrying an N-terminal 6× histidine tag and transformed into *Escherichia coli* BL21 DE3 (Novagen). Cells were cultured in Luria-Bertani (LB) medium with 50 μg/mL kanamycin until the OD_{600} was approximately 0.8, and then protein expression was induced with 400 μM of isopropyl β-D-1-thiogalactopyranoside (IPTG) at 20 °C overnight. Cells were lysed by sonication. The proteins were purified by three steps of chromatography, including Ni-NTA affinity chromatography (30210, Qiagen), HiTrap Q HP anion-exchange chromatography (17–1154-01, GE Healthcare Life Science), and size-exclusion chromatography with a HiLoad 26/600 Superdex 200 pg column (28–9893-36, GE Healthcare Life Science) using an AKTA Pure FPLC (GE Healthcare Life Science) system. Protein was eluted in a buffer containing 20 mM of Tris (pH 8.5), 100 mM of NaCl, and 2 mM of dithiothreitol (DTT). The purity of β-catenin was greater than 95% as determined by sodium dodecyl sulfate-polyacrylamide gel electrophoresis (SDS-PAGE) gel analyses. Thermal shift assays were performed on a CFX96 Real-Time System (Bio-Rad) to monitor protein stability and detect protein aggregation. Protein unfolding was evaluated through measurement of the fluorescence changes of the fluorescent dye Sypro Orange when interacting with β-catenin proteins. A temperature increment of 1°/min was applied. One set of representative results is shown in Figure S19. All proteins were stable, and no aggregation was observed under storage or assay conditions. Proteins were aliquoted and stored at −80 °C.

BCL9 Peptide Synthesis and Purification.

Human BCL9 (residues 350−375), N-terminally biotinylated human BCL9 (residues 350−375), human E-cadherin (residues 824−877), and N-terminally biotinylated human E-cadherin (residues 824−877) were synthesized by InnoPep Inc. (San Diego, CA, www.innopep.com). All synthesized peptides were purified by HPLC with purity >95%. The structures were validated by LC/MS. The sequences of the peptides are shown in Table 3 (Ahx, 6-aminohexanoic acid).

AlphaScreen Assays of β-Catenin and BCL9 Interaction.

Experiments were performed in white opaque 384-well plates from PerkinElmer (Waltham, MA), and the samples were read on a Biotek Synergy 2 plate reader (Winooski, VT) with an excitation at 680 nm and an emission at 570 nm. The standard AlphaScreen protocol was used with a sensitivity setting of 200. All dilutions were made in a 1× assay buffer containing 25 mM *N*-(2-hydroxyethyl)piperazine-*N*′ ethanesulfonic acid (Hepes) (pH 7.4), 100 mM NaCl, 0.01% Triton X-100, and 0.1% bovine serum albumin (BSA) to minimize nonspecific interactions. For the competitive inhibition assays of the β-catenin/BCL9 PPI, the negative control (equivalent to 0% inhibition) refers to 5.0 nM biotinylated BCL9, 40 nM His_6-tagged β-catenin, and 10 μg/mL donor and acceptor beads in a final volume of

Author Manuscript Author Manuscript Author Manuscript Author Manuscript

a 25 μL assay buffer, but no tested inhibitor was present. The positive control (equivalent to 100% inhibition) refers to 5.0 nM biotinylated BCL9 and 10 μg/mL donor and acceptor beads in a final volume of a 25 μL assay buffer. For the competitive inhibition assays of the β-catenin/E-cadherin PPI, the negative control (equivalent to 0% inhibition) refers to 10 nM biotinylated E-cadherin, 40 nM His_6tagged β-catenin, and 10 μg/mL donor and acceptor beads in a final volume of a 25 μL assay buffer. The positive control (equivalent to 100% inhibition) of the β-catenin/E-cadherin PPI refers to 10 nM biotinylated E-cadherin and 10 μg/mL donor and acceptor beads in a final volume of a 25 μL assay buffer.

For the β-catenin/BCL9 assay, 5 nM biotinylated BCL9 and 50 nM His_6-tagged β-catenin were incubated in an assay buffer for 30 min. For the β-catenin/E-cadherin assay, 10 nM biotinylated human E-cadherin and 50 nM His_6-tagged human β-catenin were added and incubated in an assay buffer for 30 min. Different concentrations of the tested inhibitor were added and incubated in a 20 μL assay buffer for another 1 h. All of the assay plates were covered and gently mixed on an orbital shaker. The donor and acceptor beads were then added to the plates to a final concentration of 10 μg/mL in a 25 μL assay buffer. The mixture was incubated for 1 h at 4 °C before detection. The IC_{50} value was determined by the nonlinear least-square analysis of GraphPad Prism 8.0. The K_i values were derived from the IC_{50} values. The equation used is $K_i = [I]_{50}/([L]_{50}/K_d + [P]_0/K_d + 1)$ (where $[I]_{50}$ denotes the concentration of the free inhibitor at 50% inhibition, $[L]_{50}$ is the concentration of the free labeled ligand at 50% inhibition, $[P]_0$ is the concentration of the free protein at 0% inhibition, and K_d is the dissociation constant of the protein−ligand complex). This equation used free concentrations to derive K_is for competitive inhibition assays (https://bioinfo-abcc.ncifcrf.gov/IC50_Ki_Converter/index.php).[65,66] All of the experiments were performed in triplicate and carried out in the presence of 1% DMSO for small-molecule inhibitors. Each compound was assayed at least by two independent experiments. The results were expressed as mean ± standard deviation. The inhibitor selectivity for β-catenin/BCL9 over β-catenin/E-cadherin interactions was defined as the ratio of the respective K_i value of β-catenin/E-cadherin interactions over that of β-catenin/BCL9 interactions.

Fluorescence Anisotropy Binding Assays to Determine the K_D values.

The fluorescence anisotropy binding assays were performed in 96-well Microfluor 2 black plates (Thermo Fisher Scientific), and the sample signals were read by a Synergy 2 plate reader (Biotek). The experiments were performed in an assay buffer of 25 mM Hepes (pH 7.4), 100 mM NaCl, 0.01% Triton X-100, and 100 μg/mL γ-globulin. The concentration of human BCL9 or E-cadherin fluorescence tracer was fixed at 5 nM. Different concentrations of full-length human β-catenin were added to the assay buffer giving a final volume of 100 μL. After the addition, each assay plate was covered and gently mixed on an orbital shaker for 2 h before the data were recorded at room temperature with an excitation wavelength at 485 nm and an emission wavelength at 535 nm. Each experiment was repeated three times, and the results were expressed as mean ± standard deviation. The parallel fluorescence intensity (I_s), the perpendicular fluorescence intensity (I_p), and the anisotropy (r) were recorded directly by the plate reader. The total intensity (I) and the fraction ligand bound (L_b) are calculated by eqs 1 and 2 shown below[67,68]

Author Manuscript Author Manuscript Author Manuscript Author Manuscript

$$I = 2 \times I_p \times G + I_s \quad (1)$$

G is the G factor. It was 0.993 for the instrument used

$$L_b = \frac{r - r_{min}}{\lambda \times (r_{max} - r) + (r - r_{min})} \quad (2)$$

r_{min} is the average anisotropy value for the fluorescently labeled peptide, and r_{max} is the average anisotropy value for the fluorescently labeled peptide with saturated β-catenin

$$\lambda = \frac{I_{bound}}{I_{unbound}}$$

I_{bound} is the average intensity value for the fluorescently labeled peptide with saturated β-catenin, and $I_{unbound}$ is the average intensity value for the fluorescently labeled peptide

The above data were then imported to GraphPad Prism 8.0, and the K_D value for the protein−protein interaction (PPI) between β-catenin and BCL9 or E-cadherin was analyzed by the nonlinear regression equation (eq 3) shown below

$$\begin{aligned} Y = [&(K_D + X + [\text{fluorescent} - \text{peptide}]) \\ &- \{(K_D + X + [\text{fluorescent} - \text{peptide}])^2 \\ &- 4 \times X \times [\text{fluorescent} - \text{peptide}]\}^{1/2}]/2 \end{aligned} \quad (3)$$

$Y = L_b \times$ [fluorescent-peptide]. [fluorescent-peptide], the concentration was 5 nM. $X =$ [β-catenin].

AlphaScreen Competitive Binding Assays to Determine the K_D Values.

AlphaScreen competitive binding experiments were performed to determine the apparent K_D values of β-catenin/BCL9 and β-catenin/E-cadherin.[44] In the competitive binding experiments to determine the K_D value of full-length β-catenin/BCL9 interaction, 5 nM of N-terminally biotinylated BCL9, 0.5 nM of N-terminally full-length His_6-tagged β-catenin, and different concentrations of unlabeled BCL9 peptide (0−50 μM) were incubated at 4 °C in a 20 μL assay buffer for 2 h. In the competitive binding experiments to determine the K_D value of full-length β-catenin/E-cadherin interactions, 5 nM of N-terminally biotinylated E-cadherin, 0.5 nM of N-terminally full-length His_6-tagged β-catenin, and different concentrations of unlabeled E-cadherin peptide (0−2000 nM) were incubated at 4 °C in a 20 μL assay buffer for 2 h. The streptavidin-coated donor beads and nickel chelate acceptor beads were added to a final concentration of 10 μg/mL in a 25 μL assay buffer. The mixture was covered black and incubated for 2 h before detection. The IC_{50} values, which were also the apparent K_D values from the AlphaScreen assay, were determined by nonlinear least-squares analyses using GraphPad Prism 8.0. The IC_{50} values were determined by nonlinear regression (curve fit) by using a one-site competition binding model (Y = bottom + (top − bottom)/(1 + 10X − Log IC_{50})), X is the logarithm of concentration, and Y is the

Author Manuscript Author Manuscript Author Manuscript Author Manuscript

bound form. Each experiment was repeated three times. The results were expressed as mean ± standard deviation.

β-Catenin Pull-Down Experiments.

SW480 cancer cells with adherently hyperactive β-catenin signaling (70−80% confluency) in T75 flask were lysed first in 1 mL buffer A containing 50 mM Tris (pH 7.4), 150 mM NaCl, 1% Nonidet P-40, 2 mM ethylenediaminetetraacetic acid (EDTA), and protease inhibitors. Cell debris was removed by centrifugation at 10 000*g* for 20 min at 4 °C. In 500 μL SW480 cell lysates or 3 μg purified full-length β-catenin protein in 300 μL buffer B (20 mM Tris pH 7.4,150 mM NaCl, and 0.5% NP-40), 1 or 10 μM biotinylated inhibitor was added in and incubated at 4 °C for 3 h. Then, 25 μL of streptavidin sepharose beads (S-1638, Sigma) was added to the lysate mixture and rotated at 4 °C for 2 h. The lysate mixture was centrifuged at 4000 rpm for 2 min at 4 °C. The beads were washed with buffer B four times. The beads were resuspended in 60 μL of 2× SDS sample buffer. After boiling, the samples were loaded onto an 8% SDS polyacrylamide gel for electrophoretic analysis. Separated proteins were transferred onto nitrocellulose membranes for immunoblot analysis. The antibody against β-catenin (610153, BD Biosciences. Immunogen: mouse β-catenin residues 571−781) was incubated with the membranes. IRDye 800CW goat antirabbit IgG (926–32211, LiCOR) was used as the secondary antibody. The images were detected by the Odyssey Infrared Imaging System (LiCOR). Experiments were performed in triplicate.

SPR Experiments.

Experiments were performed on a Biacore T100 instrument (GE Healthcare). N-Terminally biotinylated human BCL9 (residues 350−375) was immobilized to the surface of a Series S Sensor Chip SA (GE Healthcare) by streptavidin−biotin capturing. Approximately 630 RUs of peptide were immobilized on flow cell 2 (Fc-2). N-Terminally biotinylated mutant human BCL9 (residues 350−375) was immobilized on flow cell 1 (Fc-1) with around 630 RU immobilization as reference surface. Serially diluted inhibitors (0.0013−30 μM) were mixed with full-length β-catenin (residues 1−781) 700 nM in running buffer (20 mM Tris·HCl, pH 7.5, 100 mM NaCl, 0.005% P-20, 1% DMSO) and incubated for 1 h at room temperature. Then, the mixtures were injected over surfaces at 25 °C at a flow rate of 20 μL/min for 600 s with a dissociation time of 420 s. Regeneration was a 75 s injection once with buffer (10 mM glycine· HCl and 5% glycerol, pH 3.0) at 30 μL/min. To subtract background noise from each data set, all samples were also run over reference surface, and random injections of running buffer were performed throughout every experiment (double referencing). Data were fit to a simple 1:1 interaction with the global data analysis program GraphPad Prism 8.0.

Co-IP Experiments.

HCT116 cancer cells with hyperactive β-catenin signaling at 1×10^6 cells/mL were treated with different concentrations of the inhibitor for 24 h. Cells were lysed in buffer containing 50 mM Tris, pH 7.4, 150 mM NaCl, 1% Nonidet P-40, 2 mM EDTA, and protease inhibitors. For Pygo2-BCL9 and Pygo-β-catenin co-IP experiments, HCT116 cell nuclear extracts were used. The nuclear extracts were prepared using the NE-PER Nuclear and Cytoplasmic Extraction Reagents (78835, Thermo Scientific). The cell lysates or nuclear

Author Manuscript Author Manuscript Author Manuscript Author Manuscript

extracts were preadsorbed to A/G plus agarose (sc-2003, Santa Cruz Biotechnology) at 4 °C for 1 h. Preadsorbed lysates were incubated with a specific primary antibody against β-catenin (610153, BD Biosciences) or Pygo2 (MA524240, Invitrogen. Immunogen: human Pygopus-2 residues 160−336) overnight at 4 °C. A/G plus agarose was then added to the lysate mixture and incubated for 3 h. The beads were washed four times with the lysis buffer at 4 °C. The bound protein was eluted by boiling in the SDS sample buffer and loaded onto an 8% SDS polyacrylamide gel for electrophoretic analysis. Separated proteins were transferred onto nitrocellulose membranes for immunoblot analysis. The antibodies against BCL9 (ab37305, Abcam. Immunogen: human BCL9 residues 800−900), β-catenin (610153, BD Biosciences), E-cadherin (610404, BD Biosciences. Immunogen: human E-cadherin residues 735−883), Pygo2 (MA524240, Invitrogen), β-tubulin (sc-55529, Santa Cruz Biotechnology. Immunogen: human β-tubulin residues 210−444), and lamin B1 (sc-374015, Santa Cruz Biotechnology. Immunogen: mouse lamin B1 residues: 559−586) were incubated with the membranes. IRDye 680LT goat antimouse IgG (827–11080, LiCOR) and IRDye 800CW goat antirabbit IgG (926–32211, LiCOR) were used as the secondary antibodies. The images were detected by the Odyssey Infrared Imaging System (LiCOR). Experiments were performed in triplicate.

Cell Transfection and Luciferase Assays.

A FuGENE6 (E269A, Promega) 96-well plate format was used for the transfection of cells according to the manufacturer's instruction. HEK293 cells were cotransfected with 45 ng of TOPFlash or FOPFlash reporter gene, 135 ng of pcDNA3.1−β-catenin, and 20 ng of pCMV-RL normalization reporter gene. SW480 or MDA-MB-468 cells were cotransfected with 60 ng of TOPFlash or FOPFlash firefly luciferase reporter gene and 40 ng of renilla luciferase pCMV-RL normalization reporter. HEK293 or SW480 cells were cultured in DMEM and 10% FBS at 37 °C for 24 h, and different concentrations of inhibitors or DMSO were added and incubated in DMEM with 5% FBS. MDA-MB-468 cells were treated with Wnt3a (100 ng/mL) (rmW3aL-010, Time Bioscience) for 30 min, and different concentrations of inhibitors or DMSO was added and incubated in DMEM with 5% FBS. After the 24-h incubation, the luciferase reporter activity was measured using the Dual-Glo system (E2940, Promega). Normalized luciferase activity in response to the treatment with inhibitors was compared with that obtained from the cells treated with DMSO. Experiments were performed in triplicate.

qPCR Analyses.

SW480 cells at 1×10^6 cells/mL were treated with inhibitors at different concentrations for 24 h. MDA-MB-231 cells at 1×10^6 cells/mL were treated with Wnt 3a (100 ng/mL) for 30 min, and then the inhibitors at different concentrations were added and incubated for 24 h. Total RNAs were extracted with TRIzol (15596026, Life Technologies), and the cDNA was synthesized with the superscript III first-strand kit (18080–051, Invitrogen). qPCR experiments were performed using the iQTM SYBR green supermix kit (170–8880, BIO-RAD) on a CFX96 Real-Time System (BIO-RAD). The threshold cycle (CT) values were normalized to that of internal reference GAPDH. Experiments were performed in triplicate. The primer pairs are human *GAPDH* forward: 5′-GAAGGTGAAGGTCGGAGTC-3′, reverse: 5′-GAAGATGGTGATGGGATTTC-3′;

Author Manuscript Author Manuscript Author Manuscript Author Manuscript

human *HPRT* forward: 5′-GCTATAAATTCTTTGCTGACCTGCTG-3′, reverse: 5′-AATTACTTTTATGTCCCCTGTTGACTGG-3′; human *AXIN2* forward: 5′AGTGTGAGGTCCACGGAAAC-3′, reverse: 5′-CTTCACACTGCGATGCATTT-3′; human *LEF1* forward: 5′-GACGAGATGATCCCCTTCAA-3′, reverse: 5′-AGGGCTCCTGAGAGGTTTGT-3′; human *LEF1* forward: 5′-CCAATCTCAGCACCAGAATGTG-3′, reverse: 5′-TTGCTAGGCGAGATCTGGTTG3′; human *cyclin D1* forward: 5′-ACAAACAGATCATCCGCAAACAC-3′, reverse: 5′-TGTTGGGGCTCCTCAGGTTC-3′; human *TWIST* forward: 5′-GTCCGCAGTCTTACGAGGAG-3′, reverse: 5′-TGGAGGACCTGGTAGAGGAA-3′; human *SNAIL* forward: 5′-GGTTCTTCTGCGCTACTGCT-3′, reverse: 5′-TAGGGCTGCTGGAAGGTAAA-3′; human *TENASCIN C* forward: 5′-GAGATTTAGCCGTGTCTGAGGTTG-3′, reverse: 5′-GCCATCCAGGAGAGATTGAAGC-3′; human *LGR5* forward: 5′TGCTGGCTGGTGTGGATGCG-3′, reverse: 5′-GCCAGCAGGGCACAGAGCAA-3′; human *VEGF-A* forward: 5′ -CTTGCCTTGCTGCTCTACC-3′, reverse: 5′-CACACAGGATGGCTTGAAG-3′; human *CD44* forward: 5′CGCTTTGCAGGTGTATTCCA-3′, reverse: 5′-ACCACGTGCCCTTCTATGAA-3′; human *Slug* forward: 5′-GGGGAGAAGCCTTTTTCTTG-3′, reverse, 5′-TCCTCATGTTTGTGCAGGAG-3′.

Western Blotting of Wnt Target Genes.

SW480 cells at 1×10^6 cells/mL were treated with different concentrations of inhibitors for 24 h. MDA-MB-231 cells at 1×10^6 cells/mL were treated with Wnt3a (100 ng/mL) for 30 min, then the inhibitors at different concentration were added and incubated for 24 h. Cells were lysed in buffer containing 50 mM Tris (pH 7.4), 150 mM NaCl, 1% Nonidet P-40, 0.5% sodium deoxycholate, 0.1% SDS, and protease inhibitors. After centrifugation at 12 000 rpm for 20 min at 4 °C, the supernatant was loaded onto an 8% SDS polyacrylamide gel for electrophoretic analysis. Separated proteins were transferred onto nitrocellulose membranes for immunoblot analysis. The antibodies against Axin2 (MA5–15015, Thermo Fisher. Immunogen: residues surrounding Pro566 of human Axin2), cyclin D1 (sc-853, Santa Cruz Biotechnology. Immunogen: human cyclin D1 residues 1−295), and β-tubulin (sc-55529, Santa Cruz Biotechnology) were incubated with the membranes overnight at 4 °C. IRDye 680LT goat antimouse IgG (827–11080, LiCOR) or IRDye 800CW goat antirabbit IgG (827–08365, LiCOR) was used as the secondary antibody. The images were detected by the Odyssey Infrared Imaging System (LiCOR). Experiments were performed in triplicate.

MTS Cell Growth Inhibition Experiments.

Colorectal cancer cells (SW480 and HCT116) and TNBC cells (MDA-MB-231, MDA-MB-468) were seeded in 96-well plates at 5×10^3 cells/well in DMEM with 10% fetal calf serum (FCS), maintained overnight at 37 °C, and then incubated with the tested compounds at various concentrations in DMEM with 5% FBS. Human mammary epithelial cell MCF10A was seeded in 96-well plates at 1×10^4 cells/well in MEGM (CC-3150, Lonza) with 100 ng/mL cholera toxin, maintained overnight at 37 °C, and incubated with the tested compounds at various concentrations. Cell viability was monitored after 72 h using a

Author Manuscript Author Manuscript Author Manuscript Author Manuscript

freshly prepared mixture of 1 part phenazine methosulfate (PMS, Sigma-Aldrich) solution (0.92 mg/mL) and 19 parts 3-(4,5-dimethylthiazol-2-yl)-5-(3-carboxymethoxyphenyl)-2-(4-sulfophenyl)-2H-tetrazolium (MTS, Promega) solution (2 mg/mL). Cells were incubated in 10 μL of this solution at 37 °C for 3 h, and A490 was measured. The effect of each compound was expressed as the concentration required to reduce A490 by 50% (IC_{50}) relative to DMSO-treated cells. Experiments were performed in triplicate.

β-Catenin Rescue Experiments.

TNBC MDA-MB-231 and MDA-MB-468 cells were seeded in 96-well plates at 5 × 10^3 cells/well in DMEM with 10% FCS, maintained overnight at 37 °C. Then, 250 ng of pcDNA3.1−β-catenin or empty vector pcDNA3.1 per well was transfected into the cells, and 1 h later, the tested compounds at various concentrations were added into the cells. Cell viability was monitored after 72 h using a freshly prepared mixture of 1 part phenazine methosulfate (PMS, Sigma-Aldrich) solution (0.92 mg/mL) and 19 parts 3-(4,5-dimethylthiazol-2-yl)-5-(3-carboxymethoxyphenyl)-2-(4-sulfophenyl)-2*H*-tetrazolium (MTS, Promega) solution (2 mg/mL). Cells were incubated in 10 μL of this solution at 37 °C for 3 h, and A490 was measured. The effect of each compound is expressed as the concentration required to reduce A490 by 50% (IC_{50}) relative to DMSO-treated cells. Experiments were performed in triplicate.

Clonogenic Assays.

Cells were plated in six-well dishes in triplicate at a density of 1000 cells per well. After incubation overnight, inhibitor or vehicle (0.1% DMSO) was added to the medium (DMEM with 10% FCS) for 72 h, and cells were allowed to grow out for 7−10 days, during which the medium was changed every 2−3 days without adding the compound. Colonies were fixed in acetic acid/methanol (1:7, v/v) for 5 min, stained with 0.5% crystal violet for 2 h at room temperature, and destained with water. Colonies with more than 50 cells were counted using a low-magnification light microscope. Experiments were performed in triplicate.

FACS Experiments.

Cells (2.5 × 10^5) seeded in triplicate in six-well dishes were cultured with compounds or vehicle (0.1% DMSO) for 72 h. Cells were then harvested and stained with annexin V−fluorescein isothiocyanate (FITC) and propidium iodide (PI) using the FITC Annexin V Apoptosis Detection Kit (556547, BD Biosciences) as per the manufacturer's instructions and analyzed with the FACSCanto II flow cytometer. Experiments were performed in triplicate.

Scratch Wound Healing Experiments.

To the confluent monolayer of MDA-MB-231 cells in 24-well plates, wounds will be made by scraping a sterile 200 μL pipette tip. Cells were maintained in DMEM containing 10% FBS with 10 μg/mL of mitomycin to inhibit cell proliferation and with different concentrations of inhibitors. Images of wounds were taken immediately and 14 h after wounding. Experiments were performed in triplicate.

Author Manuscript Author Manuscript Author Manuscript Author Manuscript

Matrigel Invasion Experiments.

MDA-MB-231 cells (5×10^4 cells) suspended in a 200 μL starvation medium were added to the upper chamber of a Matrigel-coated insert with a 6.5 mm diameter and an 8 mm pore size (353097, Corning). The insert was placed in a 24-well plate containing 600 mL of DMEM medium with 10% FBS. Inhibitors were added to both the upper and the lower chambers. Invasion assays were performed for 24 h, and cells were fixed with 3.7% formaldehyde. Cells were stained with crystal violet staining solution. The cells on the upper side of the insert were removed with a cotton swab. Five randomly selected fields (10× objectives) on the lower side of the insert were photographed, and the invaded cells were counted. Experiments were performed in triplicate.

Three-Dimensional (3D) Spheroid BME Cell Invasion Assays.

The 3D invasion assays were performed using the 96-well 3D Spheroid BME Cell Invasion Assay kit (3500–096-K, Cultrex) following the manufacturer's protocol. Briefly, MDA-MB-231 cells were mixed with the kit-supplied ECM and seeded into ultralow attachment plates (3,000 cells/well). The plates were then centrifuged at 300g for 5 min and incubated at 37 °C for 72 h for spheroid formation. After that, the kit-supplied BME matrix was added and preincubated on ice for 10 min, followed by centrifugation at 300g, 4 °C for 5 min. Then, the inhibitor at various concentrations was added. The plates were cultured for 6 days at 37 °C. The spheroid in each well was photographed every 24 h using the 4× objective. The images were analyzed using the image analysis software Image*J* to measure the changes in the area of the invasive structures to determine the extent of 3D culture BME cell invasion for each sample.

DMPK and PD Studies.

Microsome stability was evaluated by incubating 1 μM of compound with 1 mg/mL of hepatic microsomes (human, rat, or mouse) in 100 mM of potassium phosphate buffer, pH 7.4. The reactions were held at 37 °C with continuous shaking. The reaction was initiated by adding reduced nicotinamide adenine dinucleotide phosphate (NADPH) (1 mM final concentration). The final incubation volume was 300 μL, and 40 μL aliquots were removed at 0, 5, 10, 20, 40, and 60 min. The removed aliquot was added to 160 μL acetonitrile to stop the reaction and precipitate the protein. NADPH dependence of the reaction was evaluated in parallel incubations without NADPH. At the end of the assay, the samples were centrifuged through a 0.45 μm filter plate (MSRLN0450, Millipore Multiscreen Solventer low binding poly(tetrafluoroethylene) (PTFE) hydrophilic plates) and analyzed by LC-MS/MS. The data were log-transformed, and the results are reported as half-life and intrinsic clearance.

The procedures of mouse PK studies are covered under existing protocols and have been approved by the Scripps Florida IACUC (IACUC Protocol #: 15–022-02) to be conducted in the Scripps vivarium, which is fully AAALAC accredited. Pharmacokinetics were determined in $n = 3$ male C57BL/6 mice (Charles River, strain code #027). Compounds were dosed as indicated via intravenous (i.v.) injection via tail vein or oral (p.o.) gavage. Twenty-five microliters of blood was collected via a small nick in the tail using heparin-coated hematocrit capillary tubes, which were sealed with wax and kept on ice until plasma was generated by centrifugation using a refrigerated centrifuge equipped with a hematocrit

Author Manuscript Author Manuscript Author Manuscript Author Manuscript

rotor. Dose levels are provided as described. Time points for determination of PK parameters were 5 min (i.v. only), 15 min, 30 min, 1 h, 2 h, 4 h, 6 h, 8 h, and 24 h (p.o. only). Plasma concentrations were determined via LC-MS/MS using an eight-point standard curve between 2 and 2000 ng/mL prepared in mouse plasma. The PK analyses were done with WinNonLin, Pharsight Inc., using a noncompartmental model.

For PD analyses, female Fox Chase SCID-Beige mice (Charles River, strain code no. 250, $n = 4$) with orthotopically implanted PDX 4013 tumors were used. All animal studies were approved by the University of South Florida/Moffitt Cancer Center Animal Care and Use Committee (IACUC Protocol no. R IS00005598). **ZW4864** was dosed as indicated in the text via oral gavage. Tumor was snap-frozen in liquid nitrogen and kept at −80 °C until processed. The PD studies were performed from tumor samples. RNA was extracted using Qiagen RNAeasy kit (74104, Qiagen) as per the manufacturer's instructions, and qPCR experiments were performed as described above.

Supplementary Material

Refer to Web version on PubMed Central for supplementary material.

ACKNOWLEDGMENTS

This work was supported by the Susan G. Komen Career Catalyst Research Grant CCR16380693, the Floridian Breast Cancer Foundation Scientific Grant (19012901), and the 2020 Moffitt Team Science Grant. The H. Lee Moffitt Cancer Center & Research Institute is an NCI-designated Comprehensive Cancer Center, supported under NIH grant P30CA76292. The authors thank Dr. Michael Cameron and his team in the Drug Metabolism and Pharmacokinetics (DMPK) core facility at the Scripps Research Institute for microsome stability and mouse PK studies.

ABBREVIATIONS

APC	adenomatous polyposis coli
BCL9	B-cell lymphoma 9
BCL9L	BCL9-like
CBP	CREB-binding protein
CK1α	casein kinase 1α
co-IP	coimmunoprecipitation
Dvl	disheveled
FACS	fluorescence-activated cell sorting
Fzd	frizzled
GSK3β	glycogen synthase kinase 3β
K_i	inhibition constant
LEF	lymphoid enhancer-binding factor

Author Manuscript Author Manuscript Author Manuscript Author Manuscript

PAINS	pan-assay interference compounds
PNPB	3-(4-fluorophenyl)-*N*-phenylbenzamide
PP2A	protein phosphatase 2A
PPI	protein–protein interaction
Pygo	Pygopus
qPCR	quantitative real-time PCR
TCF	T-cell factor

REFERENCES

(1). Nusse R; Clevers H. Wnt/β-catenin signaling, disease, and emerging therapeutic modalities. Cell 2017, 169, 985–999. [PubMed: 28575679]

(2). Liu Z; Wang P; Wold EA; Song Q; Zhao C; Wang C; Zhou J. Small-molecule inhibitors targeting the canonical WNT signaling pathway for the treatment of cancer. J. Med. Chem 2021, 64, 4257–4288. [PubMed: 33822624]

(3). Liu J; Pan S; Hsieh MH; Ng N; Sun F; Wang T; Kasibhatla S; Schuller AG; Li AG; Cheng D; Li J; Tompkins C; Pferdekamper A; Steffy A; Cheng J; Kowal C; Phung V; Guo G; Wang Y; Graham MP; Flynn S; Brenner JC; Li C; Villarroel MC; Schultz PG; Wu X; McNamara P; Sellers WR; Petruzzelli L; Boral AL; Seidel HM; McLaughlin ME; Che J; Carey TE; Vanasse G; Harris JL Targeting Wnt-driven cancer through the inhibition of Porcupine by LGK974. Proc. Natl. Acad. Sci. U.S.A 2013, 110, 20224–20229. [PubMed: 24277854]

(4). Madan B; Ke Z; Harmston N; Ho SY; Frois AO; Alam J; Jeyaraj DA; Pendharkar V; Ghosh K; Virshup IH; Manoharan V; Ong EH; Sangthongpitag K; Hill J; Petretto E; Keller TH; Lee MA; Matter A; Virshup DM Wnt addiction of genetically defined cancers reversed by PORCN inhibition. Oncogene 2016, 35, 2197–2207. [PubMed: 26257057]

(5). Yang D; Fu W; Li L; Xia X; Liao Q; Yue R; Chen H; Chen X; An S; Zeng C; Wang WE Therapeutic effect of a novel Wnt pathway inhibitor on cardiac regeneration after myocardial infarction. Clin. Sci 2017, 131, 2919–2932.

(6). Bhamra I; Armer R; Bingham M; Eagle C; Cook AE; Phillips C; Woodcock S. Porcupine inhibitor RXC004 enhances immune response in pre-clinical models of cancer. Cancer Res. 2018, 78, No. 3764.

(7). Le PN; McDermott JD; Jimeno A. Targeting the Wnt pathway in human cancers: therapeutic targeting with a focus on OMP-54F28. Pharmacol. Ther 2015, 146, 1–11. [PubMed: 25172549]

(8). Jimeno A; Gordon M; Chugh R; Messersmith W; Mendelson D; Dupont J; Stagg R; Kapoun AM; Xu L; Uttamsingh S; Brachmann RK; Smith DC A first-in-human phase I study of the anticancer stem cell agent Ipafricept (OMP54F28), a decoy receptor for Wnt ligands, in patients with advanced solid tumors. Clin. Cancer Res 2017, 23, 7490–7497. [PubMed: 28954784]

(9). Gurney A; Axelrod F; Bond CJ; Cain J; Chartier C; Donigan L; Fischer M; Chaudhari A; Ji M; Kapoun AM; Lam A; Lazetic S; Ma S; Mitra S; Park IK; Pickell K; Sato A; Satyal S; Stroud M; Tran H; Yen W-C; Lewicki J; Hoey T. Wnt pathway inhibition via the targeting of Frizzled receptors results in decreased growth and tumorigenicity of human tumors. Proc. Natl. Acad. Sci. U.S.A 2012, 109, 11717–11722. [PubMed: 22753465]

(10). Lyou Y; Habowski AN; Chen GT; Waterman ML Inhibition of nuclear Wnt signalling: challenges of an elusive target for cancer therapy. Br. J. Pharmacol 2017, 174, 4589–4599. [PubMed: 28752891]

(11). Cui C; Zhou X; Zhang W; Qu Y; Ke X. Is β-catenin a druggable target for cancer therapy? Trends Biochem. Sci 2018, 43, 623–634. [PubMed: 30056837]

(12). Wang Z; Li Z; Ji H. Direct targeting of β-catenin in the Wnt signaling pathway: Current progress and perspectives. Med. Res. Rev 2021, 41, 2109–2129. [PubMed: 33475177]

Author Manuscript Author Manuscript Author Manuscript Author Manuscript

(13). Sampietro J; Dahlberg CL; Cho US; Hinds TR; Kimelman D; Xu W. Crystal structure of a β-catenin/BCL9/Tcf4 complex. Mol. Cell 2006, 24, 293–300. [PubMed: 17052462]

(14). Graham TA; Weaver C; Mao F; Kimelman D; Xu W. Crystal structure of a β-catenin/Tcf complex. Cell 2000, 103, 885–896. [PubMed: 11136974]

(15). Poy F; Lepourcelet M; Shivdasani RA; Eck MJ Structure of a human Tcf4-β-catenin complex. Nat. Struct. Biol 2001, 8, 1053–1057. [PubMed: 11713476]

(16). Graham TA; Ferkey DM; Mao F; Kimelman D; Xu W. Tcf4 can specifically recognize β-catenin using alternative conformations. Nat. Struct. Biol 2001, 8, 1048–1052. [PubMed: 11713475]

(17). Sun J; Weis WI Biochemical and structural characterization of β-catenin interactions with nonphosphorylated and CK2phosphorylated Lef-1. J. Mol. Biol 2011, 405, 519–530. [PubMed: 21075118]

(18). Huber AH; Weis WI The structure of the β-catenin/Ecadherin complex and the molecular basis of diverse ligand recognition by β-catenin. Cell 2001, 105, 391–402. [PubMed: 11348595]

(19). Ha NC; Tonozuka T; Stamos JL; Choi HJ; Weis WI Mechanism of phosphorylation-dependent binding of APC to βcatenin and its role in β-catenin degradation. Mol. Cell 2004, 15, 511–521. [PubMed: 15327768]

(20). Xing Y; Clements WK; Le Trong I; Hinds TR; Stenkamp R; Kimelman D; Xu W. Crystal structure of a β-catenin/ APC complex reveals a critical role for APC phosphorylation in APC function. Mol. Cell 2004, 15, 523–533. [PubMed: 15327769]

(21). Fiedler M; Graeb M; Mieszczanek J; Rutherford TJ; Johnson CM; Bienz M. An ancient Pygo-dependent Wnt enhanceosome integrated by Chip/LDB-SSDP. Elife 2015, 4, No. e09073.

(22). van Tienen LM; Mieszczanek J; Fiedler M; Rutherford TJ; Bienz M. Constitutive scaffolding of multiple Wnt enhanceosome components by Legless/BCL9. Elife 2017, 6, No. e20882.

(23). Mani M; Carrasco DE; Zhang Y; Takada K; Gatt ME; Dutta-Simmons J; Ikeda H; Diaz-Griffero F; Pena-Cruz V; Bertagnolli M; Myeroff LL; Markowitz SD; Anderson KC; Carrasco DR BCL9 promotes tumor progression by conferring enhanced proliferative, metastatic, and angiogenic properties to cancer cells. Cancer Res. 2009, 69, 7577–7586. [PubMed: 19738061]

(24). Elsarraj HS; Hong Y; Valdez KE; Michaels W; Hook M; Smith WP; Chien J; Herschkowitz JI; Troester MA; Beck M; Inciardi M; Gatewood J; May L; Cusick T; McGinness M; Ricci L; Fan F; Tawfik O; Marks JR; Knapp JR; Yeh H-W; Thomas P; Carrasco DR; Fields TA; Godwin AK; Behbod F. Expression profiling of in vivo ductal carcinoma in situ progression models identified B cell lymphoma-9 as a molecular driver of breast cancer invasion. Breast Cancer Res. 2015, 17, No. 128.

(25). Huge N; Sandbothe M; Schröder AK; Stalke A; Eilers M; Schäffer V; Schlegelberger B; Illig T; Vajen B; Skawran B. Wnt status-dependent oncogenic role of BCL9 and BCL9L in hepatocellular carcinoma. Hepatol. Int 2020, 14, 373–384. [PubMed: 31440992]

(26). Li J; Chen X; Ding X; Cheng Y; Zhao B; Lai ZC; Al Hezaimi K; Hakem R; Guan KL; Wang CY LATS2 suppresses oncogenic Wnt signaling by disrupting β-catenin/BCL9 interaction. Cell Rep. 2013, 5, 1650–1663. [PubMed: 24360964]

(27). Adachi S; Jigami T; Yasui T; Nakano T; Ohwada S; Omori Y; Sugano S; Ohkawara B; Shibuya H; Nakamura T; Akiyama T. Role of a BCL9-related β-catenin-binding protein, B9L, in tumorigenesis induced by aberrant activation of Wnt signaling. Cancer Res. 2004, 64, 8496–8501. [PubMed: 15574752]

(28). de la Roche M; Worm J; Bienz M. The function of BCL9 in Wnt/β-catenin signaling and colorectal cancer cells. BMC Cancer 2008, 8, No. 199.

(29). Brembeck FH; Schwarz-Romond T; Bakkers J; Wilhelm S; Hammerschmidt M; Birchmeier W. Essential role of BCL9–2 in the switch between β-catenin's adhesive and transcriptional functions. Genes Dev. 2004, 18, 2225–2230. [PubMed: 15371335]

(30). Brembeck FH; Wiese M; Zatula N; Grigoryan T; Dai Y; Fritzmann J; Birchmeier W. BCL9–2 promotes early stages of intestinal tumor progression. Gastroenterology 2011, 141, 1359.e3–1370.e3. [PubMed: 21703997]

(31). Gay DM; Ridgway RA; Muller M; Hodder MC; Hedley A; Clark W; Leach JD; Jackstadt R; Nixon C; Huels DJ; Campbell AD; Bird TG; Sansom OJ Loss of BCL9/9l suppresses Wnt driven tumourigenesis in models that recapitulate human cancer. Nat. Commun 2019, 10, No. 723.

Author Manuscript Author Manuscript Author Manuscript Author Manuscript

(32). Moor AE; Anderle P; Cantú C; Rodriguez P; Wiedemann N; Baruthio F; Deka J; André S; Valenta T; Moor MB; Győrffy B; Barras D; Delorenzi M; Basler K; Aguet M. BCL9/ 9L-β-catenin signaling is associated with poor outcome in colorectal cancer. EBioMedicine 2015, 2, 1932–1943. [PubMed: 26844272]

(33). Mieszczanek J; van Tienen LM; Ibrahim AEK; Winton DJ; Bienz M. Bcl9 and Pygo synergise downstream of Apc to effect intestinal neoplasia in FAP mouse models. Nat. Commun 2019, 10, No. 724.

(34). Kawamoto SA; Coleska A; Ran X; Yi H; Yang CY; Wang S. Design of triazole-stapled BCL9 α-helical peptides to target the β-catenin/B-cell CLL/lymphoma 9 (BCL9) protein-protein interaction. J. Med. Chem 2012, 55, 1137–1146. [PubMed: 22196480]

(35). Takada K; Zhu D; Bird GH; Sukhdeo K; Zhao JJ; Mani M; Lemieux M; Carrasco DE; Ryan J; Horst D; Fulciniti M; Munshi NC; Xu W; Kung AL; Shivdasani RA; Walensky LD; Carrasco DR Targeted disruption of the BCL9/β-catenin complex inhibits oncogenic Wnt signaling. Sci. Transl. Med 2012, 4, No. 148ra117.

(36). Feng M; Jin JQ; Xia L; Xiao T; Mei S; Wang X; Huang X; Chen J; Liu M; Chen C; Rafi S; Zhu AX; Feng YX; Zhu D. Pharmacological inhibition of β-catenin/BCL9 interaction overcomes resistance to immune checkpoint blockades by modulating Treg cells. Sci. Adv 2019, 5, No. eaau5240.

(37). Sang P; Zhang M; Shi Y; Li C; Abdulkadir S; Li Q; Ji H; Cai J. Inhibition of β-catenin/B cell lymphoma 9 protein-protein interaction using α-helix-mimicking sulfono-γ-AApeptide inhibitors. Proc. Natl. Acad. Sci. U.S.A 2019, 116, 10757–10762. [PubMed: 31088961]

(38). de la Roche M; Rutherford TJ; Gupta D; Veprintsev DB; Saxty B; Freund SM; Bienz M. An intrinsically labile α-helix abutting the BCL9-binding site of β-catenin is required for its inhibition by carnosic acid. Nat. Commun 2012, 3, No. 680.

(39). de la Roche M; Ibrahim AE; Mieszczanek J; Bienz M. LEF1 and B9L shield β-catenin from inactivation by Axin, desensitizing colorectal cancer cells to tankyrase inhibitors. Cancer Res. 2014, 74, 1495–1505. [PubMed: 24419084]

(40). Hoggard LR; Zhang Y; Zhang M; Panic V; Wisniewski JA; Ji H. Rational design of selective small-molecule inhibitors for βcatenin/B-cell lymphoma 9 protein-protein interactions. J. Am. Chem. Soc 2015, 137, 12249–12260. [PubMed: 26352795]

(41). Zhang M; Wang Z; Zhang Y; Guo W; Ji H. Structure-based optimization of small-molecule inhibitors for the β-catenin/Bcell lymphoma 9 protein–protein interaction. J. Med. Chem 2018, 61, 2989–3007. [PubMed: 29566337]

(42). Wisniewski JA; Yin J; Teuscher KB; Zhang M; Ji H. Structure-based design of 1,4-dibenzoylpiperazines as β-catenin/B-cell lymphoma 9 protein–protein interaction inhibitors. ACS Med. Chem. Lett 2016, 7, 508–513. [PubMed: 27190602]

(43). Li Z; Zhang M; Teuscher KB; Ji H. Discovery of 1Benzoyl 4-Phenoxypiperidines as Small-Molecule Inhibitors of the β-Catenin/B-Cell Lymphoma 9 Protein–Protein Interaction. J. Med. Chem 2021, 64, 11195–11218. [PubMed: 34270257]

(44). Zhang M; Wisniewski JA; Ji H. AlphaScreen selectivity assay for β-catenin/B-cell lymphoma 9 inhibitors. Anal. Biochem 2015, 469, 43–53. [PubMed: 25312469]

(45). Wang Z; Zhang M; Luo W; Zhang Y; Ji H. Discovery of 2-(3-(3-carbamoylpiperidin-1-yl)phenoxy)acetic acid derivatives as novel small-molecule inhibitors of the β-catenin/B-cell lymphoma 9 protein-protein interaction. J. Med. Chem 2021, 64, 5886–5904. [PubMed: 33902288]

(46). Choi H-J; Huber AH; Weis WI Thermodynamics of β-catenin-ligand interactions: the roles of the N- and C-terminal tails in modulating binding affinity. J. Biol. Chem 2006, 281, 1027–1038. [PubMed: 16293619]

(47). Choi H-J; Gross JC; Pokutta S; Weis WI Interactions of plakoglobin and β-catenin with desmosomal cadherins: basis of selective exclusion of α- and β-catenin from desmosomes. J. Biol. Chem 2009, 284, 31776–31788. [PubMed: 19759396]

(48). Emami KH; Nguyen C; Ma H; Kim DH; Jeong KW; Eguchi M; Moon RT; Teo JL; Oh SW; Kim HY; Moon SH; Ha JR; Kahn M. A small molecule inhibitor of β-catenin/ CREB-binding protein transcription. Proc. Natl. Acad. Sci. U.S.A 2004, 101, 12682–12687. [PubMed: 15314234]

Author Manuscript Author Manuscript Author Manuscript Author Manuscript

(49). Kaelin WG Jr. Common pitfalls in preclinical cancer target validation. Nat. Rev. Cancer 2017, 17, 441–450.

(50). Howe LR; Watanabe O; Leonard J; Brown AM Twist is up-regulated in response to Wnt1 and inhibits mouse mammary cell differentiation. Cancer Res. 2003, 63, 1906–1913. [PubMed: 12702582]

(51). Yook JI; Li X-Y; Ota I; Fearon ER; Weiss SJ Wnt-dependent regulation of the E-cadherin repressor snail. J. Biol. Chem 2005, 280, 11740–11748. [PubMed: 15647282]

(52). Yook JI; Li X-Y; Ota I; Hu C; Kim HS; Kim NH; Cha SY; Ryu JK; Choi YJ; Kim J; Fearon ER; Weiss SJ A Wnt-Axin2-GSK3β cascade regulates Snail1 activity in breast cancer cells. Nat. Cell Biol 2006, 8, 1398–1406. [PubMed: 17072303]

(53). Scheel C; Eaton EN; Li SH-J; Chaffer CL; Reinhardt F; Kah K-J; Bell G; Guo W; Rubin J; Richardson AL; Weinberg RA Paracrine and autocrine signals induce and maintain mesenchymal and stem cell states in the breast. Cell 2011, 145, 926–940. [PubMed: 21663795]

(54). DiMeo TA; Anderson K; Phadke P; Fan C; Perou CM; Naber S; Kuperwasser C. A novel lung metastasis signature links Wnt signaling with cancer cell self-renewal and epithelial-mesenchymal transition in basal-like breast cancer. Cancer Res. 2009, 69, 5364–5373. [PubMed: 19549913]

(55). Wu Y; Ginther C; Kim J; Mosher N; Chung S; Slamon D; Vadgama JV Expression of Wnt3 activates Wnt/β-catenin pathway and promotes EMT-like phenotype in trastuzumab-resistant HER2-overexpressing breast cancer cells. Mol. Cancer Res 2012, 10, 1597–1606. [PubMed: 23071104]

(56). Beiter K; Hiendlmeyer E; Brabletz T; Hlubek F; Haynl A; Knoll C; Kirchner T; Jung A. β-Catenin regulates the expression of tenascin-C in human colorectal tumors. Oncogene 2005, 24, 8200–8204. [PubMed: 16091738]

(57). Oskarsson T; Acharyya S; Zhang XH-F; Vanharanta S; Tavazoie SF; Morris PG; Downey RJ; Manova-Todorova K; Brogi E; Massagué J. Breast cancer cells produce tenascin C as a metastatic niche component to colonize the lungs. Nat. Med 2011, 17, 867–874. [PubMed: 21706029]

(58). Barker N; van Es JH; Kuipers J; Kujala P; van den Born M; Cozijnsen M; Haegebarth A; Korving J; Begthel H; Peters PJ; Clevers H. Identification of stem cells in small intestine and colon by marker gene Lgr5. Nature 2007, 449, 1003–1007. [PubMed: 17934449]

(59). Plaks V; Brenot A; Lawson DA; Linnemann JR; Van Kappel EC; Wong KC; de Sauvage F; Klein OD; Werb Z. Lgr5-expressing cells are sufficient and necessary for postnatal mammary gland organogenesis. Cell Rep. 2013, 3, 70–78. [PubMed: 23352663]

(60). Yang L; Tang H; Kong Y; Xie X; Chen J; Song C; Liu X; Ye F; Li N; Wang N; Xie X. LGR5 promotes breast cancer progression and maintains stem-like cells through activation of Wnt/β-catenin signaling. Stem Cells 2015, 33, 2913–2924. [PubMed: 26086949]

(61). Hou M-F; Chen P-M; Chu P-Y LGR5 overexpression confers poor relapse-free survival in breast cancer patients. BMC Cancer 2018, 18, No. 219.

(62). Hagerling C; Owyong M; Sitarama V; Wang C-Y; Lin C; van den Bijgaart RJE; Koopman CD; Brenot A; Nanjaraj A; Wärnberg F; Jirström K; Klein OD; Werb Z; Plaks V. LGR5 in breast cancer and ductal carcinoma in situ: a diagnostic and prognostic biomarker and a therapeutic target. BMC Cancer 2020, 20, No. 542.

(63). Zhang X; Claerhout S; Prat A; Dobrolecki LE; Petrovic I; Lai Q; Landis MD; Wiechmann L; Schiff R; Giuliano M; Wong H; Fuqua SW; Contreras A; Gutierrez C; Huang J; Mao S; Pavlick AC; Froehlich AM; Wu MF; Tsimelzon A; Hilsenbeck SG; Chen ES; Zuloaga P; Shaw CA; Rimawi MF; Perou CM; Mills GB; Chang JC; Lewis MT A renewable tissue resource of phenotypically stable, biologically and ethnically diverse, patient-derived human breast cancer xenograft models. Cancer Res. 2013, 73, 4885–4897. [PubMed: 23737486]

(64). Rosenberg LH; Lafitte M; Quereda V; Grant W; Chen W; Bibian M; Noguchi Y; Fallahi M; Yang C; Chang JC; Roush WR; Cleveland JL; Duckett DR Therapeutic targeting of casein kinase 1δ in breast cancer. Sci. Transl. Med 2015, 7, No. 318ra202.

(65). Nikolovska-Coleska Z; Wang R; Fang X; Pan H; Tomita Y; Li P; Roller PP; Krajewski K; Saito NG; Stuckey JA; Wang S. Development and optimization of a binding assay for the XIAP

Author Manuscript Author Manuscript Author Manuscript Author Manuscript

BIR3 domain using fluorescence polarization. Anal. Biochem 2004, 332, 261–273. [PubMed: 15325294]

(66). Cer RZ; Mudunuri U; Stephens R; Lebeda FJ IC50-toKi: a web-based tool for converting IC50 to Ki values for inhibitors of enzyme activity and ligand binding. Nucleic Acids Res. 2009, 37, W441–W445. [PubMed: 19395593]

(67). Plante JP; Burnley T; Malkova B; Webb ME; Warriner SL; Edwards TA; Wilson AJ Oligobenzamide proteomimetic inhibitors of the p53-hDM2 protein-protein interaction. Chem. Commun 2009, 5091–5093.

(68). Yeo DJ; Warriner SL; Wilson AJ Monosubstituted alkenyl amino acids for peptide “stapling”. Chem. Commun 2013, 49, 9131–9133.

Author Manuscript Author Manuscript Author Manuscript Author Manuscript

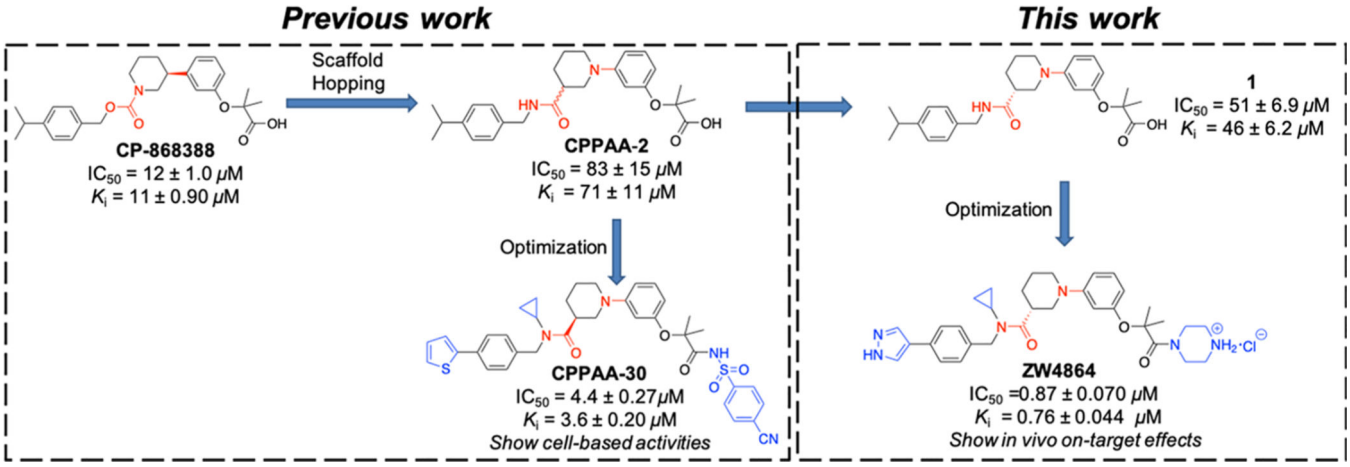

Figure 1.
Design of new β-catenin/BCL9 PPI inhibitor **ZW4864**.

Author Manuscript Author Manuscript Author Manuscript Author Manuscript

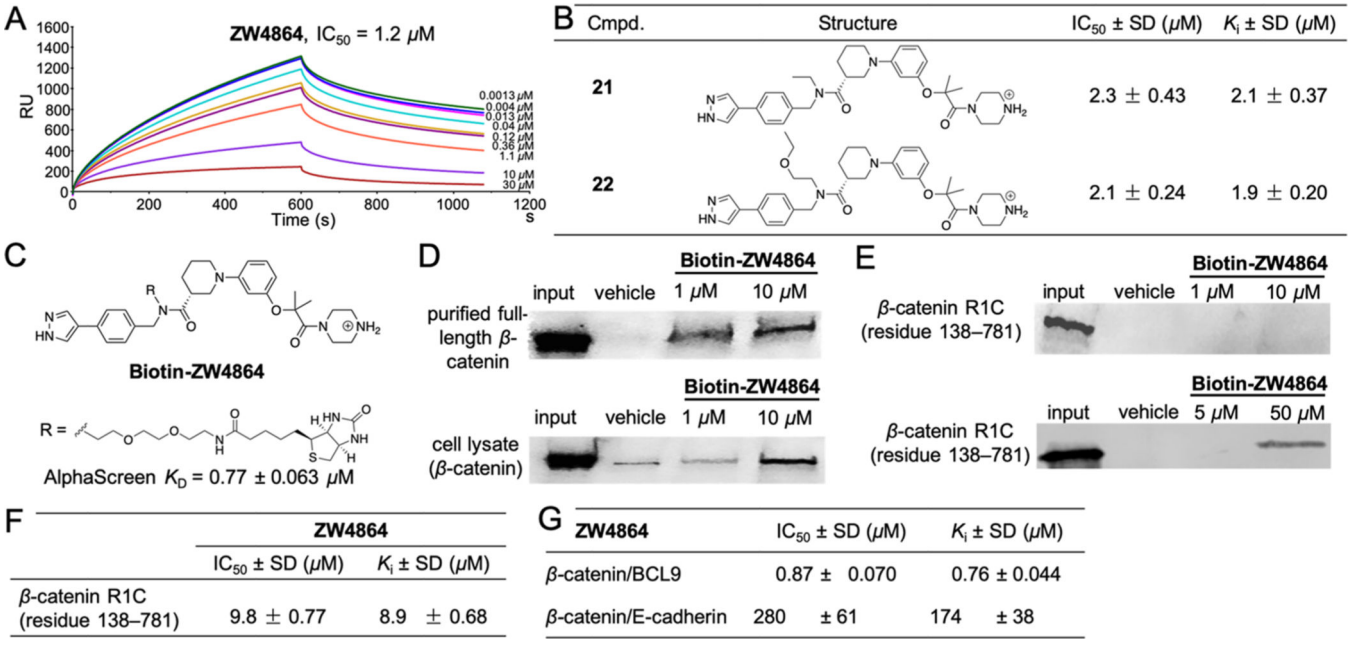

F

	ZW4864	
	IC_{50} ± SD (μM)	K_i ± SD (μM)
β-catenin R1C (residue 138–781)	9.8 ± 0.77	8.9 ± 0.68

G

ZW4864	IC_{50} ± SD (μM)	K_i ± SD (μM)
β-catenin/BCL9	0.87 ± 0.070	0.76 ± 0.044
β-catenin/E-cadherin	280 ± 61	174 ± 38

Figure 2.

Biochemical characterizations of **ZW4864** and derivatives. (A) SPR competitive inhibition assay results of **ZW4864**. The dose–response curves of SPR assays of **ZW4864** are shown in Figure S2. (B) Chemical structures of **21** and **22**, and their IC_{50} and K_i values for disrupting β-catenin/BCL9 PPI in AlphaScreen assays. The dose–response curves are provided in Figure S1. (C) Chemical structure of **Biotin-ZW4864**. TFA: trifluoroacetic acid. (D) Protein pull-down experiment results of **Biotin-ZW4864** with β-catenin. Purified full-length β-catenin (upper panel) and SW480 cell lysates (lower panel) were incubated with **Biotin-ZW4864**, followed by streptavidin pull-down. Input: 5% β-catenin or cell lysate. Vehicle: 0.1% dimethyl sulfoxide (DMSO) in buffer. Uncropped Western blot gels are shown in Figure S4. (E) Protein pull-down experiment results of **Biotin-ZW4864** with β-catenin R1C truncate (residues 138–781). Input: 5% β-catenin RIC. Uncropped Western blot gels are provided in Figure S5. (F) AlphaScreen assay results of **ZW4864** to disrupt β-catenin R1C/BCL9 PPI. (G) AlphaScreen selectivity results of **ZW4864** between β-catenin/BCL9 and β-catenin/E-cadherin PPIs. The K_Ds of wild-type full-length β-catenin with wild-type E-cadherin peptide (residues 824–877) in fluorescence anisotropy (FA) binding and AlphaScreen competitive binding assays are shown in Figure S6. The dose–response curves of AlphaScreen selectivity assays of **ZW4864** are shown in Figure S7. Each experiment was performed in triplicate. Each set of the inhibitory activity data was expressed as mean ± standard deviation (n = 3).

Author Manuscript Author Manuscript Author Manuscript Author Manuscript

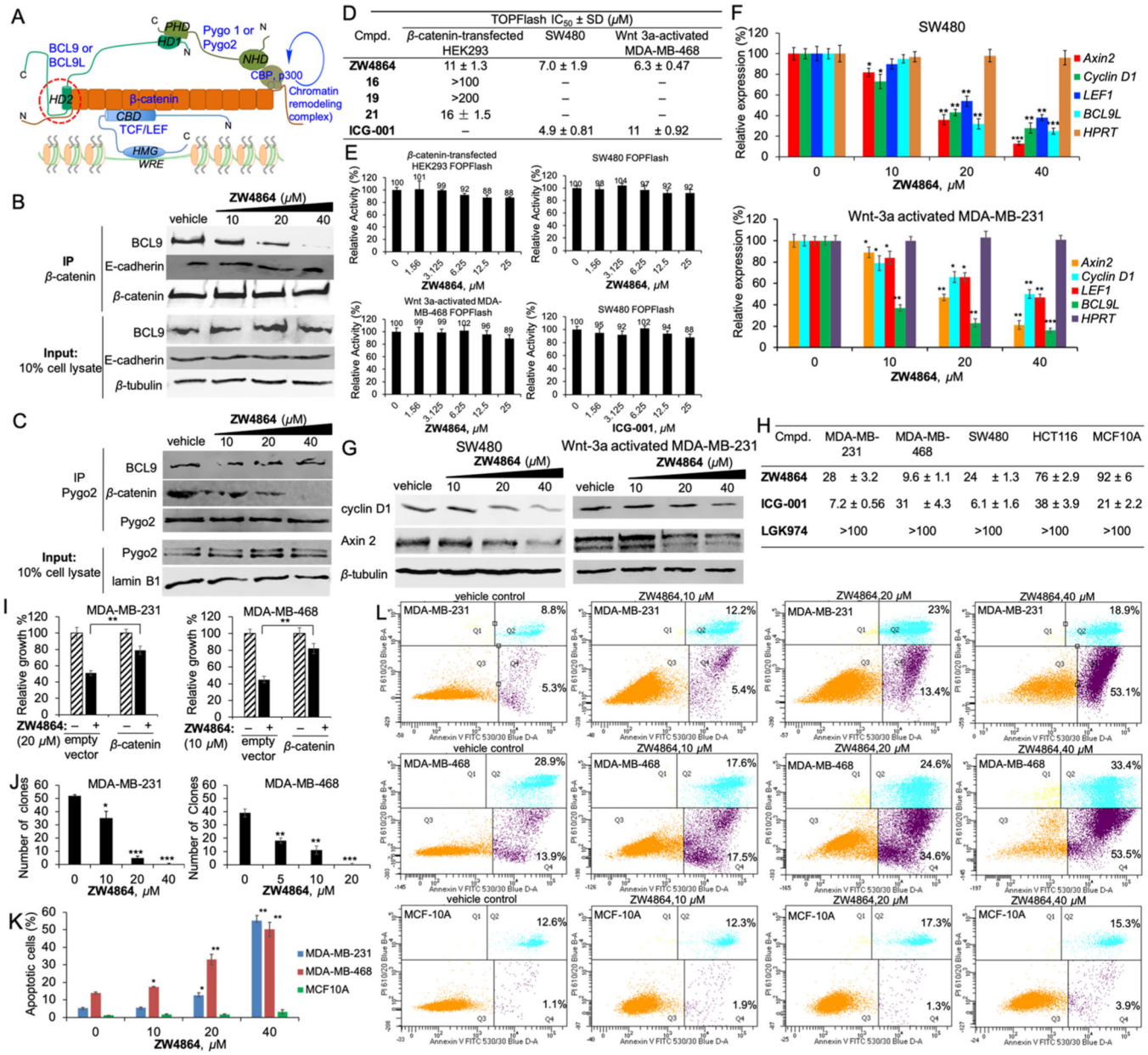

Figure 3.

(A) Illustration of β-catenin/TCF/BCL9/Pygo complex. (B) Cell-based co-IP assays to assess effects of **ZW4864** for β-catenin/BCL9 PPI disruption and the inhibitory selectivity between β-catenin/BCL9 over β-catenin/E-cadherin PPIs. (C) Cell-based co-IP assays to evaluate effects of **ZW4864** for disruption of BCL9/Pygo and β-catenin/Pygo interactions after a 24 h incubation. IB, immunoblotting; IP, immunoprecipitation; and input, 10% amount of cell lysate. (D) TOPFlash luciferase reporter assay results of **ZW4864**, its derivatives, and **ICG-001** after a 24 h incubation. (E) Results of FOPFlash luciferase reporter assays of **ZW4864** and **ICG-001** after a 24 h incubation. (F) Quantitative real-time polymerase chain reaction (qPCR) to examine changes of mRNA expression of *AXIN2, cyclin D1, LEF1*, and *BCL9L* when treated with various concentrations of

Author Manuscript Author Manuscript Author Manuscript Author Manuscript

ZW4864 (24 h incubation). House-keeper gene *HPRT* was used as the negative control. (G) Western blot to monitor the expression changes of protein Axin2 and cyclin D1 when treated with various concentrations of **ZW4864** (24 h incubation). β-Tubulin was used as the internal reference. (H) 3-(4,5-Dimethylthiazol-2-yl)-5-(3-carboxymethoxyphenyl)-2-(4-sulfophenyl)-2H-tetrazolium (MTS) IC_{50} (μM) results of **ZW4864**, the CBP/β-catenin inhibitor **ICG-001**, and the porcupine inhibitor **LGK974** on β-catenin-hyperactive cancer cells and normal breast epithelial cells after a 72 h treatment. (I) Results of β-catenin rescue experiments. The effects of **ZW4864** on growth inhibition of TNBC cells after a 72 h treatment were determined by MTS assays. The vector with constitutively active β-catenin or an empty vector was transfected in MDA-MB-231 and MDA-MB-468 cells. (J) Effects of **ZW4864** on the clonogenic growth of TNBC cells. (K) The percent of apoptosis and (L) the effects on apoptosis by fluorescein isothiocyanate (FITC) annexin V/propidium iodide (PI) fluorescence-activated cell sorting (FACS) after 72 h treatment with the indicated doses of **ZW4864**. Each experiment was performed in triplicate. Each set of quantitative data was expressed as mean ± standard deviation ($n = 3$). *$p < 0.05$, **$p < 0.01$, and ***$p < 0.001$ determined by the unpaired, two-tailed Student's t test. Uncropped Western blot gels and dose–response curves are provided in Figures S8–S15. The original FACS reports are included in the Supporting Information.

Author Manuscript Author Manuscript Author Manuscript Author Manuscript

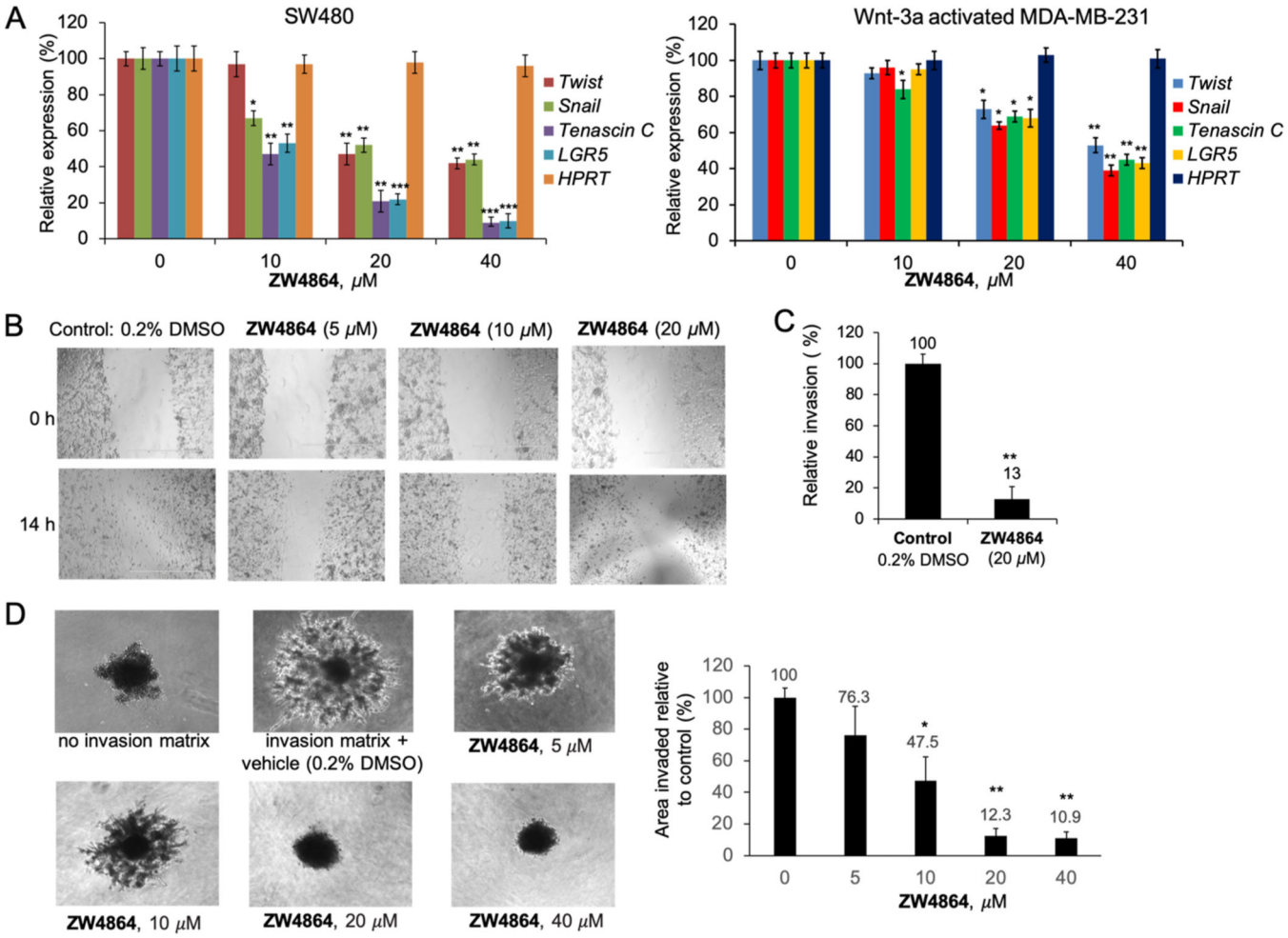

Figure 4.

(A) Changes of mRNA expression of *Twist, Snail, tenascin C*, and *LGR5* were determined by qPCR studies when SW480 and Wnt 3a-activated MDA-MB-231 cells were treated with various concentrations of **ZW4864**. House-keeper gene *HPRT* was used as the negative control. (B) Scratch wound healing assays demonstrated that **ZW4864** suppressed the migration of TNBC MDA-MB-231 cells that was induced by serum (10% in media). Mitomycin (10 μg/mL) was used to suppress cell proliferation, which allows examination of the effects on cell migration. Vehicle control: 0.2% DMSO in 10% fetal bovine serum (FBS). (C) Matrigel invasion assays showed that **ZW4864** (20 μM) impeded the invasion of MDA-MB-231 cells. Control, 0.2% DMSO in 10% FBS. (D) Cultrex 3D spheroid BME cell invasion assay results of **ZW4864** on day 6 using MDA-MB-231 cells. Left panel, representative images. Right panel, area of invasion when compared with that of the control spheroids. Each experiment was performed in triplicate. $*p < 0.05$, $**p < 0.01$, and $***p < 0.001$ determined by the unpaired, two-tailed Student's *t* test. All the original images are shown in Figures S17 and S18.

Author Manuscript Author Manuscript Author Manuscript Author Manuscript

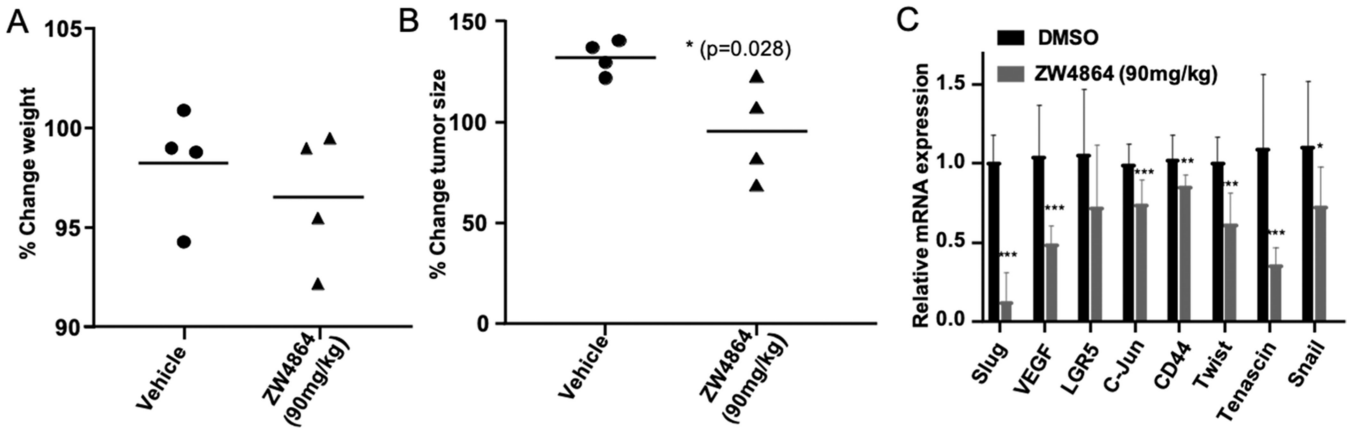

Figure 5.

(A) Weight analysis on mice treated with **ZW4864** at 90 mg/kg or saline normalized against their weight before treatment. (B) Percent change in tumor size in the 5 day course of treatment as indicated. (C) qRT-PCR analyses of the expression of the indicated genes in tumors from mice treated with **ZW4864** at 90 mg/kg or vehicle performed in triplicates. All data are presented as mean values ± SD ($n = 4$). *$p < 0.05$, **$p < 0.01$ ***$p < 0.001$ by *t*-test.

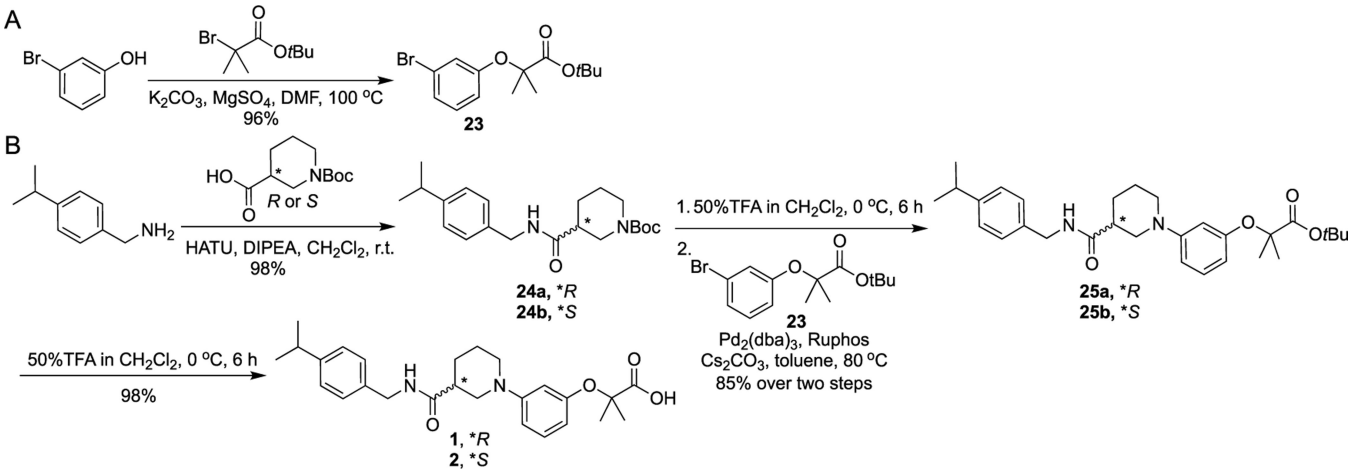

Scheme 1.
Synthetic Route of 1 and 2

Author Manuscript Author Manuscript Author Manuscript Author Manuscript

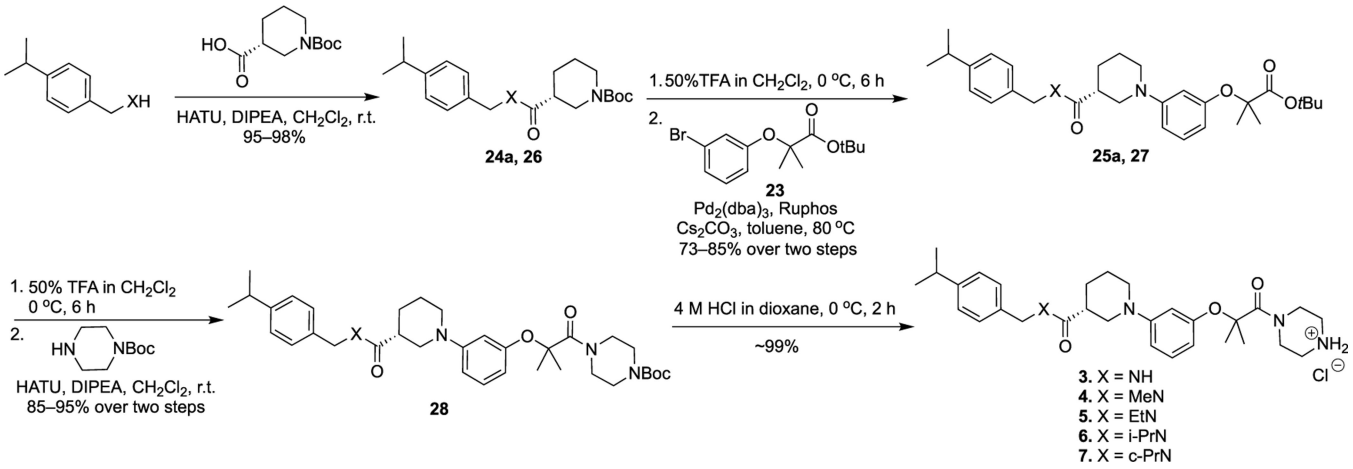

Scheme 2.
Synthesis of 3–7

Author Manuscript Author Manuscript Author Manuscript Author Manuscript

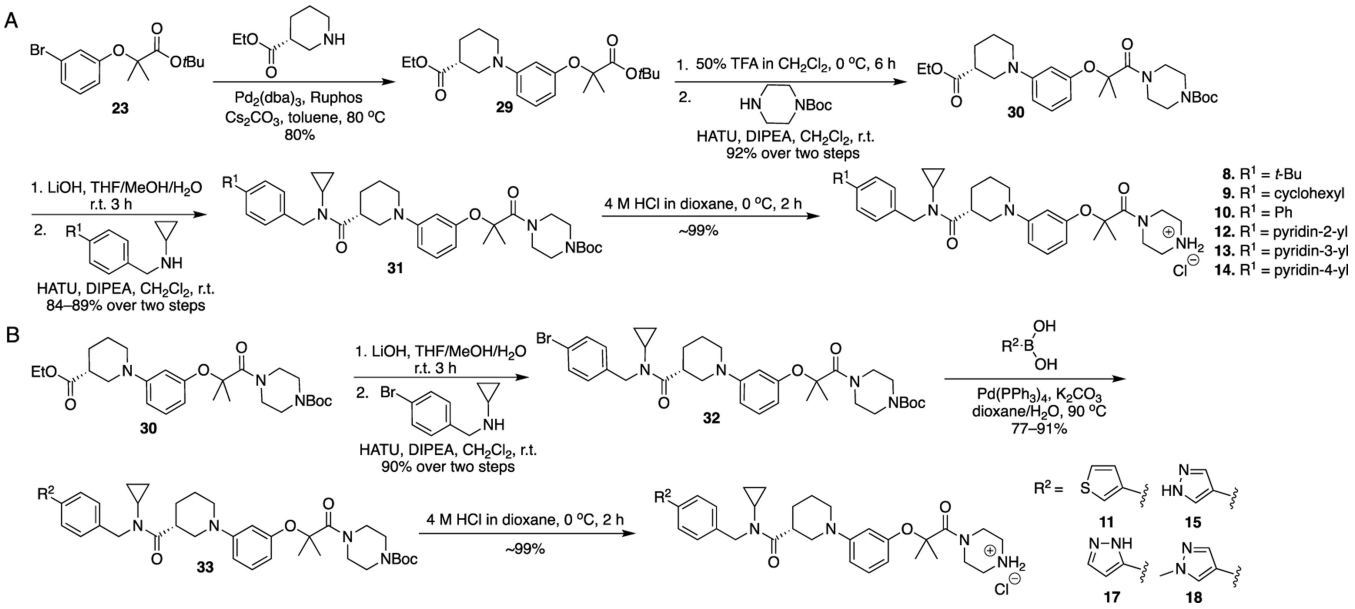

Scheme 3.
Synthesis of 8–15, 17, and 18

Author Manuscript Author Manuscript Author Manuscript Author Manuscript

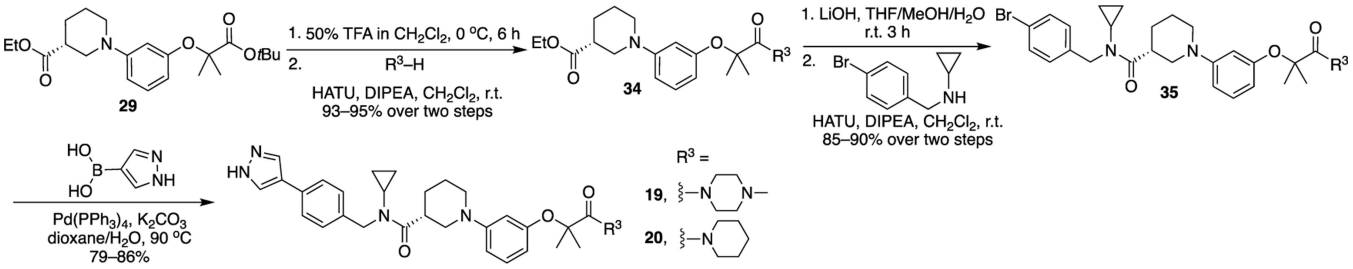

Scheme 4.
Synthesis of 19 and 20

Author Manuscript Author Manuscript Author Manuscript Author Manuscript

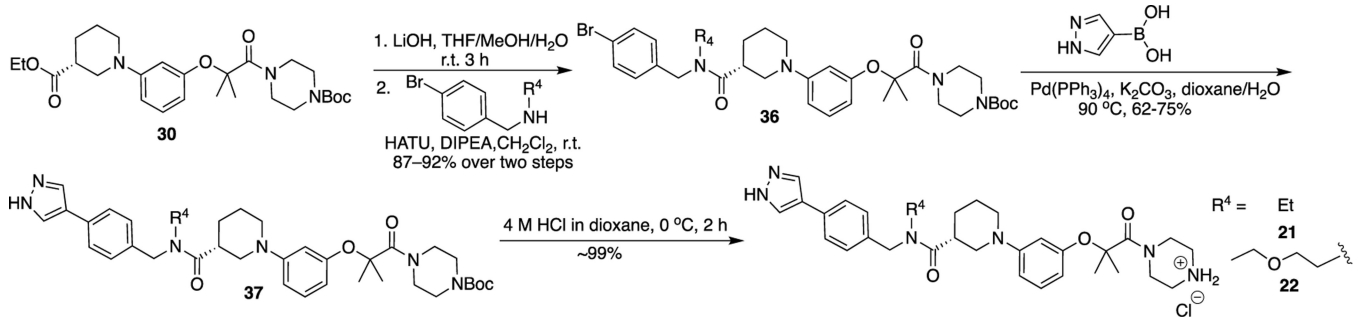

Scheme 5.
Synthesis of 21 and 22

Author Manuscript Author Manuscript Author Manuscript Author Manuscript

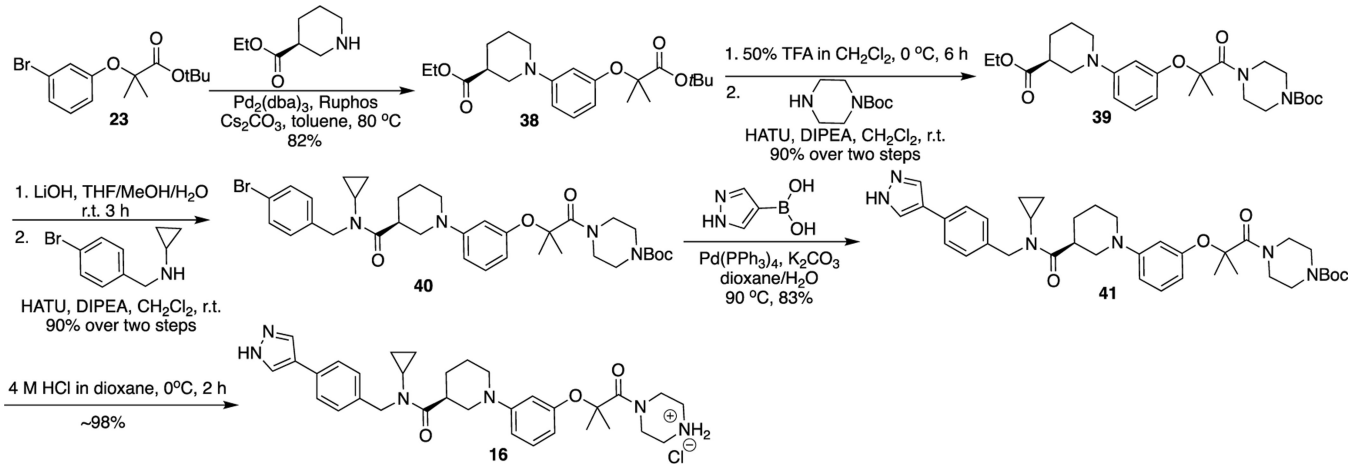

Scheme 6.
Synthesis of 16

Author Manuscript Author Manuscript Author Manuscript Author Manuscript

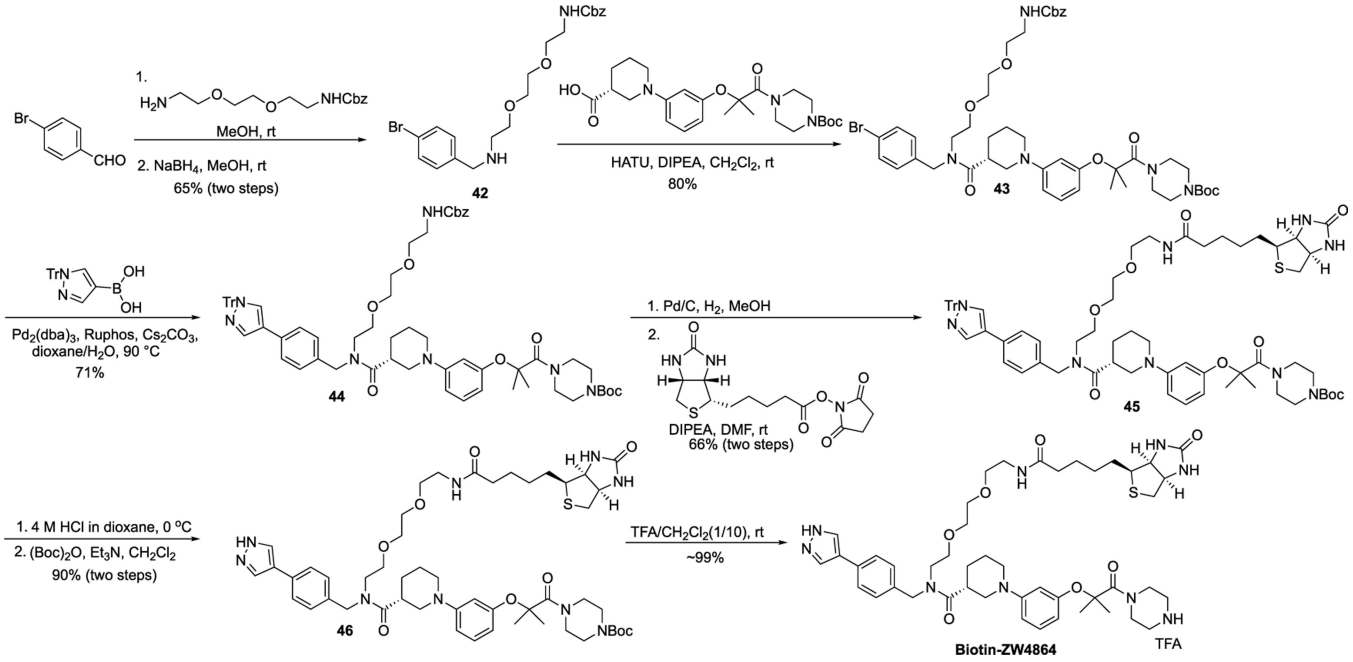

Scheme 7.
Synthesis of Biotin-ZW4864

Author Manuscript Author Manuscript Author Manuscript Author Manuscript

Author Manuscript

Author Manuscript

Author Manuscript

Author Manuscript

Table 1.

Author Manuscript
Author Manuscript
Author Manuscript
Author Manuscript

J Med Chem. Author manuscript; available in PMC 2022 August 26.

AlphaScreen Competitive Inhibition Assay Results of 1–20[a]

Cmpd.	Structure	$IC_{50} \pm SD$ (μM)	$K_i \pm SD$ (μM)
1	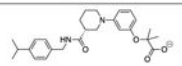	51 ± 6.9	46 ± 6.2
2	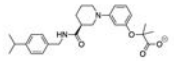	>100	>90
3	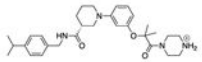	6.4 ± 1.4	5.8 ± 1.2
4	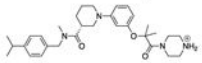	15 ± 3.1	14 ± 2.8
5	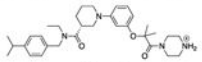	12 ± 3.1	11 ± 2.8
6	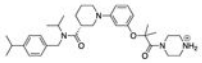	5.1 ± 1.5	4.6 ± 1.3
7	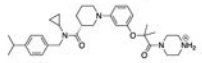	3.0 ± 0.61	2.7 ± 0.53
8	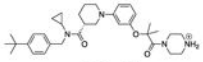	14 ± 1.6	13 ± 1.4
9	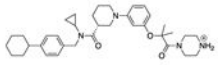	5.3 ± 0.95	4.8 ± 0.84
10	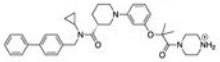	4.5 ± 0.46	4.0 ± 0.40
11	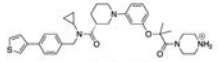	5.5 ± 0.63	5.0 ± 0.55
12	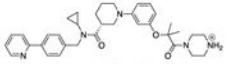	59 ± 7.1	54 ± 6.4
13	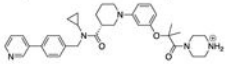	73 ± 13	66 ± 12
14	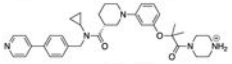	82 ± 9.2	74 ± 8.3
15 (ZW4864)	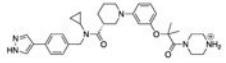	0.87 ± 0.070	0.76 ± 0.044
16	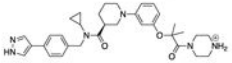	35 ± 4.7	32 ± 4.2
17	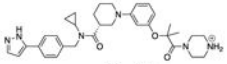	8.9 ± 0.90	8.0 ± 1.2
18	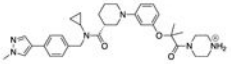	76 ± 6.3	68 ± 5.6
19	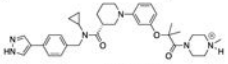	39 ± 1.3	32 ± 1.0
20	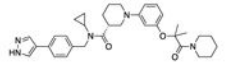	53 ± 2.0	43 ± 1.6

Author Manuscript Author Manuscript Author Manuscript Author Manuscript

[a] In AlphaScreen assays, the BCL9 peptide (residues 350–375) and full-length β-catenin (residues 1–781) were used. Each set of data was expressed as mean ± standard deviation (SD) (n = 3). The dose–response curves of the representative compounds are shown in Figure S1.

Author Manuscript Author Manuscript Author Manuscript Author Manuscript

Table 2.

Results of DMPK Studies: (A) Hepatic Microsome Stability of ZW4864 (15), 21, and Positive Control Sunitinib; and (B) Mouse PK Data of ZW4864[a]

(A)

	$t_{1/2}$ (min)		CL_{int} (μM/(min mg))	
cmpd.	**human**	**mouse**	**human**	**mouse**
sunitinib	27.8	13.0	25	53
ZW4864 (15)	38.4	9.6	18	72
21	28.3	7.7	24	90

(B)

cmpd.	**route**	**dose (mg/kg)**	C_{max} (μM)	**AUC (μM h)**	**Vd (L/kg)**	**CL (mL/(min kg))**	$t_{1/2}$ **(h)**	**%*F***
ZW4864	i.v.	1	0.79	0.71	8.0	44.20	3.51	
ZW4864	p.o.	20	3.21	11.71		51.10	3.07	83

[a]The original data plots of PK studies are shown in Figure S16

J Med Chem. Author manuscript; available in PMC 2022 August 26.

Author Manuscript Author Manuscript Author Manuscript Author Manuscript

Table 3.

Sequences of Peptides

	peptide	sequence
AlphaScreen	BCL9 26-mer	H-^{350}GLSQEQLEHRERSLQTLRDIQRMLFP^{375}-NH_2
	biotinylated BCL9 26-mer	Biotin-Ahx-^{350}GLSQEQLEHRERSLQTLRDIQRMLFP^{375}-NH_2
	E-cadherin 54-mer	H-^{824}APPYDSLLVFDYEGSGSEAASLSSLNSSESDKDQDYDYLNEWGNRFKKLADMYG^{877}-NH_2
	biotinylated E-cadherin 54-mer	Biotin-^{824}APPYDSLLVFDYEGSGSEAASLSSLNSSESDKDQDYDYLNEWGNRFKKLADMYG^{877}-NH_2
SPR	wild-type BCL9 peptide	Biotin-$(PEG)_4$-^{350}GLSQEQLEHRERSLQTLRDIQRMLFP^{375}-NH_2
	mutant BCL9 peptide	Biotin-$(PEG)_4$-^{350}GLSQEQLEAAERSLQTARDAQRMAAP^{375}-NH_2

J Med Chem. Author manuscript; available in PMC 2022 August 26.